The Pennsylvania State University

The Graduate School

The Huck Institutes of the Life Sciences

THE DNA REPAIR PROTEIN YKU80 REGULATES THE RECOMBINATION ENHANCER DURING YEAST MATING TYPE SWITCHING

A Thesis in

Integrative Biosciences

by

Chun Ruan

Submitted in Partial Fulfillment
of the Requirements
for the Degree of

Doctor of Philosophy

May 2005

The thesis of Chun Ruan has been reviewed and approved* by the following:

Song Tan
Associate Professor of Biochemistry and Molecular Biology
Thesis Advisor
Chair of Committee

Jerry L. Workman
Paul Berg professor of Biochemistry

Ross Hardison
Professor of Biochemistry

Hong Ma
Professor of Biology

Nina V. Fedoroff
Acting Co-Director, Graduate Education
Integrative Biosciences Graduate Program
Huck Institutes of the Life Sciences

*Signatures are on file in the Graduate School.

ABSTRACT:

Recombination enhancer (RE) is essential for regulating donor preference during yeast mating type switching. In this study, we attempt to investigate the RE mechanism by identifying and characterizing proteins that bind to it.

The minichromosome affinity purification (MAP) is a useful approach to isolate protein-DNA complex in its native chromatin context. Minichromosome is an artificial yeast vector that can be assembled into nucleosomes naturally in living cells. To identify factors that regulate the RE function, a 1.5kb RE segment was cloned into the minichromosome and introduced to yeast cells. Protein components of the affinity purified RE minichromosome isolated from either **a** or α cells were separated and analyzed by mass-spectrometry. A DNA repair protein yKu80p was identified by Matrix-Assisted Laser Desorption-Ionisation Mass Spectrometry (MALDI-MS) to specifically associate with minichromosome in **a** cells. Chromatin immuno-precipitation (ChIP) assay confirms the occupancy of both yKu80p and yKu70p at RE *in vivo*. Deletion of *YKU80* results in altered chromatin structure in the RE region and more importantly, causes a dramatic decrease of *HML* usage in **a** cells**.** We also detect directional movement of yKu80p from the RE towards *HML* during switching. These results indicate a novel function of yKu80p in regulating mating type switching.

To understand the molecular mechanism of yKu80p in switching, we took two biochemical approaches to search for factors that regulate RE function. The proteins identified in both methods would be our prime candidates for further study. First, we exploit the tandem affinity purification (TAP) approach coupled with multi-dimensional protein identification technique (Mud-PIT) to identify proteins that associate with

yKu80p during the course of switching. Comparison of the mass-spectrometry results of the switching and non-switching samples revealed that Rvb1p and Rvb2p, subunits of nucleosome remodeling complex INO80, bind to the yKu80p at the early stage of DSB repair. *In vitro* calmodulin pull down assay confirmed this strong but transient interaction. Moreover, ChIP assay was performed to demonstrate that Rvb1p binds to the active RE in a yKu80p dependent manner. In addition, Rvb1p exhibits a similar directional movement pattern along the left arm of Chromosome III during switching like that of the yKu80p. Second, optimized MAP approach combined with Mud-PIT analysis was used to identify the complete protein repertoire of the RE minichromosome. Various proteins have been found to associate with the RE minichromosome. They include not only proteins known to participate in minichromosome maintenance but also several novel candidates that are potentially linked to RE function. Two subunits of INO80, Arp5p and Rvb1p, were identified in this study. Since Rvb1p and Rvb2p were also detected in previous screen, we speculate that the INO80 complex might be involved in switching. To directly address this possibility, we deleted Arp5p which is required for INO80 function both *in vivo* and *in vitro*. The *ARP5* deletion strain indeed exhibits significant defect in donor preference: the *HML* usage dropped from 85% to 40%. These data collectively argue that chromatin remodeling complex INO80 play an important role in mating type switching.

Besides binding to the DSB as shown by previous study, our data suggested that both INO80 and yKu80p also bind to RE. One reasonable interpretation is that the two DNA loci could be brought together by those proteins during switching. This is consistent with the “entry point” hypothesis which proposed that, at the beginning of switching, the

double strand break (DSB) is brought to the RE vicinity, possibly by proteins that bind to both loci, and subsequently starts homolog searching and recombination. Here we provide another line of evidence that γ-H2A, a landmark of double strand break, is also enriched in the RE region upon *HO* cleavage. This enrichment requires wild type yKu80p but not functional INO80. Based on the biochemical properties of these complexes, we envision that yKu80p may mediate DSB entering RE either through self-dimerization or by interacting with DSB bound proteins. Subsequently, the nucleosome mobilization activity of INO80 may contribute to homolog searching of DSB for its donor loci.

TABLE OF CONTENTS

LIST OF FIGURES

LIST OF TABLES

ACKNOWLEDGMENTS

I want to express my sincere thanks to everyone who support me professionally or personally to finish this dissertation.

I am particularly grateful to my late advisor Dr Bob Simpson. In his lab, independent research and critical thoughts are always encouraged. In the meantime, he was always willing to help and give advice when they were needed most. He will always be remembered as a superior mentor and role model.

I would wish to express my appreciation to Dr Jerry Workman. I thank him for generously letting me finish my thesis research in his lab at the Stowers Institute for Medical Research. In addition, his extraordinary knowledge and insightful suggestions help me tremendously in the biochemistry field.

I would like to thank Drs Song Tan, Ross Hardison, Hong Ma for their suggestions and comments for my project. And Drs Joe Reese, David Gilmore, Davis Ng and Frank Pugh for their contribution to the vigorous and friendly environment of the transcriptional field in Penn State which helped me significantly ever since I came here.

Many thanks to the Simpson lab members: especially to Chuck and Mai, who help me start my project; John and Sevinc, who gave me technical advice and shared strains with me; Xi, Bob, Sangita, Alexandra and Chris, who are always supportive. I am also very grateful to all Workman lab members for their lively discussions and useful comments in the lab meeting; I thank Mark and Sam for taking time to read my manuscript and Cheri, Thomas, Dayoup, Tamaki, Sam, Summer and Leo for their input

and support. I am especially indebted to Selene, Drs Washburn and Florens who did Mud-PIT for my minichromosome samples.

I really appreciate the company of all my friends: Robert, Michelle, Mitra, Ritu, Z and Yingbao in Penn State and Yong, Jingji, Jiwang and Nancy in Stowers; your friendship is invaluable to me.

To my family, what I feel is more than obligation. I would never get as far as I am now without them. I feel extremely lucky to be my parents' daughter and to grow up in such a cozy family. And thanks to Bing, a true partner in life, this happiness continues to surround me. For them my gratitude is beyond words.

CHAPTER I INTRODUCTION

1.1 Chromatin structure and gene regulation

1.1.1 Chromatin structure

Our understanding of the chromatin began in the late 19th century when it was first described by W Flemming as a structure which strongly absorbed dye and separated into stringy objects during cell division. Later on, chromatin was found to consist of DNA, a genetic material discovered by Friedrich Miescher, and histones, a group of small basic proteins founded by A Kossel in 1884 (Olins and Olins, 2003). More than a century after these original studies, our understanding of chromatin has increased significantly, from its components, structure, sub-cellular organization to how it regulates gene expression and cell function.

In an eukaryotic cell, the nucleus contains a massive amount of genetic material. For example, the human nucleus harbors 3 billion base pairs of DNA and if linearized, the length would extend to two meters. Therefore, DNA in eukaryotic cells is organized and compacted in folded states, which are most often presented as a hierarchy. Moreover, to effectively regulate gene expression, this structure should also allow regulatory factors to access their cognate sites and also prevent other factors from binding.

The nucleosome is the basic structural unit of chromosome organization. Two molecules each of the four histones - H2A, H2B, H3 and H4 form an octamer (histone core) which then assembled to the negatively charged DNA to establish a compact spool-like structure which is known as a nucleosome core particle. In this protein-DNA complex, the H3/H4 tetramer lies at the dyad and the H2A/H2B dimers located at the end of the DNA path (Chantalat et al., 2003; Luger et al., 1997). Each of the histone has a domain consisting of three α-helices in the shape of a shallow "U" (histone fold) which

involve in the interaction between not only histones but also histones and DNA (Chantalat et al., 2003; Luger and Richmond, 1998a). Each of the four histones also has an N-terminal tail which has no fixed configuration and extends outside of the nucleosome core particle (Luger and Richmond, 1998b). It is believed that the histone tails are important for inter-nucleosome interaction (stacking). In addition, they may provide an interface which allows the binding of various factors essential in gene regulation (Widom, 1998b).

In a nucleosome core particle, a short stretch of DNA (around 147bp) wraps tightly on the histone octamer outer surface in about 1 3/4 superhelical turns. These core particles are connected to each other through linker DNA which is variable in length (ranging from about 15 to 100 bp) (Widom, 1998b). In higher eukaryotes, the linker DNA is associated with linker histones (H1 or H5) (Vignali and Workman, 1998; Widom, 1998a). However, its counterpart in yeast is less understood (Downs et al., 2003; Ushinsky et al., 1997).

The nucleosome core motif is repeated along the length of the chromosomal DNA and results in the bead-on-a-string configuration which is sometimes referred to as the "10-nm fiber" (Widom, 1998b). Under physiological conditions this structure folds into the higher order 30-nm diameter arrangements. One of the popular models for the 30-nm fiber is the “solenoid” structure in which the nucleosomes are organized into an one-start helix with six to eight nucleosomes per turn (Widom, 1998b). In contrast, a competing model proposes that the arrangement of 10 nm fiber is actually zigzag back and forth to form a two-start helix structure. This model is supported by the recent electron

microscopy study of stabilized nucleosome array (Dorigo et al., 2004). The 30 nm structure continues to fold to higher order chromatin structures (Widom, 1998b).

1.1.2 Chromatin structure and gene regulation

Packaging DNA into a chromosome was originally thought to be a mean to accommodate massive amount of genetic material into a limited cellular space. However, it has become clear that the organization of chromatin structure also plays an important role in the regulation of many cellular processes such as cell division, transcription, replication and recombination (Sivolob and Prunell, 2004).

Some structural regulations occur at the local nucleosomal level and affect the DNA-histone interaction. The tails and globular domain of histones have both been shown to be subjected to multiple post-translational modifications such as acetylation, phosphorylation, methylation, ubiquitination and ADP ribosylation (Grant, 2001). Initial studies suggested that hyper-acetylation of H3 and H4 and hyper-phosphorylation of H3 are usually linked to transcription activation (Jenuwein and Allis, 2001). In contrast, methylation at lysine 9 of histone H3 often associates with transcriptional repression (Bird and Wolffe, 1999). However, more and more evidence indicates that one modification could lead to both transcriptional activation and repression in different context. Therefore, the “histone code” model has been proposed to reconcile these seemingly conflicted observations (Jenuwein and Allis, 2001; Peterson and Laniel, 2004). In this model, it is speculated that different combinations of post-translational modification “codes” may play a role in recruiting different regulators which then determine the expression status of a gene, whether active or silent (Jenuwein and Allis, 2001). Interestingly, recent study has shown that, in a genome wide level, low density of

nucleosomes occur in the promoters of transcriptional activated genes (Lee et al., 2004). This suggests that the level of nucleosome at any given DNA region is also subjected to regulation (Ercan et al., 2004).

Besides local regulation, chromatin structure is also involved in controlling gene activity over a long distance. The mechanistic study of the Locus Control Regions (LCR) provides some insight. LCR is a group of small *cis*-elements postulated to be able to control gene expression over a large chromosome segment. Besides regulating β-globin gene expression (Li et al., 2002), LCR has also been identified to function in V(D)J recombination in mammalian cells (Roch et al., 1997). Furthermore, in the case of human dosage compensation, a small *cis*-acting element XIC is essential for inactivating one of the female X chromosome (Kay, 1998; Kay et al., 1993). In addition, a yeast recombination enhancer is able to activate a locus 20 Kb away from it during mating type switching (Wu and Haber, 1996). The mechanism of LCRs was elusive until de Bruin et al. reported that a unique looping structure formed by the telomere enables the long range activation of some enhancers that otherwise work only locally (de Bruin et al., 2001). This result suggested that the dynamic chromatin organization might play an essential role in the long range activation by LCR. Indeed, by using "chromosome conformation capture" (3C) approach, a looping structure has been found to facilitate the interaction between LCR and the β-globin gene only when the locus is transcriptional activated (Tolhuis et al., 2002).

1.1.3 Chromatin remodeling complexes

Chromatin remodeling complexes regulate the higher order structure of chromatin and modulate the gene transcription. They can be categorized into two groups: histone-

modifying enzymes and ATP-dependent chromatin remodeling complexes (Aalfs and Kingston, 2000). Histone modifying enzymes can covalently modify core histones or nucleosomes at a post-translational stage. This group includes histone acetyltransferases, histone kinases, histone methyltransferase and histone ubiquitin ligase as well as enzymes that antagonize these modification, such as histone deacetylase, histone phosphatase, histone deiminase and histone deubiquitinase (Bannister et al., 2002; Cuthbert et al., 2004; Davie and Moniwa, 2000; Peterson and Laniel, 2004). Most of these modifications are reversible to ensure the dynamic regulation of gene expression and chromatin structure (Peterson and Laniel, 2004). A recent study discovered Lsd1p, the first histone demethylase, suggesting that the most abundant modification, methylation, can also be rapidly reversed (Shi et al., 2004).

ATP-dependent remodeling complexes utilize the hydrolysis of ATP to mobilize DNA and histone interactions (Flaus and Owen-Hughes, 2001; Havas et al., 2001). Many such complexes have been identified in yeast, including SWI/SNF, RSC, INO80 and ISW (Fry and Peterson, 2001) and all of then contains an ATPase subunit from the SNF2/SWI2 superfamily (Peterson, 1996).

The SWI/SNF complex is involved in both transcriptional activation and repression (Becker and Horz, 2002). It contains 11 subunits with Swi2/Snf2 being the catalytic module. Swi/Snf was also shown to be required for the silencing at both telomere and rDNA loci (Dror and Winston, 2004). The RSC complex is required for cell viability and it has two isoforms, Rsc1 and Rsc2 (Cairns et al., 1999). RSC is also implied to participate in chromosome segregation (Angus-Hill et al., 2001). Indeed, a recent study demonstrated that this complex assists cohesin loading in a cell cycle-regulated manner

and the mutation of its catalytic subunit, Sth1 abolished the association of cohesin to chromosomal arm (Huang et al., 2004; Huang and Laurent, 2004). The ISW family includes two complexes with ATPase activity, Isw1 and Isw2. Both of them have nucleosome and spacing activities and Isw1 is also able to disrupt nucleosome (Tsukiyama, 2002; Tsukiyama et al., 1999). Up to now ISW has been associated with gene silencing and transcriptional repression, which is probably due to the displacement of the basal transcription machinery (Goldmark et al., 2000; Hughes et al., 2000; Morillon et al., 2003).

The INO80 complex is not only thought to regulate gene expression but also is involved in DNA damage repair (Morrison et al., 2004; Shen et al., 2000). This complex contains 12 subunits with Ino80p as the catalytic subunit. This complex also includes Rvb1p/Rvb2p, two proteins shown to be homologous to the bacterial Ruvb helicase family which is involved in branch migration (Kurokawa et al., 1999). They also have weak ATPase activity (Shen et al., 2000). Other components of the INO80 complex includes several actin related proteins (Arp) such as actin, Arp4p, Arp5p, Arp8p (Shen et al., 2003a). First discovered in the mammalian BAF complex, actin and acting related proteins have been found to play an important role in many chromatin remodeling processes (Olave et al., 2002). In the INO80 complex, Arp5p and Arp8p are crucial for its function. Deletion of either of these proteins does not affect the integrity of the complex. However, it causes the INO80 complex to lose its ATPase activity as well as the ability to bind DNA and mobilize nucleosome (Shen et al., 2003a).

INO80 was found to be essential for DNA repair and participates in both homologous recombination and non homologous end joining (NHEJ) pathways (Fritsch et al., 2004;

van Attikum et al., 2004). For instance, in yeast cell, *HO* endonuclease cleavage creates a single DSB near the *MAT* locus (Haber, 2002) and immediately two checkpoint kinases Mec1p and Tel1p are recruited to the damage site and phosphorylate histone H2A (γ-H2A) (Lowndes and Toh, 2005). γ-H2A subsequently promotes the interaction of INO80 to the DSB by direct interaction (Morrison et al., 2004; van Attikum et al., 2004). INO80's nucleosome remodeling activity are speculated to be critical in the repair process since resident nucleosomes can interfere with the downstream recombination/repair steps (Shen et al., 2000). Alternatively, Rvb1p/Rvb2p may play an essential role in the homologous recombination pathway, since the bacterial homolog, RuvB, is a helicase and it is required for bacteria DNA repair and the migration of Holliday structure (Kurokawa et al., 1999). Rvb proteins also possess ATP-dependent helicase activity. Therefore the INO80 complex might also be able to move the Holliday junction and facilitate the homologous repair pathway (Cairns et al., 1999).

1.2 Chromosome rearrangement and yeast mating type switching

1.2.1 Chromosome rearrangement

Chromosome rearrangement is an important biological process which involves the relocalization of large segment of chromosome. Programmed chromosome rearrangements allows the dramatic changes of gene expression and in some cases, the phenotype of the organism (Brandt and Roth, 2004; van der Woude and Baumler, 2004). Notable examples include the reorganizations of immunoglobulin and T-cell receptor genes (Jones and Gellert, 2004), phase variation in bacteria such as *Salmonella* (van der Woude and Baumler, 2004), the activity of transposons (Bennett, 2004) and yeast mating-type switching (Haber, 1998). Higher order chromosome structure may play an

important role in this process, but the detailed mechanism remains elusive. In this study, we investigate the yeast mating type switching in detail. The results will not only shed light on the mechanism of directional relocalization of DNA segment during switching, more importantly, it will also promote our understanding of the chromosome rearrangement in higher eukaryotes.

1.2.2 Yeast mating type switching and donor preference

1.2.2.1 Mating type switching

One cellular process that greatly increased our understanding of chromatin structure, gene regulation, DNA damage repair and homologous recombination is yeast mating type switching. Yeast *Saccharomyces cerevisiae* can exist in either haploid or diploid forms in its life cycle (Nasmyth, 1983). There are two types of haploid cells: a and α, which differ by their mating type. Like many other fungi, the haploid yeast cell can change its mating type as often as every generation (Haber, 1998). The mating type switching process is highly regulated in that only cells that have undergone previous cell division (mother cell) can transform its mating type, while the newly budded cell (daughter cell) remains unchanged (Nasmyth, 1983). The fact that in any given cell division, only half of the population can switch ensures the equal amount of cells with opposite mating types in one colony (Haber, 1998). This promotes the efficient mating to produce diploid cells. The diploid cell plays an important role in the yeast cell cycle because at this stage, both meiosis and sporulation can take place. Meiosis enables homologous recombination which provides yeast evolutionary advantages. In addition, sporulation protects the cell to survive harsh environment.

The precise cell lineage in yeast is achieved by the regulation of the *HO* endonuclease, which initiates switching. A protein called Ash1p, which inhibits the expression of *HO*, can only express in daughter cell. This is because *ASH1* mRNA is exclusively transported there during budding by the directional movement of the actin cytoskeleton (Gonzalez et al., 1999).

At molecular level, the mating type of yeast is determined by two alleles of the mating type (*MAT)* loci located on Chromosome III. They differ by about 700bp of DNA which contain either Ya or Yα sequence (Haber, 1998). First proposed in the 1960's, the "cassette" model is still thought to be the most accurate theory to explain mating-type switching (Hawthorne, 1963; Oshima and Takano, 1971). In this model, two haploid mating (*HM)* loci which contains the same mating type genes are required for switching, in addition to the *MAT* locus (Takano and Oshima, 1970). They are called the *HML* and *HMR*, located near the telomeres on the left and right arms of Chromosome III, respectively. In non switching cells, these two loci are transcriptional silent, and both DNA and protein regulators contribute to the establishment of the silencing. For the *cis*-elements, four silencer sequences: *HML*-E, *HML*-I, *HMR*-E and *HMR*-I are identified to flank the two *HM* loci, all of which contains the yeast replication origin. They interact with a larger number of *trans*-regulators, among them are Silent Information Regulator (Sir), Origin Recognition Complex (ORC), Rap1p and several other histone modification complexes. Working together, these factors pack the *HM* loci into heterochromatin and target it into the transcriptional repressed nuclear periphery to achieving its silencing state (Taddei et al., 2004). During switching, however, replicas of one of the loci can be copied into *MAT*, the active locus, where they are expressed.

The mating type switching of the yeast haploid cell begins with a specific cleavage at the *MAT* locus by the *HO* endonuclease in late G1 phase (Nasmyth et al., 1987). The cutting generates a 4-bp 3' overhang DNA end. The broken end is then processed by 5'-3' exonuclease to create long 3' tails which are protected by the binding of the Rad protein family and start searching for homologous sequence and repair the DSB using either *HML* or *HMR* as templates.

1.2.2.2 Donor preference and the recombination enhancer (RE)

This gene conversion event is highly directional: *MAT***a** recombines with *HML* 90% of the time while *MAT*α uses *HMR* as donor with an efficiency of 85% (Sprague et al., 1981). This phenomenon is called donor preference. Extensive studies on this subject demonstrated that **a** and α cells employ different mechanisms in choosing the correct donor. In **a** cells, to be used as a donor, *HML* requires activation of a large region of the left arm of chromosome III to "out compete" *HMR* (Wu and Haber, 1995). In this case, if *HML* is deleted, cells can readily use *HMR* as a template for recombination. On the other hand, *HMR* serves as the "default" donor in α cells (Wu and Haber, 1995; Wu and Haber, 1996) because the *HML*, along with the whole left arm of Chromosome III, is in a "cold" condition and is inaccessible for recombination. Therefore, if *HMR* is deleted, the majority of cells died during switching because the cleavage in the *MAT* can not be repaired properly (Wu et al., 1996).

In attempt to find essential cis-element in donor preference, Haber's lab examined the donor preference of a series of strains with various deletions in Chromosome III. A *cis*-acting element called the recombination enhancer (RE) has been identified to be crucial

in activating the *HML* in **a** cells (Wu and Haber, 1996). It is an approximately 730bp DNA sequence located ~30Kb from the left end of chromosome III, ~17Kb away from *HML* (Wu and Haber, 1996). It has been shown to activate ~40Kb region of the left arm of Chromosome III, including *HML*α, for recombination in **a** cells. In the presence of a functional RE, **a** cells use *HML* ~90% of the time. However, if the RE is deleted, *HML* usage drops to ~10% (Wu and Haber, 1996). Sequence comparison of *Saccharomyces cerevisiae* and *Saccharomyces calsbergensis* revealed four conserved sub-domains in the RE region (Wu et al., 1998): A, B, C and D. Region A and B only slightly affect the RE function whereas the C and D region are shown to be indispensable. Domain C contains a Matα2p/Mcm1p binding site and region D features unique TTT(A/G) repeats (Wu et al., 1998). Recent sequence alignment analysis of *Saccharomyces cerevisiae* and *Saccharomyces bayanus* identified a novel conserved E region which also contains the TTT(G/A) repeats (Sun et al., 2002). However, besides the above three closely related species (all within group sensu stricto), the searching for putative RE in yeast is unproductive. For example, sequence alignment of *S. cerevisae* and *S servazzii* (group sensu lato) (Masneuf et al., 1998), revealed that though the four genes surrounding RE (*PRD1*, *KAR4*, *SPB1* and *PBN1*) are preserved, the RE locus in between *KAR4* and *SPB1* is absent and replaced by an unknown Open Reading Frame (ORF) which are not functional related to RE (Zhou et al., 2001).

High resolution mapping of chromatin structure around the RE region using micrococcal nuclease digestion reveals that chromatin structure at this region is different in **a** and α cells (Weiss and Simpson, 1997). In α cells, this region is covered by well positioned nucleosomes. Both α2p and Tup1p play important roles in organizing the

chromatin structure. In contrast, those nucleosomes are replaced by a distinctive hypersensitive site flanked by two footprints in **a** cells and it has been shown that Mcm1p, along with other proteins, are essential in maintaining this unique pattern (Weiss and Simpson, 1997).

Study of the RE's role in donor preference revealed an inverse relation between its function and chromatin structure. For instance, if the RE is packed into tightly positioned nucleosomes, as the case in α cells, it can not activate *HML* to be used as a template during switching (Weiss and Simpson, 1997). However, when the nucleosomes are removed from this region in **a** cells, the RE is fully functional and makes *HML* accessible in homologous recombination (Weiss and Simpson, 1997).

The unique hypersensitive site and footprints of the RE in **a** cells strongly imply an "open" chromatin structure and binding of *trans*-acting elements. Indeed, several proteins have been found to be important in RE regulation. Among them is Mcm1p, a MADS box family transcription regulator. A 2-bp mutation of its binding site in the C region of the RE not only affects the RE chromatin structure but also completely eliminate its function: the usage of *HML* drops from 85% to 10%. Likewise, mutation in Mcm1p (mcm1-5) also shows a defect in donor preference, but to a less extent (Wu et al., 1998).

Besides Mcm1p, a putative DNA helicase Chl1p has been implicated to play a minor role in switching (Weiler et al., 1995). Recently, yeast transcriptional factors Fkh1p and Fkh2p have been shown to be recruited to the RE and affect donor preference in **a** cells (Sun et al., 2002). However, the detailed mechanisms of how these factors control mating type switching remain to be solved. Since the deletion of *CHL1, FKH1* and *FKH2* can

completely abolish the RE function, we concluded that redundant regulators must be involved in the process.

α cells, on the other hand, seem to use a difference set of proteins to ensure correct donor choice. In this case, the haploid specific α2p, along with global co-repressor Tup1p (Cooper et al., 1994; Smith and Johnson, 2000), plays an important role (Smith et al., 1995; Szeto and Broach, 1997; Szeto et al., 1997). The homeodomain protein Matα2p and the SRF-like protein Mcm1p bind to the RE and in turn recruit Tup1p to exert repression. Tup1p certainly plays an important role in organizing the nucleosome array in the RE since in a *tup1* deletion strain, these tightly positioned nucleosomes all disappeared (Weiss and Simpson, 1997). Several models have been proposed to explain how Tup1p functions (Smith and Johnson, 2000). For example, it could directly interfere with activators or interact with the transcriptional machinery (Gavin and Simpson, 1997; Smith and Johnson, 2000). Alternatively, Tup1p can repress gene expression by changing the chromatin structure of the regulated gene by either directly interacting with the histone tails (Edmondson et al., 1996) or recruit histone deacetylases (Watson et al., 2000).

1.2.2.3 Models of yeast mating type switching and donor preference

There are two distinct models to explain the directionality of yeast mating type switching. The first hypothesis suggests that a looping chromatin structure may brings the *MAT* locus to its potential donor and the close vicinity of the two loci before *HO* cleavage promotes the correct recombination (Kostriken and Wedeen, 2001). However, live-cell fluorescent microscopy showed that the relative position of *MAT* locus and its destined

donor is mating type independent. In addition, they are not prealigned before the start of switching (Bressan et al., 2004; Simon et al., 2002). Even tethering the wrong donor to *MAT* locus could not significantly affect the donor preference (Simon et al., 2002). The above data suggested that instead of "physical contact" before *HO* cutting, a mechanism assisting the *MAT* locus to "commit" recombination with the correct donor after the generation of DSB is crucial for donor preference. In this model, *cis*- and *trans*- elements would facilitate the processes of either the strand invasion of DSB or the maturation of strand exchange intermediates which dictate the commitment of the recombination between the *MAT* and donor locus. For example, in **a** cells, RE could serve as an "entry point" for the DSB and promote the strand invasion at *HML*. Though the mechanism of RE's action remains largely unknown, it has been shown that RE does influence the nuclear localization of *HML*, indicating the interaction between the two loci (Bressan et al., 2004).

1.3 yKu80p in DNA damage repair

DNA double strand break is a potentially lethal cellular event that is generated by ionizing irradiation or normal DNA metabolism (Haber et al., 2004). In eukaryotes, DSB is repaired through either homologous recombination or non-homologous end joining pathway (NHEJ) (Ward and Chen, 2004). One of the important protein families which involve in both pathways is the Ku complex (Doherty and Jackson, 2001; Haber, 1999).

Homologs of the Ku family have been identified in human, plant, yeast and bacteria (Boulton and Jackson, 1996; Doherty et al., 2001; Feldmann et al., 1996; Feldmann and Winnacker, 1993; Tamura et al., 2002). This protein is part of an evolutionarily

conserved protein complex that has been shown to be critical in many DNA repair events. For example, it is required for immunoglobulin isotype switching in mammals (Casellas et al., 1998), γ-irradiation induced DSB repair in plants (Tamura et al., 2002) and recombination in yeast cells (Mages et al., 1996).

1.3.1 Structure of the Ku heterodimer

Ku70 and Ku80 form a heterodimer. The crystal structure of the Ku heterodimer was first elucidated by Goldberg's group (Walker et al., 2001). Since Ku70 and Ku80 are evolutionary related proteins, their fold similarly to form a quasi-symmetrical heterodimer. Each subunit consists a three-domain structure including an N-terminal α/β domain, a β-barrel domain, and a helical C-terminal tail. The Ku70 and Ku80 subunits then form an open ring-like structure which allows the DNA strand to thread through. Especially important in the structure is the β-barrel domain because it provides the interface for DNA binding. The arrangement of the Ku heterodimer explains the preferred binding of Ku complex to DNA end, such as DSB, and offers insight to how it work in DNA damage repair (Doherty and Jackson, 2001).

1.3.2 Ku regulates telomere function

Telomeres form a protective end of chromosomes and are transcriptionally repressed. The Ku80 complex, along with the Silent information regulator (Sir) proteins, plays a very important role in maintaining the structure, function and sub-cellular location of the telomere (Wai, 2004). Like Sir proteins, yKu80p has been shown to bind to the telomere region by ChIP assay (Gravel et al., 1998). And the fact the yKu80p and another telomere

associated protein Cdc13p are synthetically lethal suggests its role in protecting the telomere end structure (Nugent et al., 1998). The Ku proteins also regulate the telomere silencing and like the Sir proteins and deletion of the Ku complex results in the loss of telomere silencing (Nugent et al., 1998). In addition, yKu80p is involved in the localization of the telomere to the nuclear envelope (Taddei et al., 2004). It is reported that in the absence of yKu80p, the telomere delocalizes from its usual residence: the nuclear periphery (Taddei and Gasser, 2004).

1.3.3 Ku in DNA damage repair and recombination

The mechanism of how Ku works first came from the studies in mammalian cells. It has been proposed that Ku80p is an important component in the NHEJ process, the major pathway for DNA repair in higher eukaryotes (Doherty and Jackson, 2001). The complex binds to the DSB and recruits DNA-dependent protein kinase (DNA-PK). Subsequently, broken DNA ends can be tethered through Ku protein self-association and interaction with DNA-PK (Cary et al., 1997; Walker et al., 2001). Slightly different from its mammalian counterpart, the yeast Ku homolog has been shown to be involved in both homologous recombination and NHEJ (Clikeman et al., 2001; Feldmann et al., 1996; Mages et al., 1996). For instance, yeast Ku70 has been shown to regulate the homologous recombination in mating type switching. As been shown by Mages et al, deletion of yKu70p in **a** cells caused dramatic drop of *HML* usage (Mages et al., 1996).

Efficient NHEJ repairing in yeast also requires yKu80p (Martin et al., 1999). The ring-like structure of the Ku heterodimer may protect the DNA ends upon binding and promote the subsequent ligation (Walker et al., 2001). Interestingly, cytological evidence

has shown that upon DNA damage, both yKu80p and Sir3p relocalize from telomere to the damage site (Martin et al., 1999; Mills et al., 1999). Indeed, this recruitment to the DSB was confirmed by ChIP assay (Martin et al., 1999).

In addition, mammalian Ku80 has been shown to involve in V(D)J recombination. Both T and B lymphocyte development was found to arrest in Ku80 deletion mouse (Nussenzweig et al., 1996). In this process, Ku80 is essential for the intermediate cleavage process which ensure the proper recombination between the different segments of the antigen receptor (Sandor et al., 2004)

Moreover, yKu80p plays an important role in DNA replication. It not only assists the formation of replication complex at the replication origin (Shakibai et al., 1996), but also controls the timing of replication initiation of DNA in telomere region (Cosgrove et al., 2002).

1.4 Methods for study the component and structure of chromatin

Regulation of gene expression and cell function occur at the chromatin level. This makes it important to understand the components and dynamic structure of the chromatin in its native condition.

1.4.1 Traditional endonuclease mapping

Attempt to understand the structure of chromatin, traditional methods rely on DNA restriction enzymes or chemicals that detect the protected sites on the chromosome which result from protein binding (Simpson, 1999). Since these agents usually can not penetrate the nuclear membrane, nuclei must first be isolated from living cells. After this step, DNA can be treated with either non specific endonucleases (such as DNase I and

micrococcal nuclease (MNase)) (Ravindra et al., 1999) or specific restriction endonucleases (Li and Reese, 2001). Subsequently, nucleosome position can be revealed by primer extension, which map chromatin regions with high resolution, or indirect end labeling analysis, which is convenient to perform but usually provides less structural information (Ducker and Simpson, 2000; Weiss and Simpson, 1997). In these types of assays, the presence of positioned nucleosome is represented by ~150bp nuclease resistant sequence separated by linker regions that are sensitive to cleavage.

Tremendous structural information has been provided by these methods at several chromatin loci and under various conditions (Lohr, 1997; Pazin et al., 1998). One good example is the study of the promoter of an inducible gene *PHO5*. Using restriction enzyme, MNase and DNase I mappings, it was found that under repressed condition, an essential upstream activation site of *PHO5* is covered by nucleosome array which prevents the binding of transcriptional activator (Lohr, 1997). However, positioned nucleosomes are disrupted and the activator binding site revealed when the gene is activated by phosphate starvation (Svaren and Horz, 1995). This examination connects the expression status of a gene and the specific nucleosome structure on its promoter and provides great insight into the role chromatin structure at gene regulation.

1.4.2 Electron Microscopy

Besides endonuclease mapping, Electron Microscopy (EM), with its ability to image DNA and nucleosomes, offers a direct visual tool in understanding the chromatin structures of a particular region. In fact, the “beads-on-string” model of nucleosome arrangement was first confirmed by this method (Olins and Olins, 1974). In this approch, chromatin liberated from purified nuclei is first fixed with gluraldehyde, applied to a

glow-discharged carbon film and observed by electron microscopy (Woodcock and Horowitz, 1997; Woodcock and Horowitz, 1998). By using EM along with Minichromosome Affinity Purification (MAP), Ducker et al were able to present a model of how the co-repressor Tup1p organizes repressed chromatin structure. Previous investigation showed that the **a**-cell specific gene *STE6* is repressed in α cells where it is covered by nucleosome arrays. And for each positioned nucleosome there are two molecules of the co-repressor Tup1p binding to it (Ducker and Simpson, 2000). The EM examination of the *STE6* minichromosome in α cells revealed a condensed hairpin structure which is relaxed when the gene is expressed in **a** cells (Ducker and Simpson, unpublished). The result leads to the hypothesis that Tup1p interacted with the histone tails of both H3 and H4 in a cross-over fashion to pack the gene into condensed chromatin structure which is inaccessible for transcription.

Though widely applied, these traditional mapping methods have their limitations in illustrating dynamic chromatin structure in living cells. Since the nuclei prep takes as long as 4 hours and undergoes various purification steps, the data generated after that may not reflect the native chromatin structure or its *bona fide* protein partners. To this end, several methods were established in recent years, to name a few, Chromatin IP (ChIP), *in vivo* endonuclease mapping and directed visualization of chromatin dynamics. All of these approaches avoid the nuclei isolation step used in traditional mapping thus better preserving the native protein-DNA binding information.

1.4.3 Expressing endonuclease in living cells

Expressing endonucleases in living cells and let them digest chromatin in vivo is advantageous in that it gets around the long process of nuclei isolation. Our lab, as well as others, has tried to introduce various enzymes into the yeast cells. Some examples include DNA methylase (Kladde et al., 1999b; Xu et al., 1998), DNase I (Wang and Simpson, 2001) and restriction enzymes (Mai et al., 2000).

Since the yeast genome is naturally unmethylated, expressing foreign DNA methyltransferases (MTases) enables the study of chromatin structure *in vivo*. However, since its target sites in yeast is limited, the resolution of this mapping method is low (Kladde et al., 1999a; Kladde et al., 1999b). To solve this problem, a bacterial cytosine-5-DNA methyltransferase with smaller and more frequent recognition sites was introduced into yeast and showed some potential in chromatin mapping (Xu et al., 1998). Similarly, a restriction enzyme *HinfI* has also been expressed in yeast under the control of inducible promoter (Iyer and Struhl, 1995). This system has been used to examine the chromatin structure on the *HIS3* promoter under physiological conditions (Iyer and Struhl, 1995; Mai et al., 2000). However, this method is also limited by the availability of recognition sites.

Wang et al have introduced the bovine DNase I gene into yeast cells. And since the gene is under control of an inducible galactose promoter, active DNase I can digest the chromatin under its native context for a very short time. Therefore the data collected in this experiment will better represent the chromatin structure *in vivo*. Indeed, using this technique, they were able to discover different protection patterns of several chromatin domains compared to *in vitro* DNase mapping. For instance, the binding of α2p to the RE

is detected by this method but not by traditional mapping of isolated nuclei, probably because of the short half life of α2p (Wang and Simpson, 2001).

1.4.4 Chromatin Immuno-precipitation (ChIP)

The ChIP assay has been widely used to study the interaction of proteins and DNA in its native chromatin context. The first step of this method is to fix cells with formaldehyde so that the endogenous association of the protein and DNA is preserved. The cells are then lysed to release the chromatin which is afterward sonicated into small fragments. Presumably all proteins associated with the native chromatin are still attached to it at this stage. The DNA fragment containing the binding site of a specific protein is purified by immunoprecipitation with antibody against that protein. The cross-link between the DNA and protein is then reversed so that the DNA fragments can be purified and analyzed by quantitative PCR (Hecht et al., 1999; Orlando, 2000).

The major advantage of this method is that it "freezes" the cells very quickly and allows the examination of the dynamic interaction of a specific protein with a certain segment of DNA in the exact time of interest. It can also determine the contact region with relative good resolution (about 500bp). Moreover, the use of different antibodies against the various modification of a protein makes it possible to explore the relations between protein function and its modification state. For example, ChIP assays showed that different forms of histone modifications were linked with the different expression status of genes. This is the foundation of the "histone code" theory (Jenuwein and Allis, 2001; Rea et al., 2000).

Intriguingly, ChIP allows us to monitor protein binding at various DNA segments at different stages of a cellular event. This can elucidate the intricate dynamics and synchronization of the protein participants that regulate the cellular process. One example is the repair of DNA damage caused by *HO* cleavage. Right after the generation of DSB near the *MAT* locus, many proteins are found to be cross-linked to it. For instance, both yKu80p and Sir4p are shown to leave the telomere and relocalize to DSB (Martin et al., 1999). In addition, rapid γ-H2A formation are detected in this region upon *HO* cleavage which then recruits the INO80 complex (van Attikum et al., 2004). The Rad protein family involved in recombination is also associated with the DSB (Morrison et al., 2004; Unal et al., 2004). This information provides an overview of importance of DSB binding factors. And more significantly, it may indicate how the regulators interact with each other to promote the DNA repair in yeast cells.

The ChIP method has become even more powerful when combined with the microarray (genome chip) technique (Lieb, 2003). The ChIP on chip approach makes possible a genome wide analysis of protein-DNA interaction. With the whole genome sequences of more than one organisms becoming available (such as yeast, fly, mouse and chicken), this method provides the potential to reveal every binding site of any protein of interest. Exploiting ChIP-chip led to the intriguing finding of a genome wide phenomenon that histones are depleted in the promoter region of almost all actively transcribed gene (Lee et al., 2004).

On the other hand, there are also some drawbacks of the ChIP. First, it can only detect the binding site of known protein. Second, it may not completely represent the *in vivo*

protein-DNA association, because in this method, the detection of the target DNA sequence is completely depend on the interaction between the specific protein, presumably remain bound after the purification, and the antibody raised against it. This reaction can be affected by many factors such as the intensity of the formaldehyde cross-linking, the quality of the antibody or binding condition of the protein and antibody.

1.4.5 Direct visualization of chromatin

Lately the development of a new method enables us to directly visualize chromatin organization and its dynamic morphological changes in living cells. This system uses tandem repetition (several hundreds) of the *lac* operators to tag the DNA region of interest. The operator array is detected by the interaction of the *lac* operator and its green fluorescent protein (GFP) labeled repressor, which is introduced to cells by micro-injection (Belmont, 2001; Tsukamoto et al., 2000).

At present, this technique has been successfully applied to many organisms from prokaryotic, yeast, to fly and mammalian cells. Its ability to directly visualize gene expression in living cells provides a powerful system to study the dynamics of chromatin architecture, transcription, cell division, and DNA repair. For instance, Spector's group reported that chromatin undergoes a structural change from condensed to more open upon gene activation, indicating the role chromatin structure played in gene regulation (Tsukamoto et al., 2000). Also using this method, Gasser's lab was able to study the detailed subnuclear localization of the telomere and how factors like the Sir2p, Ku80p and Esc1p affect the tethering of the telomeres (Taddei and Gasser, 2004; Taddei et al., 2004). Most intriguingly, Bressan and colleagues applied this method to investigate the

behavior of *HML*, *HMR* and the *MAT* loci during yeast mating type switching. Their data showed that the movement of *HML* locus in α cells or in RE deleted **a** cells is more constrained which is consistent with the established theory that without a functional RE, *HML* is inaccessible for recombination (Bressan et al., 2004).

CHAPTER II IDENTIFYING PROTEINS THAT BIND TO THE RECOMBINATION ENHANCER USING MINICHROMOSOME AFFINITY PURIFICATION (MAP) AND MASS-SPECTROMETRY

Abstract:

To isolate the protein-DNA complex in its native chromatin context, minichromosome affinity purification (MAP) has been developed in our lab. The minichromosome is an artificial vector that can be kept as an episome in yeast cells. It contains three main elements: an autonomous replication sequence (ARS), a *TRP1* selection marker and a bacteria *lac* promoter. Minichromosomes can be assembled naturally into nucleosomes in yeast cells. The original MAP procedure is a single step affinity purification based on the strong interaction between the *lac* promoter DNA and its binding protein *lac*I/Z repressor. Crude extracts of minichromosome were passed through a chitin column charged with *lac* repressor and retained in the beads. Minichromosome bound beads were then extensively washed to eliminate non-specific protein binding. Finally, the minichromosome complex is eluted by adding IPTG to the column to dissociate the binding of *lac* operator and the *lacI-Z* repressor under appropriate ionic strength.

In this study, the original MAP method was used as a tool to investigate novel proteins factors that bind to the recombination enhancer (RE). A 1.5Kb DNA fragment of the RE region, which contains two Mcm1p/α2p binding sites were cloned into the minichromosome backbone. We also inserted a ~400bp insulator sequence between the RE and the selection marker *TRP1* in order to achieve efficient transformation in α cells. Different binding and eluting situations have been tested to optimize the purification and promote the specificity of protein binding. We also attempted to further purify the minichromosome complex by chromatography and sucrose gradient.

Protein components of the RE minichromosome isolated from either **a** or α cells are analyzed by two types of mass-spectrometry: the MALDI-MS or the Mud-PIT. From MALDI-MS approach, we identified a DNA repair protein yKu80p which associates with the RE only in **a** cells. On the other hand, Mud-PIT presented a broader view of proteins controlling the whole minichromosome activity. Besides RE regulators, we also detected proteins involved in gene regulation and insulator function.

2.1 Introduction

2.1.1 Identification of DNA binding proteins

2.1.1.1 One hybrid system

Yeast one hybrid system is a powerful tool than can be used to discover proteins that interact with a special DNA sequence (Sieweke, 2000). In this method, the yeast protein expression library is fused to a Gal4 activation domain (Gal4-AD). The potential interaction of a DNA binding protein with its regulatory elements will tether the Gal4-AD to a *HIS3* reporter gene and activate its expression as a selective marker (Liao and Fang, 2000). The method has been applied to identify proteins that interact with the RE. By transforming the yeast expression library to a *MAT***a** strain that carries an integrated genomic copy of partial RE sequences upstream of a *HIS3* reporter, McCray et al. were able to identify several proteins that bound to different regions of the RE and potentially regulated its function (McCray and RTS, unpublished).

2.1.1.2 Minichromosome Affinity Purification (MAP)

Minichromosomes provided a convenient system to study chromatin structure because they are stably packaged, maintained as native chromatin and are also easily manipulated (Dean et al., 1989). It is especially useful to examine the structure and composition of a DNA segment in different functional states. In yeast cells, the minichromosome usually exists in multicopies (Ducker and Simpson, 2000). In addition, each minichromosome contains an Autonomous Replicating Sequence (ARS). This

replication origin allows the minichromosome to replicate in yeast cells as an autosome. A previous study has shown that the ARS sequence can be dissected into four sub domains and some are not essential for replication (Marahrens and Stillman, 1992). This finding implies that a DNA sequence could be inserted in this region without sacrificing the minichromosome copy numbers. An *E coli lac* operator was placed between the ARS element B2 and B3 for the purpose of affinity purification (Simpson et al., 2004). The minichromosome backbone also contains a gene for *N*-phosphoribosylanthranilate isomerase (*TRP1*) which can be used as a selection marker in when transforming the minichromosome into yeast cells.

The chromatin structure of the minichromosome is well studied (Simpson et al., 2004). There are four loosely positioned nucleosomes on the *TRP1* coding sequence. Another three precisely positioned nucleosomes cover the remainder of the vector. In between of these two organized chromatin structures are two ~100bp nucleosome free regions. We created a multi-linker cloning site in one of them that located downstream of *TRP1*. This linker will be convenient for introducing a DNA segment of interest into the minichromosome (Ducker and Simpson, 2000).

The minichromosome affinity purification (MAP), initially developed by Dean and Simpson (Dean et al., 1989), is based on the strong interaction between the lac promoter and its repressor. The recombinant protein is designed with *N*-LacI/Z repressor and C-chitin binding domain with self-cleaving intein domain in the middle. Upon expression, this fusion protein binds to the chitin matrix and provides an interface for minichromosome binding.

As illustrated in Fig. 2.1, cells carrying minichromosomes were lysed by Zymolyase and homogenized. The minichromosome, along with proteins binding to it, is allowed to passively diffuse out of the nuclear membrane. The precleared supernatant containing minichromosomes is incubated with the *lac* repressor charged chitin beads. After intensive washing to get rid of non-specific binding contaminant, the minichromosome is eluted with IPTG in 300mM NaCl which dissociates the interaction between the *lac* promoter and its repressor.

Since its establishment, MAP has been applied questions about chromosome components and structure as well as gene regulation (Ducker and Simpson, 2000; Morse et al., 1987; Roth et al., 1992; Simpson, 1990). For instance, MAP can be used to determine the stoichiometry of proteins interacting with a particular DNA segment. By MAP and quantitative western blotting, Ducker et al has found that the **a**-specific gene *STE6*, when repressed, is assembled into organized chromatin. In addition, an essential repressor of this gene, Tup1p, bound with a protein/nucleosome ratio of 2:1 (Ducker and Simpson, 2000). Moreover, when coupled with electronic microscopy (EM), MAP enables us to directly visualize the 3-D chromatin structure of a DNA section. Under EM, the *STE6* minichromosome showed a unique condensed hairpin structure, perhaps stabilized by the interaction of Tup1p and histone tails (Ducker and Simpson, unpublished).

2.1.2 Protein identification by mass spectrometry

Mass spectrometry provides a very powerful tool to identify proteins in a biological mixture. The principle of this method is to classify proteins based on their unique mass-

to-charge ratios (Ferguson and Smith, 2003). This technology is applied to not only pre-purified proteins (Neverova and Van Eyk, 2005) but also proteomic samples such as whole cell extract (Washburn et al., 2001).

The Mass spectrometer can be divided into three fundamental parts, namely the ionisation source, the analyser, and the detector (Ferguson and Smith, 2003). Protein or protein mixtures are first digested with trypsin or other proteases to generate short peptides. They are then introduced to the ionization source and blasted with electrons which turns them into positively charged ions. As the ions continue through the MS, they travel through the analyzer: an electromagnetic field that filters the ions based on mass-to-charge ratios. The filter continuously scans through the range of masses as the stream of ions come from the ion source. Then a detector counts the number of ions with a specific mass. This information is sent to a computer and a mass spectrum is created. The mass spectrum is a graph of the number of ions with different masses that traveled through the filter. By comparing the peptide fragment fingerprints to a database, proteins in the mixture can be identified (Ferguson and Smith, 2003; Liebler, 2002).

In this study, two mass spectrometry approaches were used: Matrix-Assisted Laser Desorption-Ionisation Mass Spectrometry (MALDI-MS) and Multi-dimensional Protein Identification Technology (Mud-PIT).

2.1.2.1 MALDI-MS

The Matrix-Assisted Laser Desorption-Ionisation Mass Spectrometry (MALDI-MS) was a commonly used method when this project was started (Corona and Toffoli, 2004). In this method, isolated proteins, presumably with high purity and less complexity, are digested with trypsin and co-crystallized with a UV-absorbing matrix compound. The

matrix plays a key role in allowing efficient and directed energy transfer during a laser-induced desorption event which provides high ion yields and produces data with high accuracy and sensitivity.

2.1.2.2 Mud-PIT

A new technology Multi-dimensional Protein Identification Technology (Mud-PIT) was first developed in the Yates' lab and it enables us to analyze the proteome in a larger scale and with more complexity (Link et al., 1999). After digestion with trypsin, proteins samples are subjected to multidimensional liquid chromatography (LC) to fractionate the peptide mixture which is then continuously applied to tandem mass spectrometry (MS/MS) to separate and fragment peptides. The data collected was linked to a powerful analytic tool: the SEQUEST algorithm which relies upon translated genomic sequences to identify amino acid sequences from the fragment ions (Yates et al., 1995) . This method proved to be a rapid and sensitive process for comprehensively identifying proteins in macromolecular complexes. For example, a total of 1,484 proteins were identified from yeast BJ5460 cells. More importantly, this method appears to be unbiased in detecting the presence of proteins of very low abundance or with extreme pI or molecular weight (Washburn et al., 2001).

In this study, we used the minichromosome purification combined with mass spectrometry to identify and characterize proteins that bind to the RE and regulate its function. A 1.5Kb DNA fragment of the RE region was cloned into the minichromosome backbone. Different binding and eluting situations have been tested to optimize the purification and promote the specificity of protein binding. Protein components of the RE minichromosome isolated from either **a** or α cells are analyzed by two types of mass-

spectrometry: the MALDI-MS or the Mud-PIT. From the MALDI-MS approach, we identified a DNA repair protein yKu80p which associates with the RE only in **a** cells. In addition, Mud-PIT presented a broader view of proteins controlling the whole minichromosome activity.

2.2 Materials and methods

2.2.1 Plasmid construction

The ALT minichromosome backbone used in this study is described previously (Ducker and Simpson, 2000). A 1.5Kb RE segment flanked by two Mcm1p/α2p binding sites was PCR amplified and cloned into the SacII site in the multi-linker region. A ~400bp tRNA gene, a published insulator (Donze et al., 1999), was inserted between the α2p binding site and the *TRP1* gene using a *EcoRI* restriction site. The plasmid was then digested with *SphI* to remove the bacterial sequence and transformed to yeast.

2.2.2 Cell growth and media

Synthetic medium containing the appropriate supplements was used to select and maintain the*TRP1* minichromosome. For minichromosome purification, cells were allowed to grow in YPD (2% dextrose) media until OD600 reached 1.0-1.2.

2.2.3 *lac* repressor affinity column

Bacteria strain pTLIZ which contains the LacI/Z-intein-CBD gene was grown in 2XYT media to OD600 of0.6-0.8 with 100μg/ml ampicillin for selection. The culture was cooled on ice for 15 minutes. IPTG was added to a final concentration of 40μM to induce the expression of the fusion protein at 15°C overnight. Cells were harvested by centrifugation using Sorvall GS-3 rotor at 5000 rpm for 10 minutes at 4°C. The bacteria was then lysed in chitin column buffer (CCB: 20mM HEPES, 1mM EDTA, 0.1% Tween 20 and 500mM NaCl) by sonication. The condition we used is 6 times 10-second burst at duty cycle of 50% at setting 4 in a Branson Ultrasonic machine. Soluble proteins were then cleared by centrifugation using a Sorvall SS-34 rotor at 12,000 rpm for 20 minutes at

4°C. The supernatant was mixed with chitin beads (NEB) and incubated for 1 hour at 4°C. They were loaded to the column and packed by gravity flow. The column was washed by 10 volumes of CCB followed by 5 volumes minichromosome binding buffer (MBB: 20mM HEPES, 1mM EDTA, 0.1% Tween 20, 5mM MgCl2, 5mM KCl). The quality of the affinity column was tested by the β-galactosidase activity of the resin. 1μl resin and 5μl flowthrough were mixed with 1ml Z buffer (60mM Na_2HPO_4, 40mM NaH_2PO_4, 10mM KCl, 1mM $MgSO_4$**,** and 5mM β-mercaptoethanol) and incubated at 28°C for 5 minutes. 200μl 4mg/ml ONPG were added to the mixture and incubated in 28°C for 5-10 seconds. Reaction was stopped by adding 500μl 1M Na_2CO_3. The β-galactosidase activity was measured by the OD 420nm of the final product.

2.2.4 Minichromosome affinity purification

The minichromosome was isolated as previously described, but with some additional modifications (Ducker and Simpson, 2000). Yeast cells carrying the RE minichromosome were collected at OD600 of 0.8-1.0 by centrifugation. The cells were then treated with 0.5mg/ml Zymolyase (Seikagaku, 100T) at 30°C for 15 minutes. The formation of spheroplasts was determined microscopically. The spheroplasts were then gently wash twice with 30ml sorbitol buffer [1.4M sorbitol; 20mM HEPES, pH8.0; 5mM MgCl and 5mM KCl] and resuspended in 10ml minichromosome binding buffer (MBB) [20mM HEPES, pH 8.0; 1mM EDTA; 150mM NaCl and 0.1% Tween20] plus complete protease inhibitors [10ug/ml A-protinin; 2ug/ml Pepstatin A; 2ug/ml Leupeptin and 1mM PMSF]. After chilling on ice for 15 minutes, the spheroplasts were homogenized in a Thomas® glass homogenizer and a Telflon motor driven pestle with six strokes. Minichromosomes were allowed to passively diffuse out of the nuclei by putting the

lysate on ice for three hours with occasional agitation. The lysate was then clarified by centrifugation at 4°C for 20 minutes at 40,000g using a Sorvall SS-34 rotor. The supernatants were then collected and loaded onto the *lac*I-Z affinity column described above (Ducker and Simpson, 2000; Ercan and Simpson, 2004).

2.2.5 Protein separation and mass spectrometry

The minichromosome samples purified from the affinity column were concentrated using Amicon protein concentrators with a cutoff range of 30 kDa. The concentrated proteins were resolved by 10% SDS-PAGE electrophoresis. The amount of sample loaded on the gel was normalized according to its minichromosome DNA content which is determined by Southern blotting using a probe to detect the lac operator. All the protein components of the minichromosome were visualized by silver stain.

For the MALDI-MS analysis, a protein band around 75KDa was excised, digested with trypsin and sent to the Mass-Spectrometry facility at Penn State University. For Mud-PIT analysis, the RE minichromosome elution from the affinity column was concentrated, treated with benzonase to remove DNA contaminants, precipitated with TCA and sent to the mass spectrometry facility in the Stowers Institute of Medical Research.

2.3 Results

2.3.1 Minichromosome construction and the introduction of insulator

To identify and characterize novel proteins that bind to the RE, I cloned a ~1.5 kb DNA segment (29192-30612) containing the conserved C, D and part of the E regions into the minichromosome pALT backbone (Fig. 2.2) at the HSR B site (Ducker and Simpson, 2000). In this segment of DNA, there are several domains that are important for RE function including a Mcm1p binding site in the C domain. A two base pair mutation of this site completely inactivates the RE. The tandem repeats of TTT(G/A) in the D region have also been shown to be necessary for the function of RE (Wu et al., 1998). The 1.5kb DNA sequence also included another Mcm1p/α2p binding site located in the E domain which might regulate the RE activity (Szeto et al., 1997).

The new construct pRE-ALT was digested with *SphI* to eliminate bacterial sequences. The remaining portion was then circularized and used to transform **a (**YPH499) and α (YPH500) cells. Positive clones were selected on *trp*- synthetic media and further confirmed by Southern blotting using probe that detected the *lac* operator.

My first attempt to introduce the RE minichromosome pALTRE to **a** cells was successful. However, I could not get any *TRP1* prototrophic α cells despite several tries. Since our minichromosome construct contains a Mcm1p/α2p binding site that is located upstream of the selection marker, *TRP1*, it is possible that in α cells, the binding of α2p to this site may initiate repressed chromatin structure to spread into the *TRP1* promoter thus interfering with its expression.

To avoid this potential complication, we decided to place a well characterized insulator DNA segment between the Mcm1p binding site and *TRP1* gene. The insulator sequence is a ~400bp tRNA gene near the E silencer of the *HMR* which has been shown to be sufficient to block the spread of silenced chromatin (Donze et al., 1999). Indeed, pTAIR, which contain the insulator insertion was successfully introduced into both **a** and α cells with similar efficiency.

2.3.2 Minichromosome affinity purification

The *lac*I/Z affinity column was made as described in Materials and Methods. The final quality of the column was monitored by measuring the β-galactosidase activity of both the charged resin and the flowthrough. By comparing the OD420 of both of samples, I concluded that about 30% of the total fusion protein activity is associated with the chitin matrix. In addition, the bead bound fusion protein is close to 90% homogeneity based on Coomassie stain of the SDS-PAGE gel.

Minichromosome affinity purification was carried out as previously described (Ducker and Simpson, 2000) with a few modifications. 6L of yeast cells were grown to OD of 1 and collected by centrifugation. After Zymolyase treatment, cells were homogenized to release nuclei. Minichromosomes were then allowed to diffuse passively from the nuclei on ice and subsequently loaded onto a *Lac* I-Z affinity column. After extensive washing, minichromosomes were eluted with 300 mM NaCl and 1mM IPTG. To monitor the quality of the purification, minichromosome DNA was checked on 1% agarose gel, stained with ethedium bromide and further quantified by Southern blotting. A TRP/ARS (TA) probe was used in the Southern analysis to determine the copy number of the minichromosome. This probe detected both the full sequence of *TRP1* in the

minichromosome and genomic *TRP1* gene which contains a 0.6 kb deletion in the coding area. Since we know that a haploid yeast cell only has one genomic copy of this gene, by comparing the intensity of the signal of both loci, the average copy number of minichromosomes can be determined. In conclusion, there are about twenty copies of pTAIR minichromosome per cell in both **a** and α cells.

Since we introduced about twenty copies of the RE minichromosome per cell, it is important to know whether the RE segment is still maintained as the native genomic copy. We addressed this question by high resolution MNase mapping. The minichromosome eluate was digested with MNase. Consequently DNA was purified and subjected to primer extension analysis. The primer used in this study is so designed as to anneal to only minichromosomal but not the genomic RE region. As shown in Fig. 2.3, the local chromatin structure of the minichromosomal RE is very similar to that of the genomic copy compared to previously published data (Weiss and Simpson, 1997). This assured us that protein factors which bind to the RE and regulate its structure and function in native state should still be associated with it in isolated minichromosome.

2.3.3 Using mass spectrometry to identify proteins that bind to RE

According to the unique chromatin structure of the RE, our initial goal was to identify protein regulators that specifically bound to the active RE in **a** cells. To compare the different components of the RE between mating types, proteins bound to the RE minichromosome isolated from both **a** and α cells were concentrated using Amicon protein concentrator, resolved by a 11% SDS-PAGE gel and visualized by silver staining. As shown in Fig. 2.4A, a prominent ~75 Kd band presented only in the **a** cells sample but

not that of the α cells. This band was subsequently excised, trypsinized, and subjected to MALDI-MS analysis.

The collected peptide mass peak information was imported to ExPASy Proteomics Server online and analyzed using Swiss-Prot protein sequence database for protein identification. We found seven peptide hits matched that of the yKu80p (Fig 2.4B), the yeast homolog of human DNA repair protein Ku80. The functional study of yKu80p in RE regulation will be the main focus in Chapter III.

One of the drawbacks of this method is that it requires pre-separation of the protein mixture by 1D or 2D gels. In some cases the protein band of interest has to be identified visually, excised and its content extracted from the polyacrylamide gel matrix. Bedsides being time consuming, this procedure could also be biased since it omits proteins of low concentration or extreme pI which can not be detected by silver stain. Moreover, eluting the proteins from the gel could also cause sample loss.

2.3.4 Further purification of the minichromosome by chromatography or gradient

To circumvent the drawbacks of MALDI-MS and to identify the whole protein repertoire associated with the RE minichromosome, we decided to take the advantage of Mud-PIT approach. However, for this method, the purity of the minichromosome samples needed to be further addressed.

MAP approach is based on the affinity interaction between the *lac* operator and its repressor. This single step approach can achieve up to10,000 fold purification (Simpson et al., 2004). Nonetheless, the final elution still gives rise to multiple protein bands in silver staining (Fig. 2.9) which might indicate non-specific binding. Consequently, if directly applied to Mud-PIT these contaminants could obscure the real difference

between two samples. Therefore, we further purified the minichromosome after the affinity column to ensure the accuracy of the Mud-PIT result.

2.3.4.1 Superose 6 chromatography

Superose 6 gel filtration column (Amersham Bioscience) separates macromolecules base on their sizes and shape. It was used in this study to remove the smaller RNA complex that co-elutes with the minichromosome complex by affinity purification (Simpson et al., 2004). Minichromosome eluates were concentrated by Amicon protein concentrator, loaded onto Superose 6 column and eluted with 500mM NaCl in MBB buffer. Forty 0.5ml fractions collected and 1% of which was subjected to DNA extraction and Southern blotting. Fig. 2.5A shows a minichromosome elution profile of superpose 6 column. We also monitored the elution of minichromosome by Southern blotting of DNA in each fraction using *lac* probe. The minichromosome containing fractions (13-19) were pooled and concentrated again. The protein components were then separated by 10% SDS-PAGE gel and visualized by silver staining (Fig. 2.5B).

Superose 6 chromatography was a convenient way to purify the minichromosome. By this method, the small RNA complex was separated from the minichromosome complex. However, to avoid non-specific protein binding to resin, we used 500mM NaCl in the buffer. The high ionic strength may potentially have disrupted some protein-DNA interactions.

2.3.4.2 Sucrose gradient supercentrifugaion

Sucrose gradient supercentrifugaiton is another system that separates proteins by molecular weight but under a milder condition. I used 15% to 40% sucrose buffer which contained 150mM NaCl. The gradient was poured using a gradient maker at 4°C and

chilled on ice for at least 30 minutes to achieve homogeneity. MAP purified minichromosome was concentrated using Amicon protein concentrator to 150μL and carefully loaded on top of the gradient. Minichromosome complexes were fractionated by centrifugation at 38,000 rpm using Ti 45 rotor at 4°C for 14 hours. Samples were collected from the bottom at 400μL per fraction and in most cases a total of 26 fractions were collected. 10% of each fraction was subjected to DNA extraction and Southern blotting to detect the minichromosome concentration (Fig. 2.6). A *lac* probe which detected the minichromosome *lac* promoter was used in this analysis. Three forms of the minichromosomes are detected using this probe, a supercoiled form, a nicked form and a linearized form. Those fractions containing minichromosome (11-15) were pooled and after concentration, subjected to SDS-PAGE electrophoresis and silver stain (Fig. 2.7).

Sucrose gradient supercentrifugation approach provides a gentler method to further purify minichromosome since it used a lower concentration of NaCl. However, as shown in Fig. 2.7, we found the final minichromosome complex yield was very low. This may be due to the several concentration/washing steps in this approach since the Amicom filter may retain part of the protein sample. In addition, the sucrose in the eluate interferes with the TCA precipitation, so we failed to obtain interpretable Mud-PIT results using this procedure.

2.3.5 Mud-PIT analysis

2.3.5.1 Monitoring the elution profile from the affinity column

Because of the results discussed above, we decided to optimize the eluting condition of the MAP for the Mud-PIT study. Since yKu80p has been proven to bind to RE, it could be used as an indicator for the quality of the purification. Step elutions were

preformed using increasing amount of salt and the protein constituent of the minichromosome monitored by silver stain (Fig. 2.8). Meanwhile, the yKu80p and minichromosome DNA in each fraction are also assessed by western blotting and Southern blotting, respectively. I decided to elute the minichromosome in 300mM NaCl because in this situation, the majority of minichromosome DNA and its *bona fide* protein partner yKu80p are recovered.

Proteins associated with affinity purified minichromosomes from both **a** and α cells were visualized by silver stain (Fig. 2.9). As indicated by arrows, we detected different protein components in the **a** and α RE minichromosome. Interestingly, most of the mating type specific bands appeared to be associated with the **a**-cell RE minichromosome. This result is not surprising since both the unique chromatin structure and the active function of the **a**-cell RE suggested the binding of unique proteins. Additionally, consistent with previous results, a protein migrating at about 75 Kd was found to specifically bind to the **a**-cell RE minichromosome.

The minichromosome samples were concentrated using Amicon protein concentrator, treated with benzonase and TCA precipitated. The protein pellet was sent to Mass-Spectrometry core facility in the Stowers Institute for Medical Research.

2.3.5.2 Mud-PIT analysis of the minichromosome sample

Since Mud-PIT possessed the ability to separate protein components in mixture and efficiently detected proteins of low abundance and extreme pI and molecular weight, we expected to find various proteins that may be involved in the regulation of not only RE function but also minichromosome maintenance (Table 2-1).

By exploiting Mud-PIT, we were able to detect about 100 protein partners of the RE minichromosomes and the majority of them associated with it in both **a** and α cells. We can categorize the majority of proteins into the following groups:

Histones, all H2A H2B H3 and H4 were detected with several peptide hits.

Pol II basal transcriptional machinery, most of its components including TFIID (Spt15p, Taf17p, Taf61p, Taf25p), PolII(Sin4p, Srb4p) and transcriptional factors TFIIA (Toa1p) have been identified which may be involved in the active transcription of the *TRP1*.

Pol III complex, we detect 9 components of Pol III (Rpc19p, Rpc11p, Rpc40p, Ret1p, Rpo31p, Rpc82p, Rpc34p, Rpc31p, Rpc37p) and subunits for TFIIIC (Tfc6p, Tfc7p, Tfc3p) in both **a** and α cells, which may reflect their involvement in insulator function as described by Donze et al (Donze and Kamakaka, 2001).

Replication proteins, Rfa1p, Rfa2p, Rfa3p, Mcm2p, Mcm3p, Mcm6p, Cdc46p, Cdc54p

Nucleosome modification complexes, We found several nucleosome modification complexes associated with the minichromosome, including INO80 (Ino80p, Arp5p, Arp4p, Arp8p, Act1p, Rvb1p, Rvb2p), FACT (Spt16p, Pob3p), RSC (Sth1, Rsc4p, Rsc5p, Rsc6p), SWI/SNF (Snf5p, Snf6p Swi3p Swi1p Arp7p), ISW (Isw1p, Loc2p, Itc1p), Ubiqitin ligase (Bre1p, Ige1), HIR (Hir1p, Hir2p, Hpc2p) and SAGA/SLIK(Rtg1p, Rtg2p, Rtg3p Spt20p, Ada2p, Hfi1p). Most remarkably, all the subunits of the INO80 complex have been identified in the Mud-PIT. These complexes might be involved in the active transcription of several genes including *TRP1* in the

minichromosome. In addition, they may have dual function related to RE regulation (see discussion in Chapter IV).

yKu70/80 and Rvb1/2, The main focus of this study is to identify the proteins that specifically associated with the active RE minichromosome. Consistent with MALDI-MS result, yKu80p and yKu70p have been identified to bind preferentially to the minichromosome isolated from **a** cells. In addition, Rvb1p and Rvb2p have also been identified.

Yeast Rvb ("RuVB"-like protein) proteins are homologs of bacteria RuVB family which has been shown to be involved in recombination and regulation of branch migration of the Holliday structure (Kurokawa et al., 1999). Its counterpart in yeast Rvb1p and Rvb2p, also participate in recombination and are important subunits of nucleosome modification complexes such as INO80 which has been shown to bind to the DSB and play an important role in DNA damage repair (Morrison et al., 2004; Shen et al., 2003a). The Rvb proteins also exist in SWR1 complex which catalyzes the replacement of H2A with histone variant Htz1 and is involved in establishing the boundaries of heterochromatin (Mizuguchi et al., 2004). There is another small complex that consists of only Rvb1p, Rvb2p and a protein called YHR034c although its function is not fully understood (Jonsson et al., 2004). This finding is consistent with our unpublished data (see Chapter IV). In three of five Mud-PIT analyses we performed, Rvb1p and Rvb2p, preferably associated with **a**-cell RE minichromosome. For the remaining two experiments, these two proteins also exist in the protein repertoire that binds to the α minichromosome, although in low abundance. At this point, we speculate

that Rvb1p may play a role in both transcription of *TRP1* and RE regulation which may explain its low abundance in α cells.

2.4 Discussion

In this study we used the minichromosome affinity purification combined with mass spectrometry to identify proteins that bind to the RE and contribute to its function. I cloned a 1.5kb fragment of RE into the ALT minichromosome backbone and the selection of such an RE segment is based on the following reasons: first, previous attempts to purify minichromosomes containing the essential 277bp RE alone were unsuccessful, likely due to extremely low copy numbers (Weiss and Simpson, unpublished); secondly, it has been shown that region A and B were dispensable to some degree for the RE function (Wu et al., 1998); lastly and most importantly, a second Mcm1p/α2 located in E region was also included in addition to the one that is located in the C region. Both sites may be important to establish the unique local chromatin structure that is crucial for the RE function (Szeto and Broach, 1997). In α cells, this 1.5 kb region is covered by nine positioned nucleosomes. In contrast, the local chromatin structure is more "open" in **a** cells as represented by the hypersensitive site and footprints (Weiss and Simpson, 1997).

To ensure efficient transformation of the minichromosome to the α cells, we had to insert an insulator sequence inbetween the α2p binding site and the *TRP1* gene. α2p has long been shown to possess the ability to organize nucleosome arrays and repress the transcription of **a**-specific gene such as *STE6* in α cells (Patterton and Simpson, 1994). To neutralize its effect, we chose an insulator tRNA gene which has been reported to stop the nucleosome spreading near *HMR* locus (Donze et al., 1999). Indeed, this segment of

DNA successfully protected the *TRP1* gene from α2p mediated repression and made it possible to introduce minichromosome into α cells.

The minichromosome affinity purification is a newly developed approach and there are several factors that could affect the final quality of the minichromosome. In an attempt to further optimize this method, I tried various conditions at different steps of the purification.

First, releasing the minichromosome from nuclei is a critical step which determines both the quality and yield of the purification. Since the minichromosome is a huge complex, higher detergent concentration in MBB might help relax the nuclear membrane and increase the yield. However, too much detergent may cause the nuclear membrane to dissolve which will increase the amount of genomic DNA in the mixture. To find a balance between these two scenarios, I tested the effect of two non-ionic detergents, Tween-20 and Triton X-100. I found that at 0.5%, both work similarly and there was very little genomic DNA in the final elute. However, when the detergent concentration increases to 2%, we saw little increase of minichromosome yield but a large amount of genomic contaminant emerged.

Another essential factor in this step is the NaCl concentration since high ionic strength may disrupt protein binding (Simpson et al., 2004). To this end, I lowered the concentration of NaCl in the buffer from 150mM to 50mM hoping to relax the minichromosome chromatin and facilitate the interaction of protein factors. However, I detected no difference in either the amount or the composition of the eluted proteins.

In addition, EDTA also plays an important role in minichromosome complex diffusion. EDTA depletes certain ions, such as magnesium, in the buffer. Therefore it

might disturb the association of some proteins with the minichromosome during the purification. In an attempt to preserve the minichromosome complex in its native physiological state, we substituted the 1mM EDTA in the MBB with 5mM MgCl and 5mM KCl to stabilize the minichromosome. This substitution did not affect the yield but might promote the calcium dependent binding of some proteins.

The binding of the minichromosome to the *lac* repressor matrix is a crucial step in this purification. To reduce the non-specific interactions between the proteins and chitin beads, I tested different incubation times and minichromosome/resin ratios. No significant difference in yield or protein components was detected in minichromosome samples that were incubated with the resin for either 1 hour or overnight. The minichromosome/resin ratio (up to 5mg total protein/ml resin) also did not seem to play an important role in promoting more specific binding of the protein and minichromosome.

To improve the quality of minichromosome for mass spectrometry, we further fractionated the affinity purified samples with either Superose 6 chromatography or sucrose gradient super-centrifugation. Both techniques to some extent separate the minichromosome complexes from contaminants such as small molecular weight RNA complex and genomic DNA. However, in the chromatography approach, the minichromosome was exposed to high ionic strength (500mM NaCl) which may disrupt the interactions of some proteins on the DNA target whereas in sucrose gradient purification, the final yield was lower. Moreover, the sucrose in the purified sample interfered with Mud-PIT analysis. Therefore, both approaches needed further optimization.

Using the MALDI-MS mass spectrometry, a protein that specifically interacts with the active RE minichromosome was identified. This protein, yKu80p, is the yeast homolog of human Ku proteins which are involved in DNA damage repair. Likewise, yKu80p has been shown to participate in various homologous recombination and DNA repair processes in yeast cell (Haber, 1999; Mages et al., 1996). The cellular function of yKu80p strongly implied a role in regulating the mating type switching. Its mechanism in this process will be discussed in Chapter III.

The Mud-PIT analysis gave us a comprehensive overview of the proteins that associate with the minichromosome. In this study, the results provided many potential candidates which apparently have a functional link with DNA repair and homologous recombination (Martin et al., 1999; van Attikum et al., 2004). These candidates are carefully pursued in future studies (See Chapter IV). In the mean time, to accurately identify the native minichromosome components, further optimization of the MAP approach is needed (See Chapter V).

Figure 2.1: Flow chart of the minichromosome affinity purification.

Red rings indicate the minichromosome backbone. Filled green circles represent nucleosomes. Lac repressor dimer is symbolized by yellow rods. After transforming into yeast cells, minichromosomes are assembled naturally into chromatin. The interaction between the *lac* operator and its repressor retains the minichromosomes in the column. After washing, minichromosomes are eluted with 300mM NaCl.

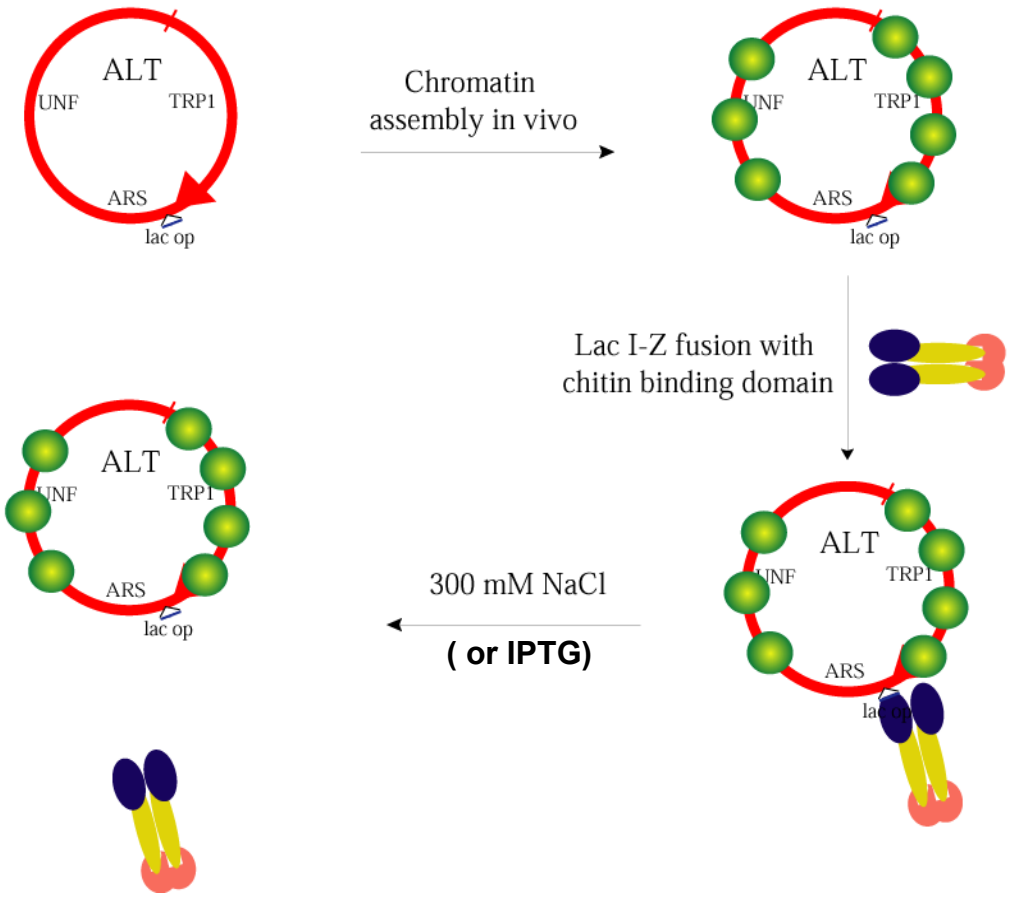

Figure 2.2: Minichromosome construct.

In the center is the TRP1/ARS1 backbone with filled light blue circles showing the positions of nucleosomes. The blue arrow represents the direction of transcription of the *TRP1* gene. A small blue ellipse shows the location of the *lac* operator. Expanded at the top are the RE inserts for the minichromosome used in this study. Patterned regions indicate the conserved domains of the RE. Insulator sequence is symbolized by red hexagon and the ARS region is indicated by red line.

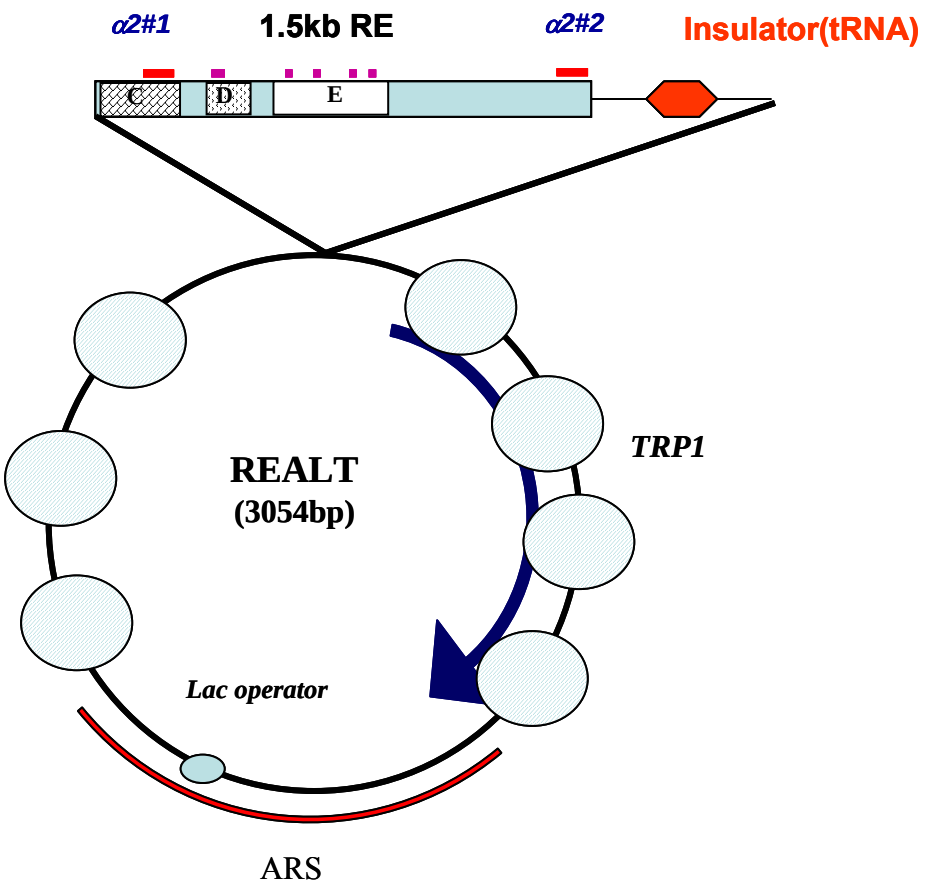

Figure 2.3: Chromatin structure of the RE region on minichromosome is similar to its genomic counterpart.

The chromatin structure of minichromosome isolated from **a** (YPH499) cells was mapped by primer extension analysis of micrococcal nuclease cleavage sites using primer c290. Solid gray and white rectangular boxes represent the location of the hypersensitive site and footprints, respectively. Lanes 1-3 represent minichromosome DNA digested with increased concentration of MNase. Lane 4 is a non-digested DNA control.

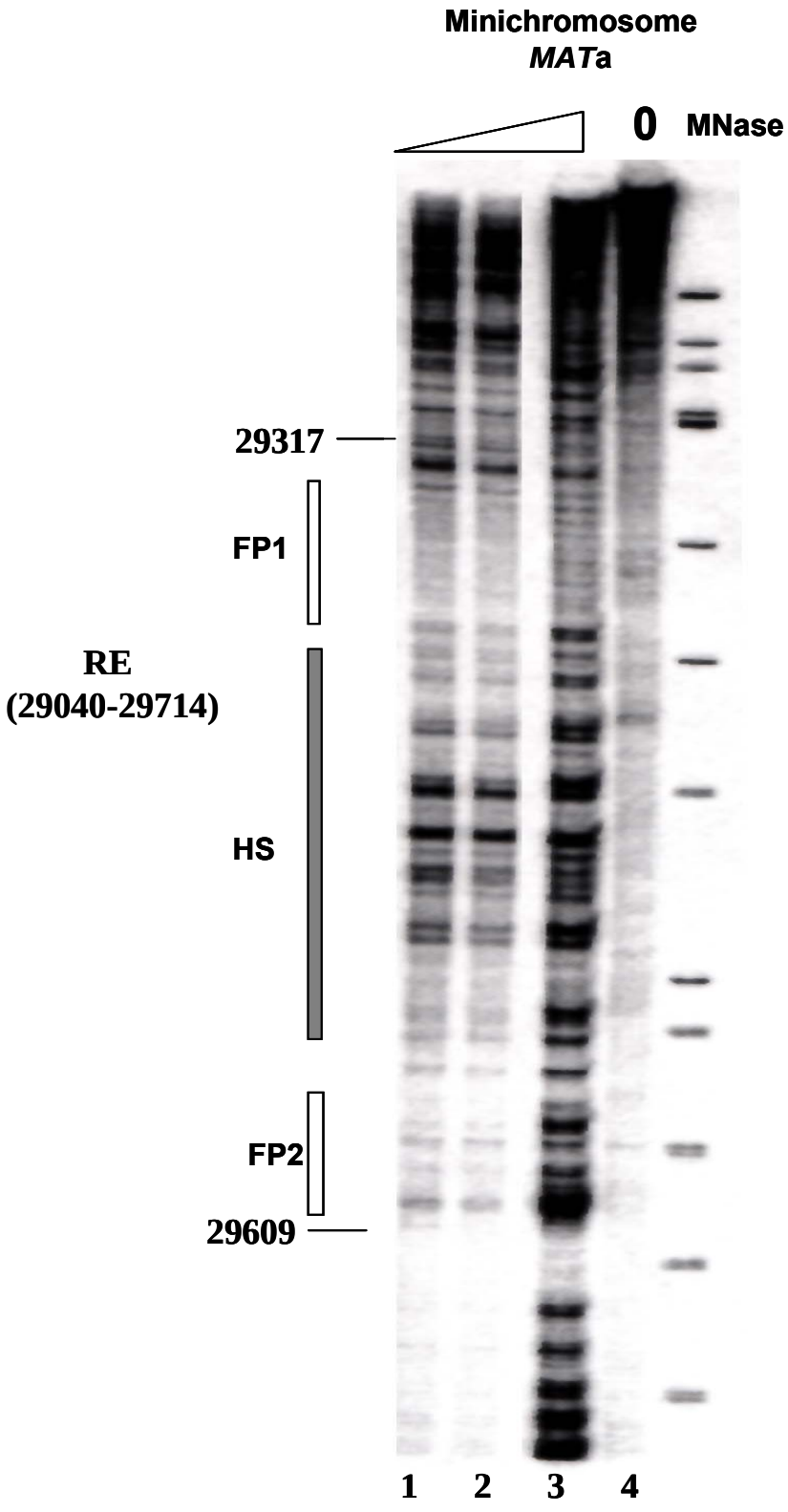
Minichromosome
MATa
0
MNase
29317
FP1
RE
(29040-29714)
HS
FP2
29609
1
2
3
4

Figure 2.4: Exploiting MAP and mass spectrometry to identify RE associating proteins.

(A) Proteins bound to the RE minichromosomes isolated from *MAT***a** cells (YCR101) (lane 2) or *MAT*α cells (YCR102) (lane 1), were separated on 10% SDS-PAGE gel and visualized with silver staining. The arrow indicates a ~75 Kd band that is present only in the *MAT***a** cell eluate but not in that from *MAT*α cells, thereby being excised and subjected to mass spectrometry. (B) Peptide sequences obtained from the mass-spectrometry of the indicated band are shown.

A.

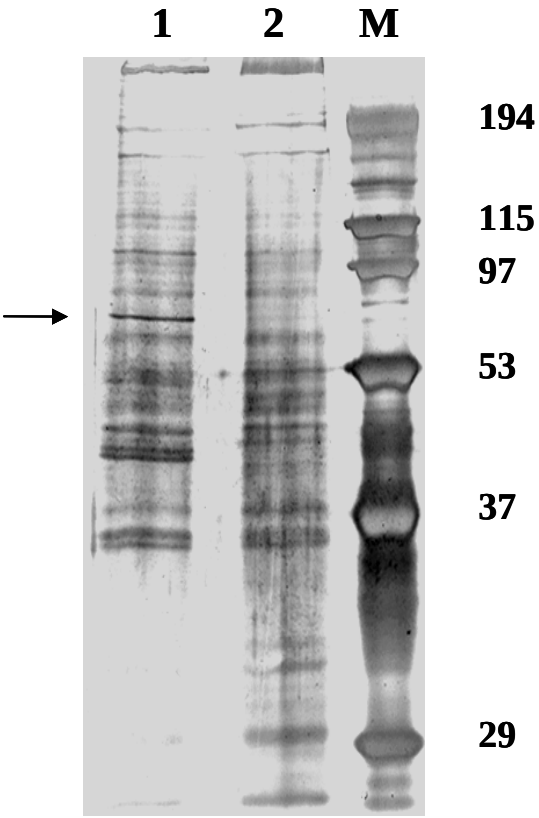

B.

```
     1         11         21         31         41         51
     |         |          |          |          |          |
  1 mssesttfiv dvspsmmknn nvsksmayle ytllnkskks rktdwiscyl ancpvsensq    60
 61 eipnvfqiqs flapvtttat igfikrlkqy cdqhshdssn eglqsmiqcl lvvsldikqq   120
121 fqarkilkqi vvftdnlddl ditdeeidll teelstriil idcgkdtqee rkksnwlklv   180
181 eaipnsrIYN MNELLVEITS PATSVVKPVR vfsgelrlga dilstqtsnp sgsmqdencl   240
241 cikVEAFPAT KAVSGLNRKt avevedsqkk eryvgvksii eyeihnegnk knvseddqsg   300
301 ssyipvtisk dsvtkayryg adyvvlpsvl vdqtvyesfp gldlrgflnr ealpryflts   360
361 essfitadtr lgcqsdlmaf salvdvmlen rkiavaryvs kkdsevnmca lcpvliehsn   420
421 insekKFVKS LTLCRLPFAE DERvtdfpkl ldrtttsgvp lkketdghqi delmeqfvds   480
481 mdtdelpeip lgnyyqpige vttdttlplp slnkdqeenk kdplriptvf vyrqqqvlle   540
541 wihqlminds refeipelpd slknkispyt hkkfdstkLV EVLGIKKVDK lkldselkte   600
601 lerekIPDLE TLLKRGEQHS Rgspnnsnn
```

Figure 2.5: Chromatography elution profile of minichromosome.

Affinity purified RE minichromosome was fractionated by Superose 6 column. (A) Chromatographic profile of minichromosome. Forty 0.5ml fractions were collected. The red and blue curves indicate UV absorption of 260nm and 280nm, respectively. (B) Silver staining of 10% pooled minichromosome eluate (fractions 13-19) separated by 10% SDS-PAGE.

A.

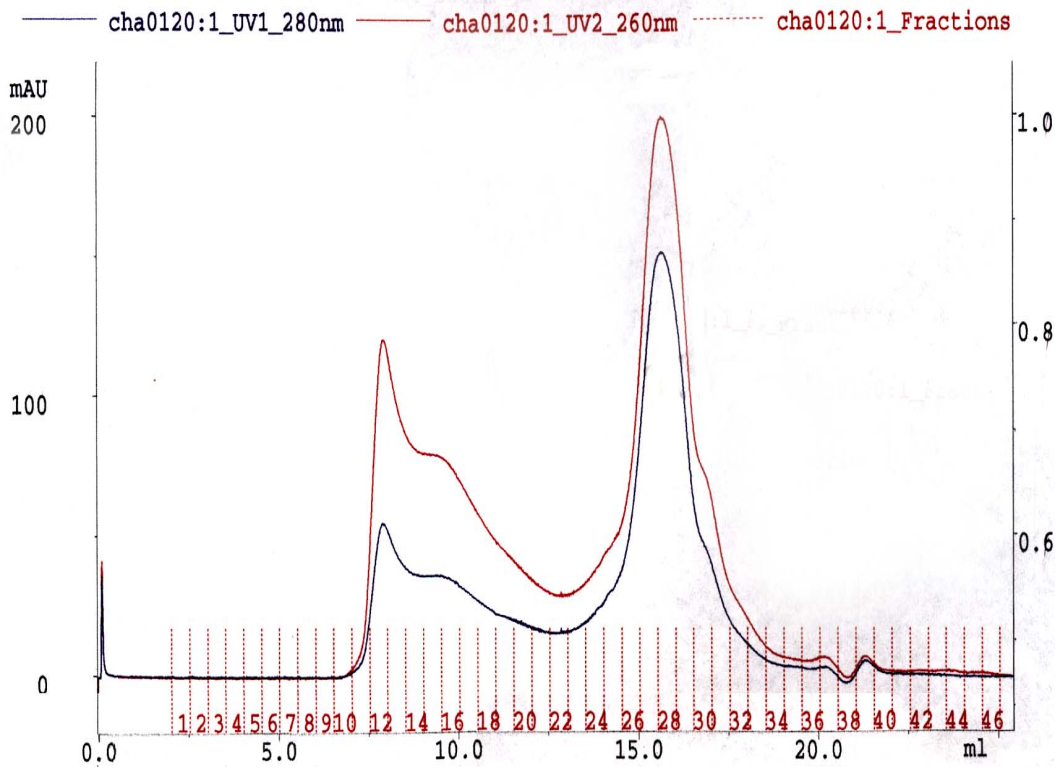

B.

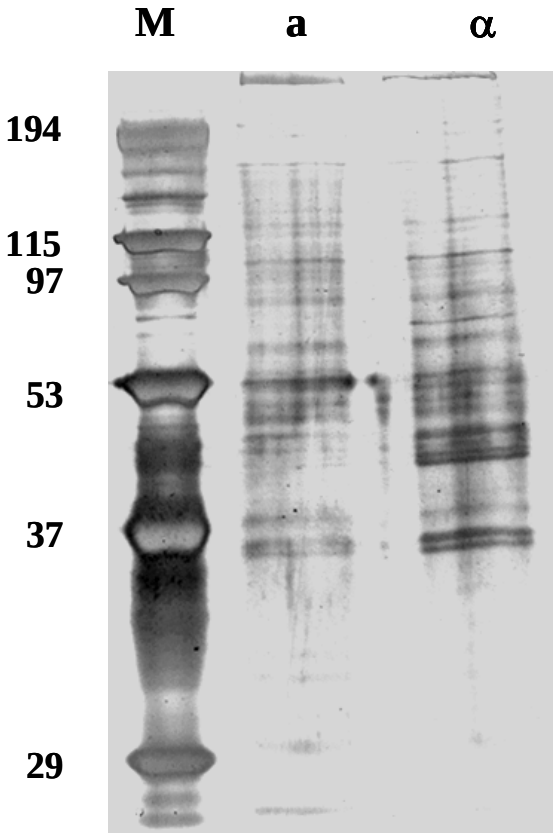

Figure 2.6: Sucrose gradient purification of minichromosome.

Minichromosome isolated from **a** (YPH499) and α (YPH500) cells by MAP were subjected to 10%-40% sucrose gradient supercentrifugation (see Materials and Methods). Twenty fractions from the bottom of the gradient were collected. 8% of the samples were subjected to DNA extraction and Southern blotting using *lac* oligos. The arrows indicate the two major forms of the minichromosomes detected by Southern blotting.

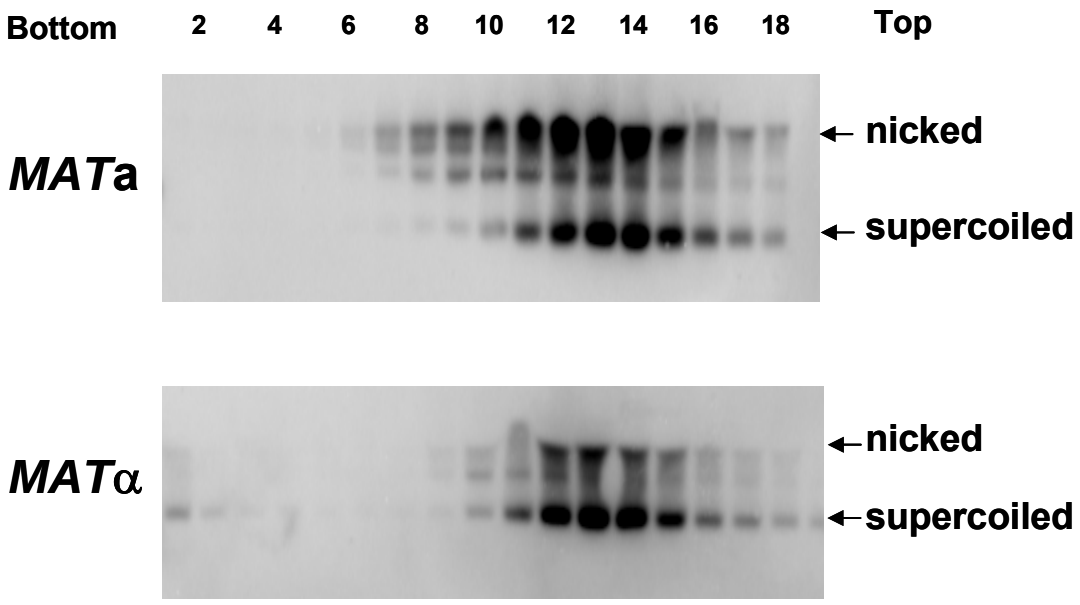

Figure 2.7: Proteins associated with the minichromosome after the sucrose gradient purification.

Proteins components of sucrose gradient purified RE minichromosome in **a** or α cells were pooled (fractions 11-15), separated by 11% SDS-PAGE and visualized by silver staining. Lanes 1-2 represent minichromosome isolated from **a** cells and lanes 3-4 represent minichromosome isolated from α cells.

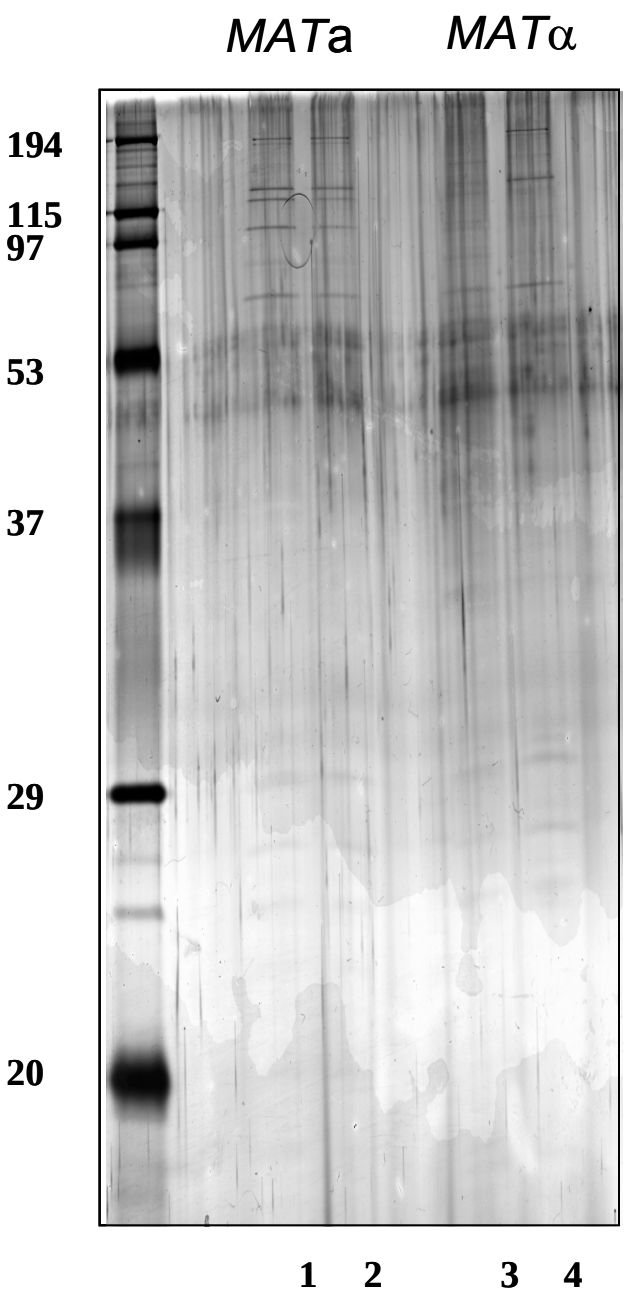
MATa
MATα
194
115
97
53
37
29
20
1
2
3
4

Figure 2.8: Step elutions of minichromosome from affinity column.

(A) Minichromosome binding to the affinity column was eluted with increasing NaCl concentration, as indicated at the top of the gel. Proteins associated with the RE minichromosome isolated in an **a** strain containing *myc*-tagged yKu80p (YCR501) were separated by 11% SDS-PAGE electrophoresis and visualized by silver staining. (B) Minichromosome DNA in each fraction was detected by Southern blotting using *lac* probe. (C) The presence of yKu80p in each fraction was assessed by western blotting of using anti *myc* antibody.

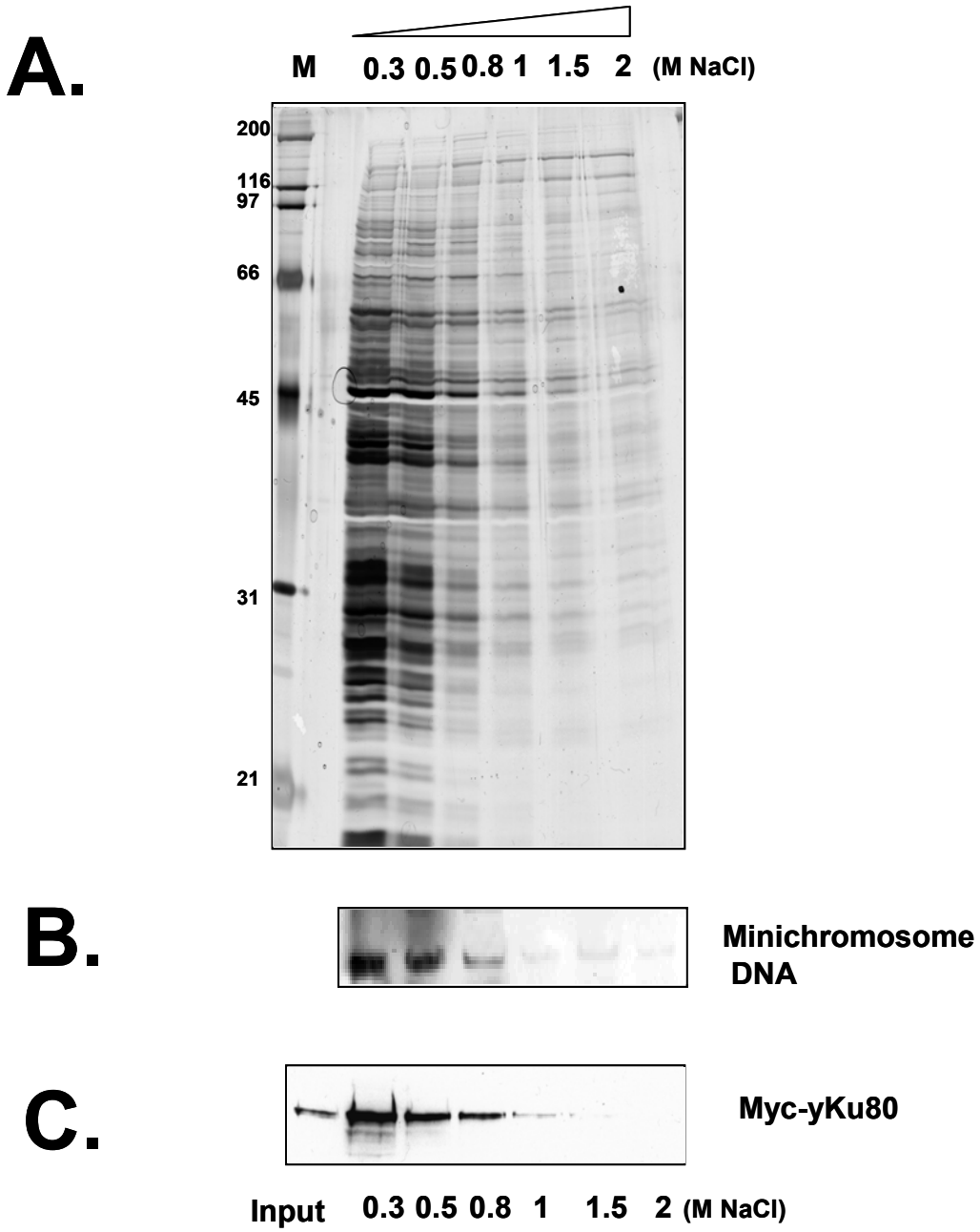
A.
M
0.3 0.5 0.8 1 1.5 2 (M NaCl)
200
116
97
66
45
31
21
B.
Minichromosome DNA
C.
Myc-yKu80
Input
0.3 0.5 0.8 1 1.5 2 (M NaCl)

Figure 2.9: Minichromosome associated proteins after affinity purification.

Proteins bound to the RE minichromosomes isolated from *MAT***a** cells (YCR101) or *MAT*α cells (YCR102) were separated on 11% SDS-PAGE gel and visualized by silver staining. As a control, we also include ALT minichromosome backbone isolated for **a** cells (YPH499). The arrows indicate proteins that bind specifically to either **a** or α RE minichromosomes.

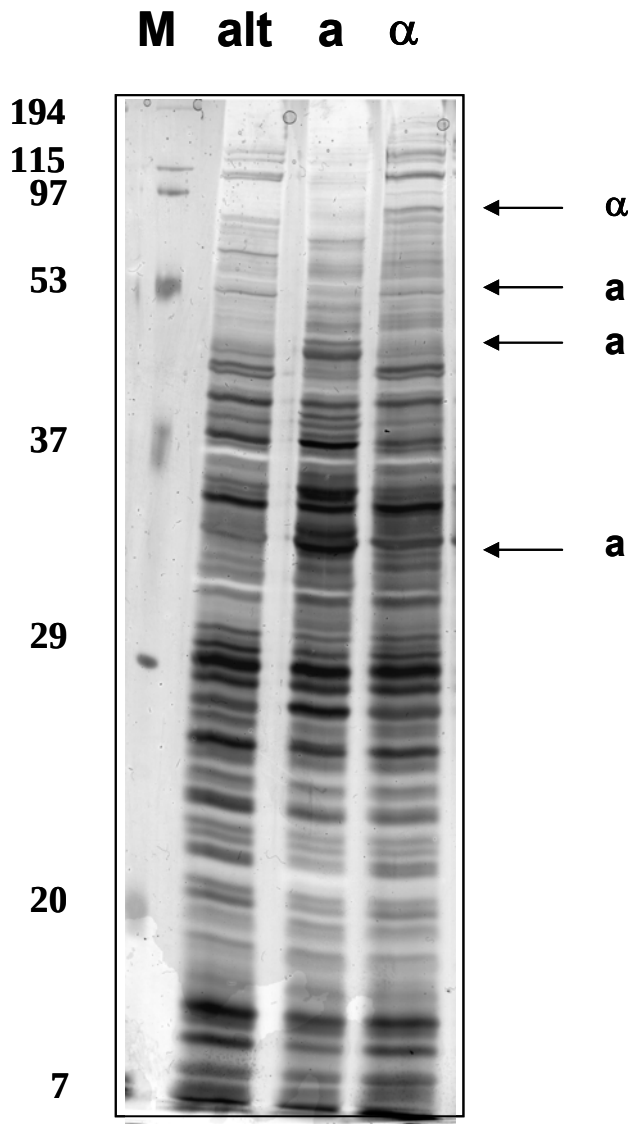

Table 2-1: Summary of Mud-PIT analysis of a-cell RE minichromosome

Complex	Protein	Peptide hits	Spec-count	Cover-age %	Sequence
yKu80	yKu80	3	5	5.6	R.IILIDCGK.D
					K.NVSEDDQSGSSYIPVTISK.D
					K.LVEVLGIK.K
	yKu70	3	8	6.6	R.SVTNAFGNSGELNDQVDETGYR.K
					K.TNFIVGVK.G
					K.DYNEGFYLYR.V
Histones	Hht1/2	1	1	5.1	
	Hhf1/2	3	6	16.5	
	Htb1/2	1	2	6.9	
	Hta3	1	2	7.5	
RNA polII	Rpc19	2	4	19	
	Rpc11	1	1	15.5	
	Rpc40	3	4	14	
	Ret1	2	3	1.5	
	Rpo31	2	3	1.4	
	Rpc82	1	1	1.8	
	Rpc34	1	1	2.8	
	Rpc31	1	1	8.8	
	Rpc37	1	3	7.4	
TFIII	Tfc6	2	4	5.8	
	Tfc7	1	2	5.1	
	Tfc3	1	2	0.6	
Replication proteins	Rfa1	4	9	5.8	
	Rfa2	3	4	15	
	Rfa3	3	6	41	
	Mcm2	2	5	4.5	
	Mcm3	1	1	0.8	
	Mcm6	1	3	1.8	
	Cdc46	1	1	1.4	
	Cdc54	1	1	2.5	
Ino80.com	Rvb1	11	30	16.6	R.TAAHTHIK.G
					R.TAAHTHIK.G
					K.GLGLDESGVAK.R
					K.GLGLDESGVAK.R
					R.AILLAGGPSTGK.T
					R.AILLAGGPSTGK.T
					K.EVYEGEVTELTPEDAENPLGGYGK.T
					T.PEDAENPLGGYGK.T
					R.LDPTIYESIQR.E
					K.EIVVNDVNEAK.L
					K.EIVVNDVNEAK.L
	Rvb2	13	39	23.1	K.TALAMGVSQSLGK.D
					K.TALAMGVSQSLGK.D
					K.TTDMETIYELGNK.M
					K.TTDMETIYELGNK.M
					K.VLAGDVISIDK.A

Table 2-1, continue

Complex	Protein	Peptide hits	Spec-count	Cover-age %	Sequence
					K.VLAGDVISIDK.A
					R.FVQCPEGELQK.R
					R.FVQCPEGELQK.R
					R.AQEEEVELSSDALDLLTK.T
					K.NNTVEVEDVK.R
					K.SADPDAMDTTE.-
	Arp5	6	9	8.7	R.NYDEDIEK.I
					K.AQMVEAEDDSHLDEMNEDK.T
					K.FDLLDIADEDLNEDQIK.E
					K.NLASLAEDNVK.Q
					K.NLASLAEDNVK.Q
					K.EYEEYGPEYIK.E
	Arp7	1	1	1.7	R.YYELAFDK.L
	Arp8	6	12	8.7	K.AAEEFAK.T
					K.NYSSDYLK.K
					R.NNNTSQISSTNTPDVIDLK.S
					R.DLFTNELNDWNSLSQFESK.E
					K.EGNLYCDLNDDLK.I
					K.ENFAPLEK.A
	Arp4	7	12	13.9	K.TFDYEVDK.S
					K.SLYDYANNR.G
					K.ETLCHICPTK.T
					K.ETLCHICPTK.T
					K.TLEETKTELSSTAK.R
					K.STSPAANSADTPNETGK.R
					R.ILTTGHTIER.Q
	Act1	4	9	10.7	K.AGFAGDDAPR.A
					K.DSYVGDEAQSK.R
					R.DLTDYLMK.I
					K.EITALAPSSMK.V
	Ino80	14	26	9.7	K.NANLSDIINEK.D
					K.DAAAAAAIGK.A
					R.FTNCIVTDYNPIDSK.L
					K.NNVGLDGNDLDNDEDGSESHK.R
					R.LVQQIQSIR.S
					K.TNELEGNNVSSNDSESQK.N
					K.NIDISALAPNK.N
					K.NIDISALAPNK.N
					R.AAENASNALAETR.A
					R.AAENASNALAETR.A
					R.ADVDSPFSFTTFGK.T
					K.FTDLIYSSR.N
					K.FTDLIYSSR.N
					K.TIEVGENDSEVTR.E
FACT	Spt16	2	2	2.2	
	Pob3	1	4	3.6	
RSC	Sth1	1	3	1.1	

Table 2-1, continue

Complex	Protein	Peptide hits	Spec-count	Cover-age %	Sequence
	Rsc4	1	2	3.7	
	Rsc5				
	Rsc6	1	1	3.1	
SAGA/SLIK	Rtg1	1	4	14.1	
	Rtg2	1	1	1.2	
	Rtg3	1	2	3.1	
	Spt20	1	1	3.5	
	Ada2	1	4	3.7	
	Hfi1	1	2	2.9	
Swi/Snf	Snf5	3	5	6	
	Snf6	1	1	3.3	
	Swi3	2	2	3.2	
	Swi1	1	1	0.6	
	Arp7	1	1	1.7	
ISW	Isw1	2	5	2	
	Loc2				
	Itc1	2	4	3.1	
Pol II GTF	Sin4				
	Srb4	1	2	3.2	
TFIID	Spt15	1	4	4.2	
	Taf17	1	5	15.9	
	Taf25	1	3	9.2	
	Taf61	1	1	2.2	
Hir.com	Hir1	1	1	2.3	
	Hir2	2	5	3.7	
	Hpc2	1	2	3	

CHAPTER III THE DNA REPAIR PROTEIN YKU80 REGULATES THE FUNCTION OF RECOMBINATION ENHANCER DURING YEAST MATING TYPE SWITCHING

Abstract

Recombination enhancer (RE) is essential for regulating donor preference during yeast mating type switching. Previous minichromosome affinity purification and mass spectrometry has identified yKu80p to be associated with RE in **a** cells. In this study, chromatin immuno-precipitation assay was performed to confirm its occupancy *in vivo*. Deletion of *YKU80* results in altered chromatin structure in the RE region and more importantly, causes a dramatic decrease of *HML* usage in **a** cells**.** We also detect directional movement of yKu80p from the RE towards *HML* during switching. These results indicate a novel function of yKu80p in regulating mating type switching.

3.1 Introduction

The mating type of yeast *Saccharomyces cerevisiae* is determined by two alleles of the mating type (*MAT*) loci which contain either **a** or α information (Nasmyth, 1983). Yeast can change mating type every other generation and during this process, two transcriptionally silent haploid mating (*HM*) loci *HML*α and *HMR***a** are required. Conversion of mating type begins with a site-specific cut of the *HO* endonuclease at the *MAT* locus. The resulting double strand break (DSB) is then repaired by homologous recombination using either *HML* or *HMR* as template (Haber, 1998). This event is highly directional. *MAT***a** recombines with *HML* 90% of the time while *MAT*α uses *HMR* as donor with an efficiency of 85% (Sprague et al., 1981).

A *cis*-acting element called the recombination enhancer (RE) has been identified as critical in regulating donor preference (Wu and Haber, 1995). It is an approximately 730bp DNA sequence located ~30kb from the left end of chromosome III ~17Kb away from *HML* (Wu and Haber, 1996). RE contains no open reading frame. However, at least two non-coding RNAs were found to be transcribed from this region (Szeto and Broach, 1997). RE has been shown to activate ~40Kb region of the left arm of chromosome III, including *HML*α, for recombination in **a** cells (Wu and Haber, 1996). In the presence of a wild type RE, **a** cells use *HML* ~90% of the time. However, in a RE deletion strain, *HML* usage drops to ~10% (Wu and Haber, 1996). Sequence comparison of *Saccharomyces cerevisiae* and *Saccharomyces carlsbergensis* revealed four conserved sub-domains in the RE region, A, B, C and D, which are indispensable for its function (Wu et al., 1998). Among these region C contains a Matα2p/Mcm1p binding site and region D features

unique TTT(A/G) repeats (Wu et al., 1998). Recent sequence alignment analysis of *Saccharomyces cerevisiae* and *Saccharomyces bayanus* identified a novel conserved E region which also contains TTT(A/G) repeats (Sun et al., 2002).

High resolution micrococcal nuclease (MNase) mapping of chromatin structure around the RE region demonstrated an inverse correlation of RE function and its organized nucleosome structure (Weiss and Simpson, 1997). In α cells, where RE is inactive, it is packaged as tightly positioned nucleosomes. In **a** cells, where RE is active, those positioned nucleosomes are replaced by a distinctive pattern of hypersensitive sites flanked by two footprints (Ercan and Simpson, 2004; Weiss and Simpson, 1997). This different chromatin structure in **a** and α cells strongly implies that *trans*-acting factors might bind to RE and regulate its function. In α cells, repressor Matα2p and Tup1p are essential for repressing RE probably by organizing the nucleosome arrays (Weiss and Simpson, 1997). By contrast, in **a** cells, Mcm1p associates with RE and is crucial for donor preference (Wu et al., 1998). In addition, Chl1p, a putative DNA helicase, has been suggested to play a minor role in switching (Weiler et al., 1995). Recently, yeast forkhead proteins Fkh1p and Fkh2p have been shown to be recruited to RE and regulate mating type switching (Sun et al., 2002). However, the deletion of *FKH1* and *FHK2* genes does not completely abolish the donor preference in **a** cells, suggesting that other factors may also contribute to this process (Sun et al., 2002).

Previously we use the Minichromosome Affinity Purification (MAP) (Ducker and Simpson, 2000) combined with mass-spectrometry to screen for proteins that bind to RE. We found that yKu80p is a protein that associates with RE *in vivo*. yKu80p is a yeast

homolog of human Ku80p, which belongs to a conserved protein family that is critical for many DNA repair events (Casellas et al., 1998; Mages et al., 1996; Tamura et al., 2002). yKu80p has been implicated in homologous recombination, non-homologous end joining (Clikeman et al., 2001), maintenance of telomeres (Laroche et al., 1998) and DNA replication (Cosgrove et al., 2002). Here we demonstrate that deletion of *YKU80* causes altered chromatin structure around the RE and defective donor preference in **a** cells, indicating a novel function of yKu80p in regulating yeast mating type switching. Moreover, the directional movement of yKu80p along the left arm of Chromosome III during switching may shed light on the molecular mechanism of donor preference.

3.2 Materials and methods

3.2.1 Strains and minichromosome construction:

The yeast strains used in this study are isogenic (except the *MAT* locus). **YCR101** *(MATa ade 2-101, ura3-52, his3-200, leu2-1, trp1-63, lys2-1 pALTRE);* **YCR102** *(MATα ade 2-101, ura3-52, his3-200, leu2-1, trp1-63, lys2-1 pALTRE);* **YCR201** *(MATa ade 2-101, ura3-52, his3-200, leu2-1, trp1-63, lys2-1 YKU80-myc KANMX6);* **YCR202** *(MATα ade 2-101, ura3-52, his3-200, leu2-1, trp1-63, lys2-1 YKU80-myc KANMX6);* **YCR203** *(MATa ade 2-101, ura3-52, his3-200, leu2-1, trp1-63, lys2-1 YKU70-myc KANMX6);* **YCR300** *(ho MATa ade 2-101, ura3-52, his3-200, leu2-1, trp1-63, lys2-1 ade3::GAL HO YKU80::KANMX6);* **YCR501** *(MATa ade 2-101, ura3-52, his3-200, leu2-1, trp1-63, lys2-1 YKU80-myc KANMX6 pALTRE);* **YCR502** *(MATα ade 2-101, ura3-52, his3-200, leu2-1, trp1-63, lys2-1 YKU80-myc KANMX6 pALTRE);* **YCR601** *(ho HMLα MATa hmrΔ::HMRα-B ade1 112 lys5 leu2-3 ura3-52 trp1::hisG ade3::GAL HO YKU80::KANMX6);* **YCR602** *(ho HMLα MATa hmrΔ::HMRα-B ade1 112 lys5 leu2-3 ura3-52 trp1::hisG ade3::GAL HO YKU70::KANMX6);* **YCR603** *(ho HMLα MATa hmrΔ::HMRα-B ade1 112 lys5 leu2-3 ura3-52 trp1::hisG ade3::GAL HO YKU80::KANMX6 FKH1::URA3-1);* **JKM161a-K** *(ho HMLα MATa HMRa ade1-112 lys5 leu2-3 ura3-52 trp1::hisG ade3::GAL HO)*(Wu and Haber, 1996)*;* **CWWT** *(ho HMLα MATa hmrΔ::HMRα-B ade1-100 ura3-53 leu2-3,112*) (S. Ercan, unpublished); **YCR604** *(ho HMLα MATa hmrΔ::HMRα-B ade1-100 ura3-53 leu2-3,112 YKU80-myc KANMX6*). All strains used for the minichromosome purification and MNase mapping are derived from YPH499 and YPH500. Strains used for the mating type switching assay are derived from either JKM161**a**-K or DBY745 (Wu and Haber, 1995). Synthetic medium containing the appropriate supplements was used to select and maintain the *TRP*1 minichromosome.

For the pRE-ALT construction, a 1.4 kb RE fragment was amplified by PCR, cloned into an engineered *AvaI* site of the minichromosome backbone pALT(Ducker and Simpson, 2000). pRE-ALT was then digested with *SphI* to remove bacterial sequences. The resulting DNA was then re-ligated (RE-ALT) and transformed into yeast. To ensure the correct transcription of *TRP1* in α cells, a ~200bp insulator was cloned between Matα2p binding site and *TRP1*(Link et al., 1999). The deletion and epitope tagged strains were generated by the standard one-step PCR method (Brachmann et al., 1998; Longtine et al., 1998).

3.2.2 Minichromosome affinity purification and mass-spectrometry

Minichromosome affinity purification was carried out as previously described (Ducker and Simpson, 2000) with a few modifications. After Zymolyase treatment and homogenization of the cells, minichromosomes were allowed to diffuse passively from the nuclei on ice then loaded onto *Lac* I-Z affinity column. They were subsequently eluted with 300 mM NaCl and 1mM IPTG. Proteins from the minichromosome eluate were resolved using 10% SDS-PAGE and silver stained. Interesting bands were excised and subjected to MALDI-MS analysis by the Mass-Spectrometry facility at the Penn State University.

3.2.3 ChIP

Chromatin immuno-precipitation were performed as described in (Li and Reese, 2001). Cells were harvest at about OD 1.0 and chromatin was sheered to ~500 bp by sonication. Immuno-precipitation was performed using 9E10 anti-*myc* antibody (Upstate) and Protein A beads (Promega). DNA was then purified and PCR was performed using primers that specific amplify the RE region.

3.2.4 MNase mapping:

The assay was preformed as previously described (Weiss and Simpson, 1997). Nuclei isolated from cells grown to log phase were digested with increasing concentrations of MNase. The cleavage sites were determined by primer extension using *Taq* polymerase (Shimizu et al., 1991). The primer used in this study was a290 (5' GCTGGAAGTGCAGAACAAAGAGG-3') (Weiss and Simpson, 1997).

3.2.5 Mating type switching assay:

Cells were grown in YPL (yeast extract, peptone and lactic acid) to OD~0.4 and then 2% galactose was added to the media to induce *HO* expression (Wu and Haber, 1995). After 40 minutes, cells were washed and resuspended in YPD (yeast extract, peptone and dextrose) to complete switching. DNA was extracted from cells collected at different time points, cut with either *StyI* or *BamHI* and *HindIII* and then analyzed by Southern blots.

3.3 Results

3.3.1 yKu80p binds to RE in vivo

Our previous study combining the minichromosome purification and the mass spectrometry identified yKu80p, the yeast homolog of DNA repair protein Ku, to bind to the RE minichromosome isolated from **a** cells but not that of the α cells. In attempt to understand the role yKu80p played in RE regulation, we examined its involvement in the local RE chromatin structure and the directionality of switching.

To confirm that yKu80p indeed associates with RE in **a** cells, we sought to detect this protein in isolated minichromosomes. To this end, RE-ALT plasmid was introduced to both **a** and α cells bearing *myc*-tagged yKu80p. Proteins bound to purified minichromosomes were analyzed by western blotting using anti-*myc* antibody. The amount of minichromosome loaded on the gel was normalized based on DNA content in each fraction, measured by ethidium bromide staining and Southern blotting (data not shown). We found a significant amount of yKu80p in the minichromosome fraction isolated from **a** cells (Fig. 3.1, lane 6), whereas minichromosomes from α cells only contain trace amount of yKu80p (lane 5). Thus, yKu80p preferentially bound to the active form of RE, which is consistent with the fact that RE only functions in **a** cells (Wu and Haber, 1996). The faint yKu80p band observed in α cells may reflect the interaction of the protein and the ARS sequence in the minichromosome backbone (Shakibai et al., 1996).

To further address the interaction between yKu80p and RE in living cells, we took advantage of chromatin immunoprecipitation (ChIP) assay. Yeast strains containing

genomic epitope tagged yKu80p were cross-linked with formaldehyde. Whole cell extracts were then subjected to sonication to shear chromatin DNA into an average size of 500 bp. Immunoprecipitation was carried out with anti-myc antibody, and precipitated DNA was detected by quantitative PCR using the primer set covering D and part of the E region within RE (Fig. 3.2 A). yKu80p cross-linked to the RE region only in **a** cells but not α cells (Fig. 3.2 B). As a positive control, we repeated the result that yKu80p binds to the sequence 0.5 Kb away from the right telomere of chromosome VI, but not to DNA 7 Kb from that telomere (Martin et al., 1999). This is a good control since the occupancy of yKu80p at the telomeric region is indistinguishable between **a** cells and α cells in contrast to its binding at RE. Together these results strongly indicate that yKu80p associates with RE in **a** cells *in vivo*.

We then sought to determine if a functional RE is required for yKu80p recruitment. One of the most important features of the RE is the Mcm1p binding site. A mere two base pair mutation GG to CC within the Mcm1p binding site completely not only strongly decreased the binding of Mcm1p (Smith and Johnson, 1994), but also abolished both RE function and its unique chromatin structure (Wu et al., 1998). Thus we tested whether this DNA segment is also essential for the binding of yKu80p to the RE. Using the ChIP approach, we analyzed the interaction of yKu80p and the RE in both wild type and a Mcm1p binding site mutation strain described above. As shown in Fig. 3.2 B, the *myc*-yKu80p cross-linking signal reduced to background level in the mutant. This indicates that an intact Mcm1p binding site is essential for the interaction of the yKu80p to this region.

3.3.2 Loss of yKu80p leads to altered nucleosome structure of RE in a cells

In α cells, where RE is inactive, tightly positioned nucleosomes cover this region. In **a** cells, where RE is active, those positioned nucleosomes are disrupted and unique hypersensitive sites and footprints appear (Weiss and Simpson, 1997). Surprisingly, when RE's function is abolished in a *MAT***a** strain containing a GG-to-CC mutation of the Mcm1p binding site, the MNase digestion pattern at the RE resembles that of the α cells (Wu et al., 1998). This suggests that local chromatin structure may play a role in regulating RE's function.

To investigate whether yKu80p affects RE chromatin structure, we mapped this region using MNase digestion in a *MAT***a** strain bearing a deletion of *YKU80*. The digestion patterns of the RE in wild type **a** (Fig. 3.3, lanes 1-3) and α (lanes 4-6) cells are consistent with previous observations (Weiss and Simpson, 1997). In *Δyku80* **a** cells, chromatin structure around the RE has undergone significant changes compared to that of wild type **a** cells (compare lanes 1-3 and 7-9), specifically, less intense hypersensitive bands and the loss of the footprints 1 and 2 flanking it. The overall digestion pattern in **a** Δ*yku80* deletion strain resembles that of wild type α cells where RE is inactive and yKu80p does not bind to it (Fig. 3.1 and 3.2), suggesting that the association of yKu80p with RE contributes to the disruption of the nucleosomes positioned in this region. The remaining weak hypersensitive site signal may indicate yKu80p is not the only factor that affects the chromatin structure of this region.

3.3.3 Donor preference is defective in Δyku80 deletion MATa strain

We next asked whether yKu80p affects mating type switching upon binding to RE. First, we monitored the kinetics of the double strand break repair during **a** to α switching

in the absence of yKu80p. *YKU80* was deleted in a *MAT***a** strain containing an *HO* gene under the control of the *GAL10* promoter. Cells were grown to OD 0.4-0.6 in lactic acid medium before induction (with 2% galactose) of *HO* expression (see Materials and Methods). After 40 minutes of induction, cells were transferred to dextrose medium to shut down *HO* expression. At this point, cells started to repair the double strand break and complete the switching process. Genomic DNA was extracted from cells collected at different time points, digested with the *StyI,* and subjected to Southern blotting using a probe adjacent to the *MAT* locus (Fig. 3.4A).

Forty minutes following *HO* induction (the zero time point), bands representing efficient cleavage of the *HO* site at the *MAT***a** locus were detected in both the wild type and the *Δyku80* strains (Fig. 3.4B lanes 2 and 6, compare bands labeled **a** and *HO*). Complete switching to *MAT*α generates a novel 1.8 kb DNA fragment (labeled α) which is visible one hour after the end of induction in the wild type cells (lane 3) and by two hours, 85% of the wild type **a** cells have successfully switched to *MAT*α (lane 4). In the *Δyku80* strain, the gene conversion event was abnormal: less than 40% of the **a** cells switched to *MAT*α at 1 and 2 hour time points as shown in Fig. 3.4 (lane 7 and 8, compare bands **a** and α). The *yku80* deletion strain does not have a defect in general DNA repair during switching, since the *HO* cleavage in both the wild type and deletion cells were almost completely repaired after 1-2 hours in dextrose medium (Fig. 3.4B, bands *HO* in lanes 2 to 4 and 6 to 8). This result strongly suggested that yKu80p is involved in yeast mating type switching by means independent of its general DNA repair function.

However, there are two possible interpretations for this observation: The deletion of *YKU80* can either specifically affect the donor preference or it may just impair the overall homologous recombination process. To distinguish between these two possibilities, we tested the direct involvement of yKu80p in donor preference in an assay where *YKU80* is deleted in a strain carrying a modified *HMR*α-B and wild type *HML*α (Wu and Haber, 1995). Following a similar switching assay procedure, DNA was extracted and digested with *BamHI* and *HindIII.* Subsequent Southern blotting was performed using probe detecting the Y_α specific sequence. Since *HMR*α-B has an engineered *BamHI* site, it can be distinguished from *HML*α by the different size of DNA fragments generated from restriction endonuclease cleavage (compare band *MAT*α-B and *MAT*α). Donor preference is directly reflected by the ratio of these two bands. Shown in Figure 3.5A, about 85% of wild type **a** cells chose *HML*α as the donor during switching. In contrast, cells without yKu80p choose the correct donor *HML*α only 40% of the time while the usage of the wrong donor *HMR*α-B increased to 60%.

Based on this result and that of the first switching assay (Figure 3.4B), we conclude that yKu80p plays an important role in **a** cells to maintain correct donor preference during switching. The *YKU70* deletion strain was also included in this assay since previous study has shown that yKu80p and yKu70p usually act as a heterodimer (Cervelli and Galli, 2000). Interestingly, we found that yKu70p only moderately affects the donor preference (65% *HML* usage, see Fig. 3.5A and B) though it does bind to the RE *in vivo* (Fig. 3.6). This is somewhat different from a previous observation (Mages et al., 1996). Mages et al. have reported that after 6 hours of *HO* induction, there was more than 60% decrease of mating type switching in a *yku70* deletion strain (from ~30% of wild type to

~10% of in Δ*yku70*) (Mages et al., 1996). However, the overall low switching rate in both WT and Δ*yku70* deletion strains in their assay, possibly due to over-exposure to the *HO* endonuclease, may cause the discrepancy between the two results. We use transient *HO* expression (< 40 minutes) in our study, thinking this better mimics the *in vivo* switching process.

It has been shown that the forkhead proteins, especially Fkh1p, is essential in the process of donor preference (Sun et al., 2002). However, like yKu80p, cells deleted of this protein still maintain partial ability to choose the correct donor (Sun et al., 2002). Thus it is possible that yKu80p and Fkh1p play partially redundant roles in donor preference. To address this possibility, we performed the switching assay using a strain deleted of both *FKH1* and *YKU80*. As shown in Figure 3.5C, the usage of *HML* in the double deletion cells drops to 22% which is significantly lower than that of either single deletion strain and close to the level of the RE deletion cells (Wu et al., 1998). This result suggests that Fkh1p and yKu80p may act in concert to regulate the RE function during switching.

3.3.4 Dynamic Interaction of yKu80p with the left arm of Chromosome III during mating type switching

One of the hypotheses regarding the function of the RE in donor preference is that the unique chromatin structure of the RE in **a** cells serves as an entry point for the DSB and the recombination machinery to start homology searching and DNA repair (Weiss and Simpson, 1997). If this is the case, it is possible that the DSB is brought about to the vicinity of the RE then tracks along the left arm of Chromosome III and samples different regions before it reaches the final destination - *HML*. Since yKu80p is one of the known

proteins that bind to both the DSB and the RE (Martin et al., 1999), we speculate that yKu80p might play a leading role in such a searching process. To monitor the kinetics of yKu80p occupancy on Chromosome III during switching, we constructed a strain containing a *myc*-tagged yKu80p in a *GAL10* controlled *HO* background. Switching was induced by addition of galactose as previously described. Cell samples were collected during the course of switching with 15 minutes intervals and subjected to ChIP analysis using primer sets designed to amplify regions from the RE towards either *HML* or *HMR* (Fig. 3.7B). In addition, genomic DNA of each sample was prepared and subjected to the switching assay described above (Fig3.4 A). The switching process of the *myc-YKU80* strain is largely similar to that of the wild type and is completed within 90 minutes (Fig. 3.7 A).

As shown in Fig. 3.7 C, consistent with previous experiment, yKu80p was cross-linked to RE before the induction of HO cleavage. The cross-linking signal remained after the generation of DSB (Fig. 3.7 C, 0 time point). However, the signal suddenly dropped to background 15 minute after the start of switching. Interestingly, 30 minutes after the beginning of switching, yKu80p was found to cross-linked to RE again. This phenomenon might be explained by masking of the the *myc*-yKu80p epitope by other proteins during the invasion of the DSB and the recombination machinery in the RE region (Fig. 4.6 B). Our data shows that the recruitment of yKu80p to the RE peaks 30 minutes after the start of switching (Fig. 3.7 C). This signal then gradually disappears. The association of yKu80p with the region at 5Kb from the RE *HML* proximal starts about the same time and the binding is weakened after 45 minutes. The strongest binding signal of the yKu80p to 11kb *HML* proximal was detected 45-60 minutes after the start of

DNA repair. By 60 minutes we saw significant association of the yKu80p and the donor sequence *HML*. Interestingly, another DSB binding protein Rad51p is shown to be associated with *HML* around the same time (Sugawara et al., 2003). At the 75 minutes time point, the cross-linking signal of yKu80 at *HML* started to decrease and when the switching is almost completed at 90 minutes, we did not find any cross-linking of yKu80p to the left arm of Chromosome III (Fig. 3.7 C). Notably, throughout the whole switching process, yKu80p does not seem to bind to *HMR* or regions from 5Kb right of the RE at any point (Fig. 3.7 E). This is consistent with the idea that yKu80p helps facilitate donor selection of the *HML*. In summary, yKu80p appears to move from its initial binding site of the RE towards the *HML* along the left arm of chromosome III in a directional manner during switching.

3.4 Discussion

In this study, we discovered a novel function of yKu80p. We report that yKu80p binds to RE and regulates RE function in mating type switching. yKu80p has previously been shown to be a DNA end binding protein (Shakibai et al., 1996). The ring-like crystal structure of the yKu80p/yKu70p heterodimer further supports its non-specific end binding activity (Walker et al., 2001). However, in this study, their association with the RE seems to require an intact binding site for a sequence-specific transcription factor (Mcm1p). Thus, yKu80p to the RE may be distinct from that occurring in its roles in DNA repair and telomere silencing.

a and α cells employ different mechanisms in choosing the correct donor during switching: The *HML* in **a** cells requires activation of a large region of the left arm of chromosome III to "out compete" *HMR* (Wu and Haber, 1995). On the other hand, in *MAT*α cells, *HMR* serves as the "default" donor (Wu and Haber, 1995; Wu et al., 1996) when the *HML* is not available for recombination. A study combined immunofluorescence and *in situ* hybridization indeed revealed that the "cold" *HML* in α cells are located near the nuclear periphery and packed into heterochromatin (Gotta and Gasser, 1996). It is speculated that in **a** cells, a change in the higher order chromatin architecture may reverse the inaccessibility of the left arm of chromosome III and make it open for recombination.

The RE has been shown to be essential in this activating process (Sun et al., 2002; Wu et al., 1998; Wu and Haber, 1996). Besides its conserved *cis*-element sub-domains,

protein factors are also required to help carry out RE function. In **a** cells, a MADS family protein, Mcm1p, regulates RE by possibly opening up the chromatin structure of this region and making it accessible for binding of other factors ((Sun et al., 2002) and S.E. and R.T.S., unpublished data). One current hypothesis is that interactions of RE with proteins such as Mcm1p, yKu80p and Fkh1/2p, may help to release the left arm of chromosome III including the *HML* from the heterochromatic nuclear periphery and make it accessible for recombination. Indeed, an *in vivo* immunofluorescence study showed that in wild type cells, the *HML* in **a** cells is located in an inner nuclear location which is considered to be more accessible to recombination. However, the deletion of Ku protein makes it targeted to the nuclear periphery where is often associated with inactive recombination (Weiss.K, personal communication). Moreover, RE may also serve as an entry point for the DSB and regulate the donor preference by assisting homology searching and recombination. Thus, proteins that are associated with RE, such as yKu80p and the forkhead proteins may promote this process by interacting with proteins that bind to the DSB and lead it to scan for the homologous sequence in the *HML*. The directional and transient interactions of the yKu80p and the left arm of chromosome III, as shown in Fig. 3.7, support this model.

Future mechanistic studies will not only help us understand RE functions during switching, but more importantly it will also shed light on how a small *cis*-acting element can control homologous recombination and chromatin structure over a large chromosome segment. Implications of these results for similar situation in the genomes of other organisms, e.g. immunoglobulin switching in human, are obvious (Casellas et al., 1998; Manis et al., 1998; Wu and Haber, 1996).

Figure 3.1 yKu80p is associated with RE containing minichromosomes in *MAT*a cells.

RE minichromosomes were isolated using the MAP method from **a** (YCR501) and α (YCR502) cells containing *myc* tagged yKu80p. The amount of minichromosomes loaded on the gel was normalized by DNA content measured both by ethidium bromide (EB) staining and Southern blotting. Western blotting was performed with an antibody against the *myc*-epitope tag. An arrow shows the molecular weight of *myc*-tagged yKu80p.

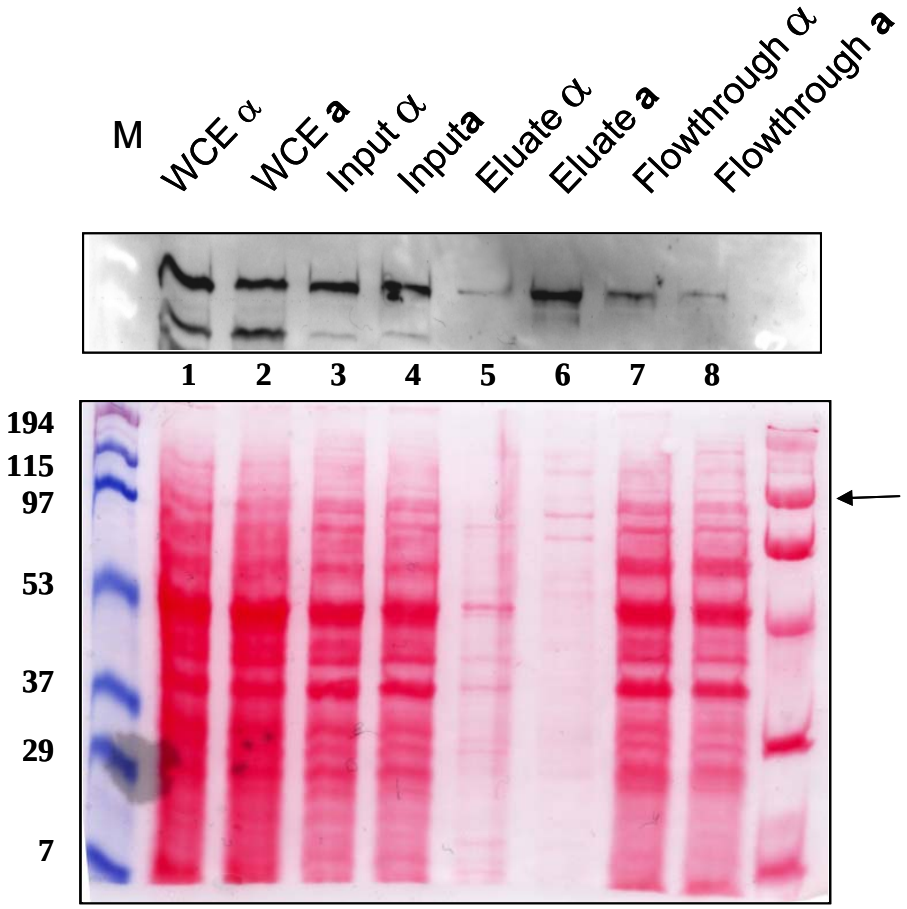

Figure 3.2: Binding of yKu80p to the RE *in vivo* requires an intact Mcm1p binding site.

(A) Schematic diagram of the RE region. Five conserved regions are labeled A, B,C,D and E. Fuchsia bars indicate putative binding sites of Fhk1p and red bars represent the two Mcm1p binding sites. Green arrows show the primer set for ChIP analysis. (B) Whole cell extracts were prepared from **a** (YCR201), α (YCR202) and **a** with GG-to-CC mutation (CW157) cells containing *myc*-tagged yKu80p, sonicated to make the average DNA fragment about 500bp and subjected to chromatin immunoprecipitation with anti-*myc* antibody. Quantitative PCR was performed in parallel on input DNA, mock (no antibody) and *myc*- yKu80p immunoprecipitated DNA (IP) with primers corresponding to the RE region. PCR with primer sets that amplify regions 0.5kb and 7kb from the right telomere of the chromosome VI were used as positive and negative controls, respectively. (B) Quantification of above experiment. Error bars indicate the results for three independent experiments.

A.

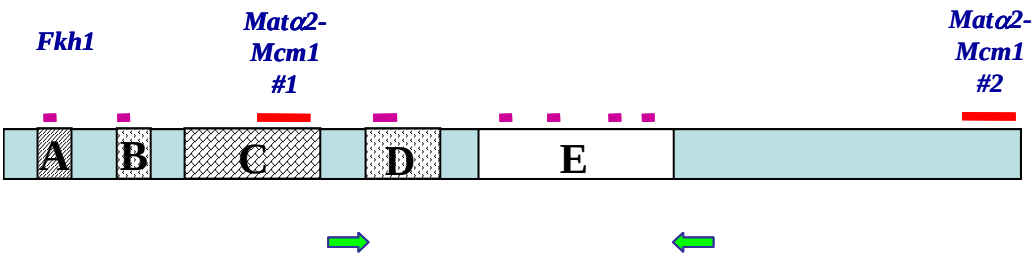

RE primers

Fkh1 binding site

Mcm1p binding site

B.

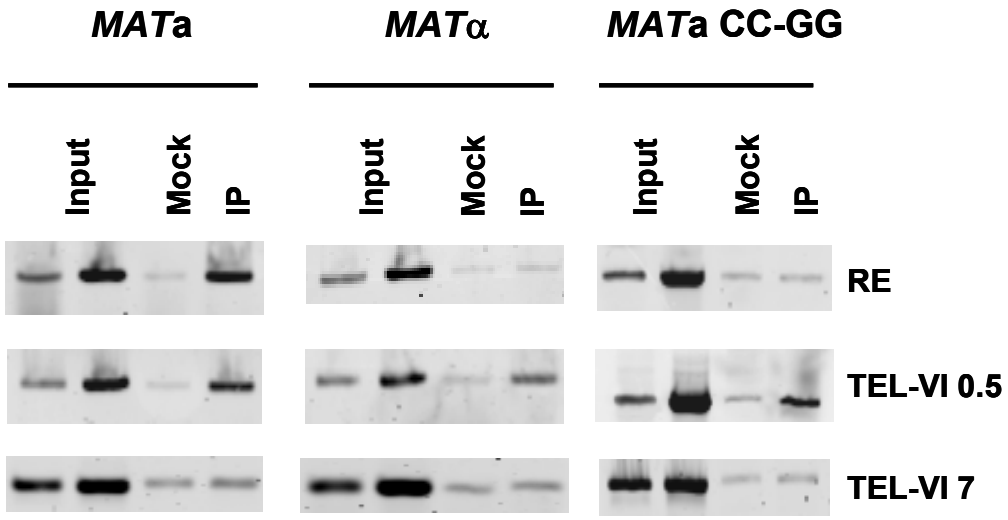
MATa
MATα
MATa CC-GG
Input
Mock
IP
Input
Mock
IP
Input
Mock
IP
RE
TEL-VI 0.5
TEL-VI 7

C.

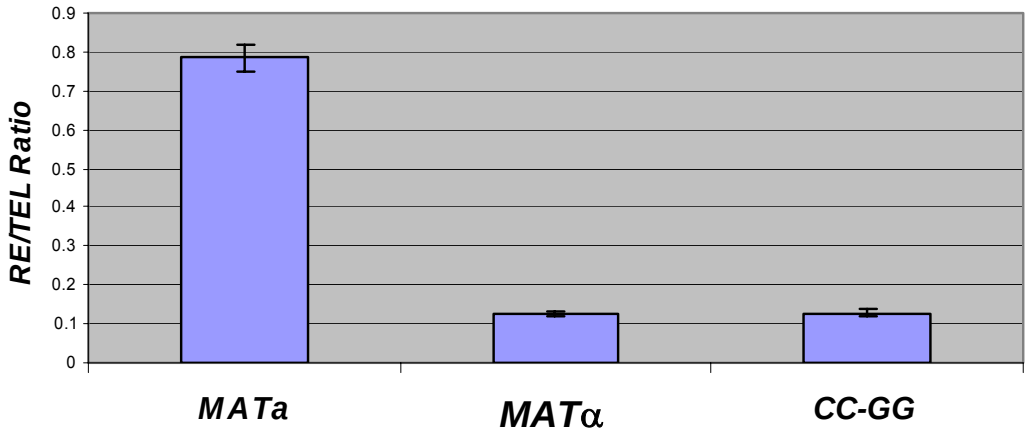
RE/TEL Ratio
0.9
0.8
0.7
0.6
0.5
0.4
0.3
0.2
0.1
0
MATa
MATα
CC-GG

Figure 3.3: Chromatin structure of RE in *MAT*a cells was altered upon deletion of the *YKU80* gene.

High resolution chromatin structure of the Watson strand of the RE region in wild type **a** (YPH499), α (YPH500) and *yku80*Δ (YCR300) strains using primer c290 (Weiss and Simpson, 1997) is shown. Solid gray and blank rectangular boxes represent the location of the hypersensitive site and footprints, respectively, in wild type **a** cells; Ellipses correspond to tightly positioned nucleosomes in α cells. The black bars indicate altered digestion patterns upon deletion of *YKU80* in **a** cells.

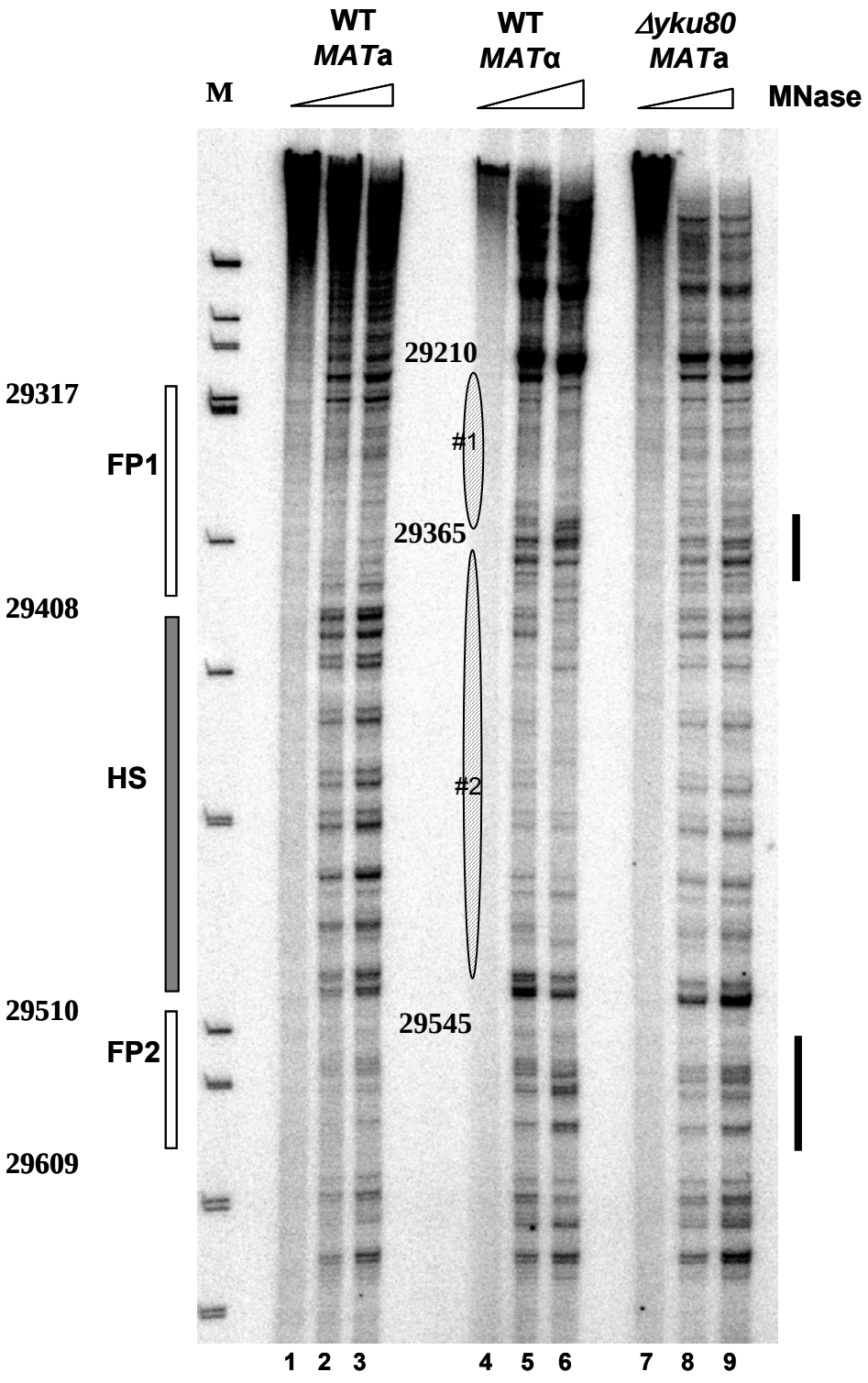
WT
MATa
WT
MATα
Δyku80
MATa
M
MNase
29317
FP1
29408
HS
29510
FP2
29609
29210
#1
29365
#2
29545
1 2 3 4 5 6 7 8 9

Figure 3.4: yKu80p affects yeast mating type switching.

(A) A schematic illustration of the physical analysis of mating type switching. The *HO* cutting site and *StyI* cleavage sites are shown as the arrows. The location of the probe for Southern blotting is indicated as a black bar. (B) Mating type switching of wild type (JKM161-K) and *yku80*Δ (YCR300) cells was initiated by galactose induction of *HO* expression. Samples were collected at four time points: before *HO* induction (lane 1 and 5, labeled as –40), 40 minutes after induction (lane 2 and 6, labeled as 0, since it is the starting point of DSB repair), one hour (lane 3 and 7), and two hours (lane 4 and 8) after transfer to YPD medium. DNA was extracted and digested with *StyI* before Southern blotting with the probe indicated in panel A. The **a**, α and *HO* specific bands generated by *StyI* digestion are indicated. The ratio of the intensity of **a** and α specific signals measured by ImageQuant software was used to determine the **a**-to-α switching efficiency.

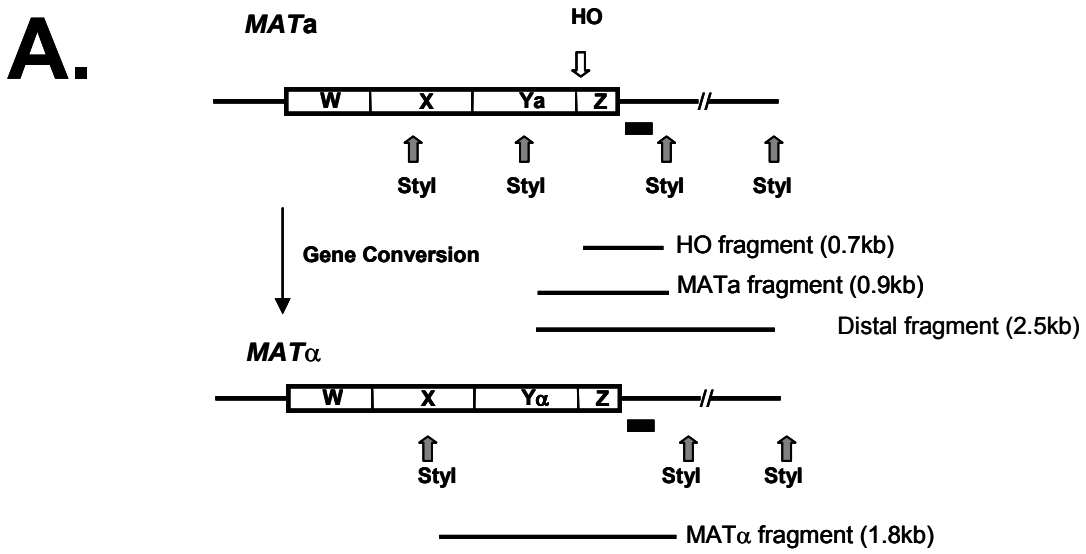
A.
MATa
HO
W
X
Ya
Z
StyI
StyI
StyI
StyI
Gene Conversion
HO fragment (0.7kb)
MATa fragment (0.9kb)
Distal fragment (2.5kb)
MATα
W
X
Yα
Z
StyI
StyI
StyI
MATα fragment (1.8kb)

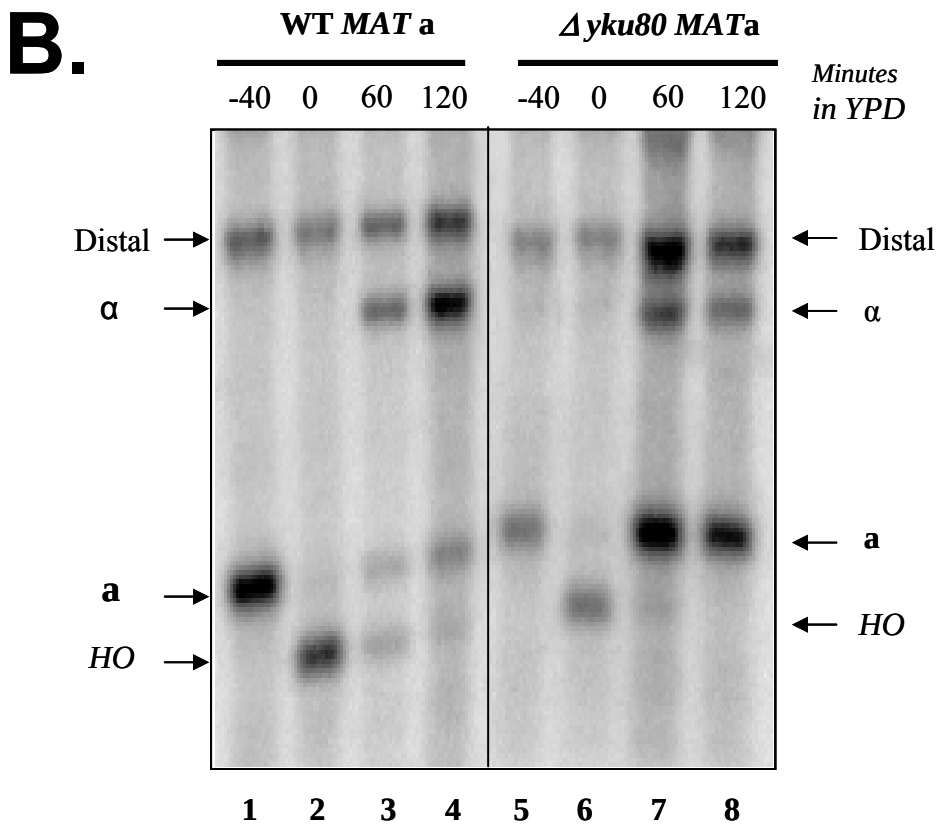
B.
WT MAT a
Δyku80 MATa
-40
0
60
120
-40
0
60
120
Minutes in YPD
Distal
α
a
HO
Distal
α
a
HO
1
2
3
4
5
6
7
8

Figure 3.5: yKu80p directly regulates donor preference

(A) DNA was extracted from wild type (CWWT), *yku80*Δ (YCR601) and *yku70*Δ (YCR602) cells 2 hours after the *HO* induction and digested with *BamHI* and *HindIII* before blotting with the Y_α probe which can detect the four specific bands labeled above. Completion of switching generates *MAT*α band when cell chooses *HML* or *MAT*α-B band when *HMR* is used as the donor. (B) Donor preference was determined by comparing the intensity of the *MAT*α and *MAT*α-B bands using ImageQuant. Error bars reflect results from three independent experiments. (C) Switching assay was performed using wild type (CWWT) and *Δyku80/Δfkh1* (YCR603) strains. Donor preference was determined as above.

A.

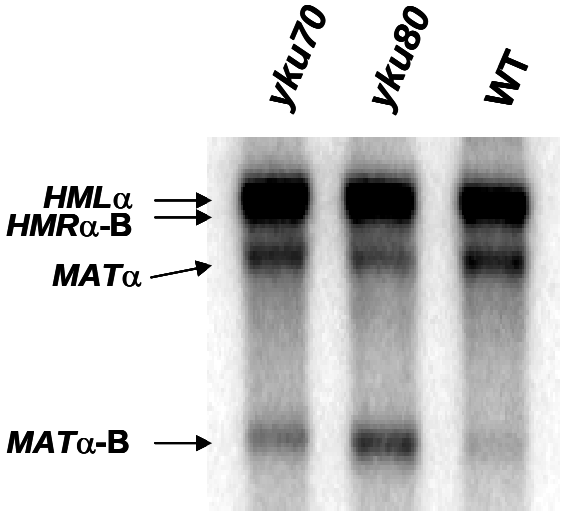
yku70
yku80
WT
HMLα
HMRα-B
MATα
MATα-B

B.

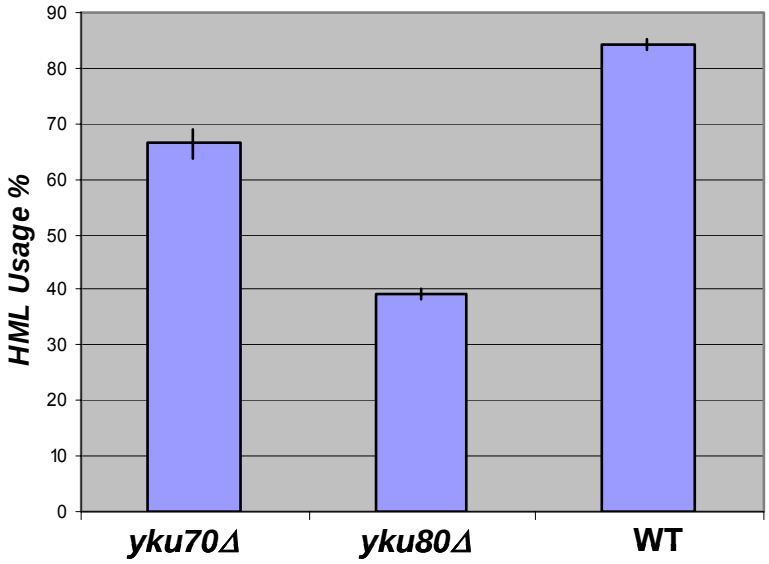
HML Usage %
90
80
70
60
50
40
30
20
10
0
yku70Δ
yku80Δ
WT

C.

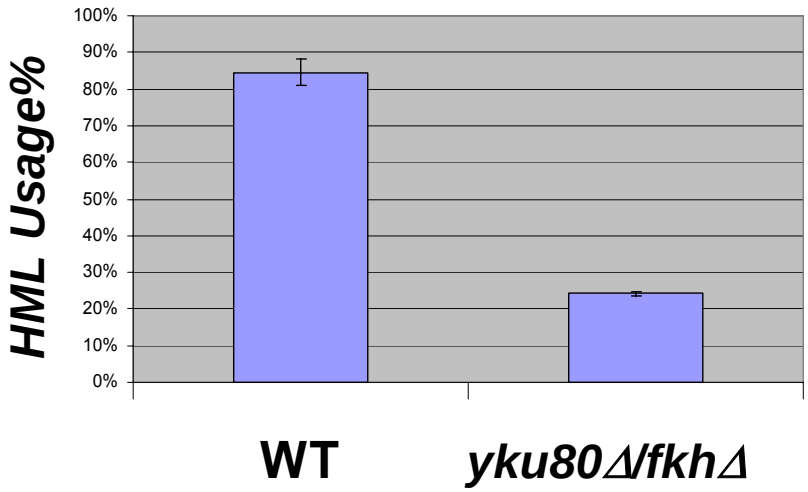

Figure 3.6: yKu70p binds to the RE in vivo

Whole cell extracts were prepared from **a** (YCR203) cells containing *myc*-tagged yKu70p, sonicated to make the average DNA fragment about 500bp and subjected to chromatin immunoprecipitation with anti-*myc* antibody. PCR was performed in parallel on input DNA, mock (no antibody) and *myc*- yKu70p immunoprecipitated DNA (IP) with primers corresponding to the RE region. PCR with primer sets that amplify regions 0.5kb from the right telomere of the chromosome VI and 5Kb from RE, *HML* proximal were used as positive and negative controls, respectively.

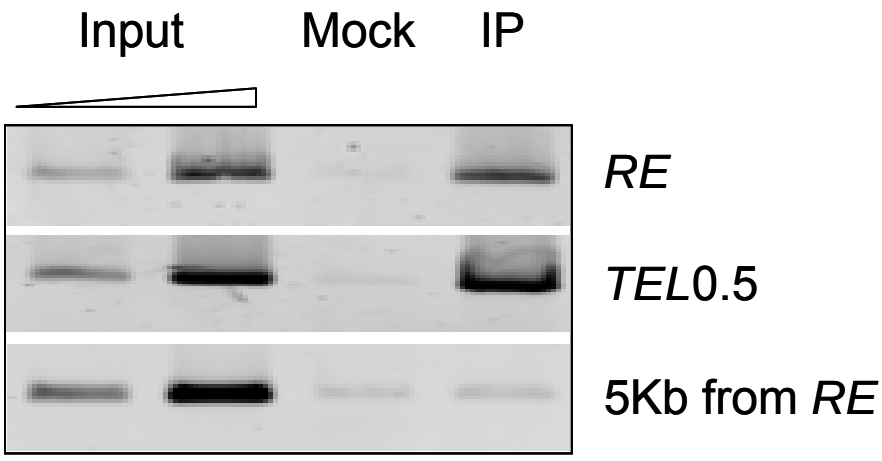

Figure 3.7: Dynamic interaction of yKu80p and the left arm of Chromosome III during switching.

(A) Physical monitoring of the switching of the strain containing a *myc*-tagged yKu80p (YCR061). Mating type switching was initiated by galactose induction of *HO* expression. Samples were collected at eight time points: before *HO* induction (labeled as –40), 40 minutes after induction (labeled as 0, since it is the starting point of DSB repair), 15, 30, 45,60, 75 and 90 minutes after transfer to YPD medium. DNA was extracted and digested with *StyI* before Southern blotting with the probe indicated in Fig 3.4 A. The **a**, α and *HO* specific bands generated by *StyI* digestion are indicated. (B) Schematic diagram of Chromosome III. Patterned or colored boxes indicate loci that are important for switching. Red bars represent seven primer sets used in ChIP assay. (C) A yeast strain containing a *myc*-tagged yKu80p (YCR061) was induced for mating-type switching as described before. Cells were collected at -40, 0, 15, 30, 45, 60, 75 and 90 minutes after the start of switching. DNA was extracted and subjected to ChIP analysis using primers designed to amplify regions of *HMR*, the RE, and 5kb and 11kb away from RE the *HML* proximal. (D) Quantification of ChIP assays from three independent experiments. The cross-linking efficiency is normalized to the mock IP for all primer sets. (E) YCR061 was induced for mating-type switching as described before. Cells were collected at -40, 0, 15, 30, 45, 60, 75 and 90 minutes after the start of switching. DNA was extracted and subjected to ChIP analysis using primers designed to amplify regions of 5kb and 11kb away from RE the *HMR* proximal and the *HMR*. The experiment was repeated once with similar results.

A.

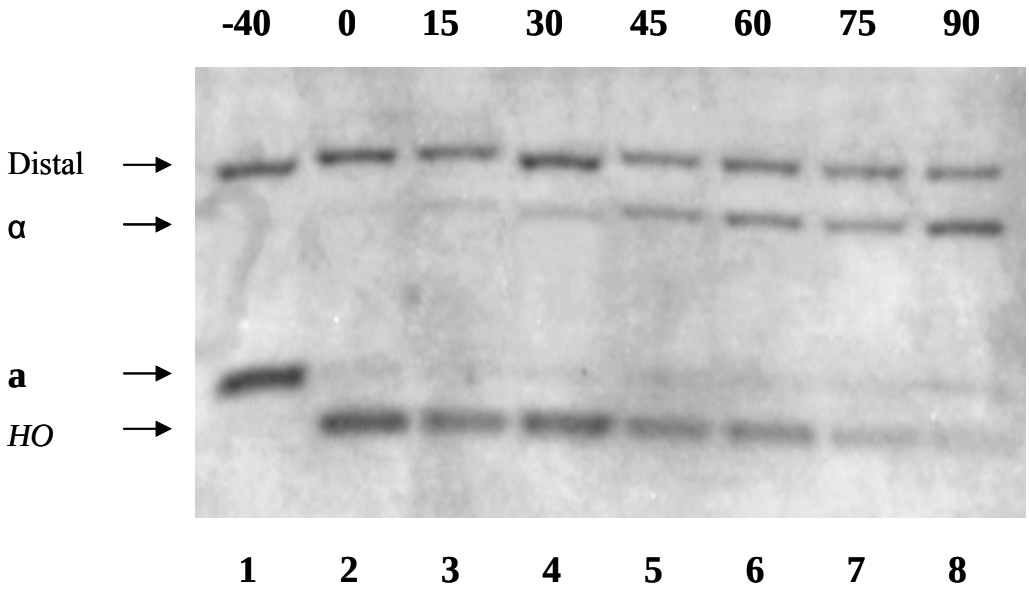
-40
0
15
30
45
60
75
90
Distal
α
a
HO
1
2
3
4
5
6
7
8

B.

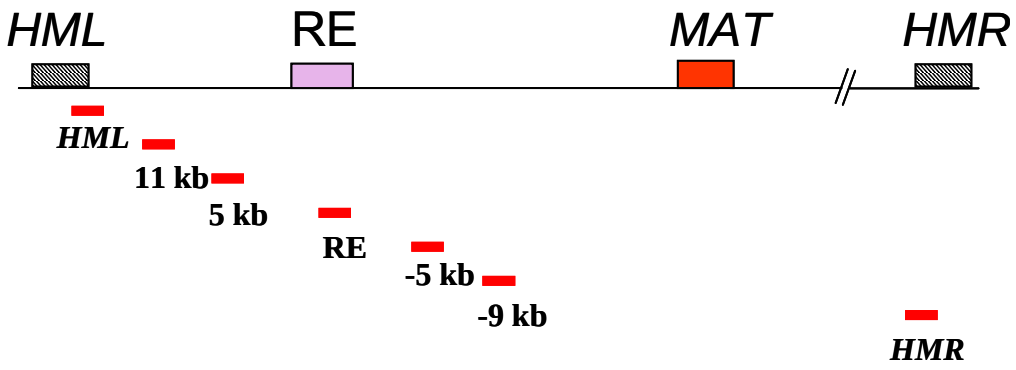
HML
RE
MAT
HMR
HML
11 kb
5 kb
RE
-5 kb
-9 kb
HMR

C.

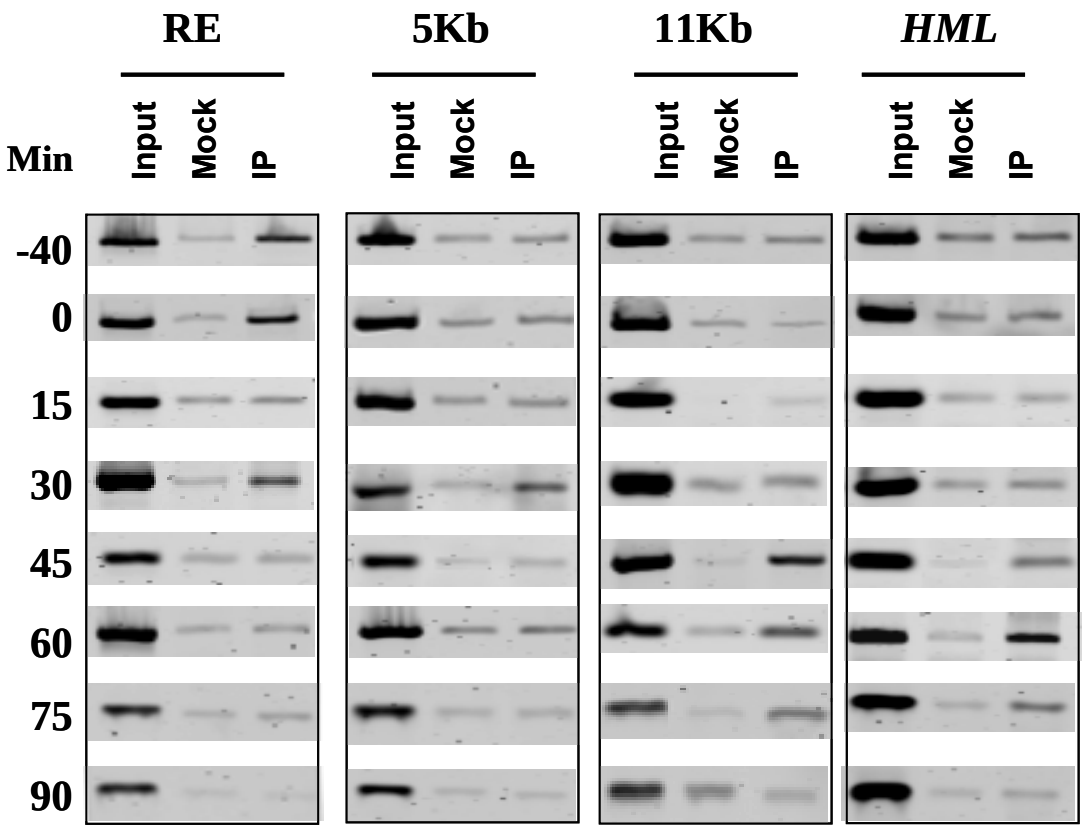

D.

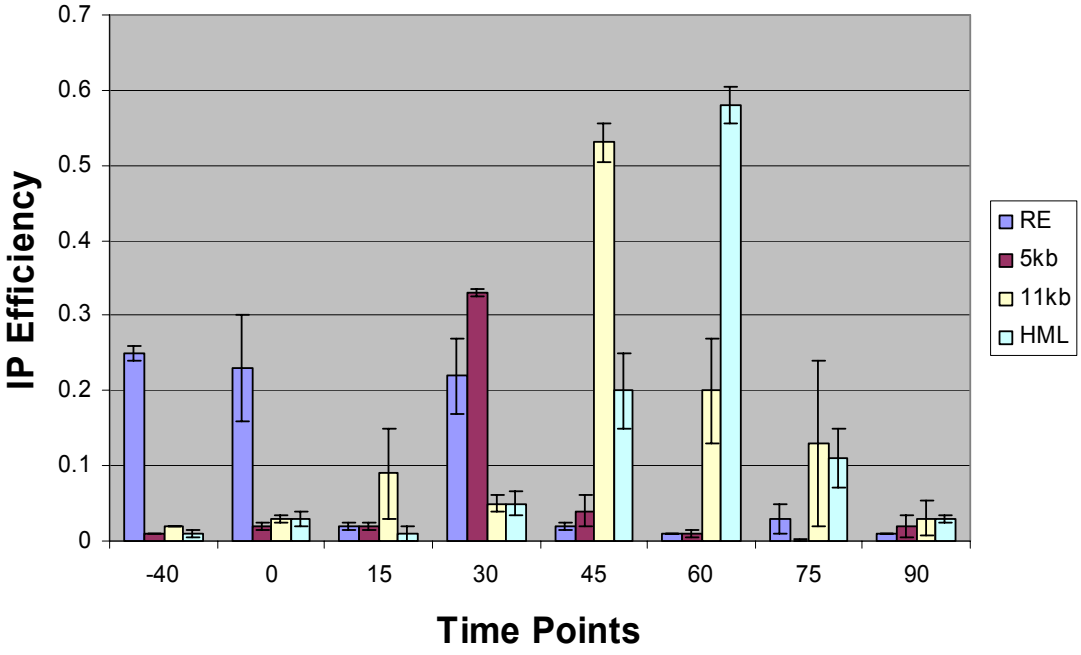
0.7
0.6
0.5
0.4
0.3
0.2
0.1
0
IP Efficiency
-40
0
15
30
45
60
75
90
Time Points
RE
5kb
11kb
HML

E.

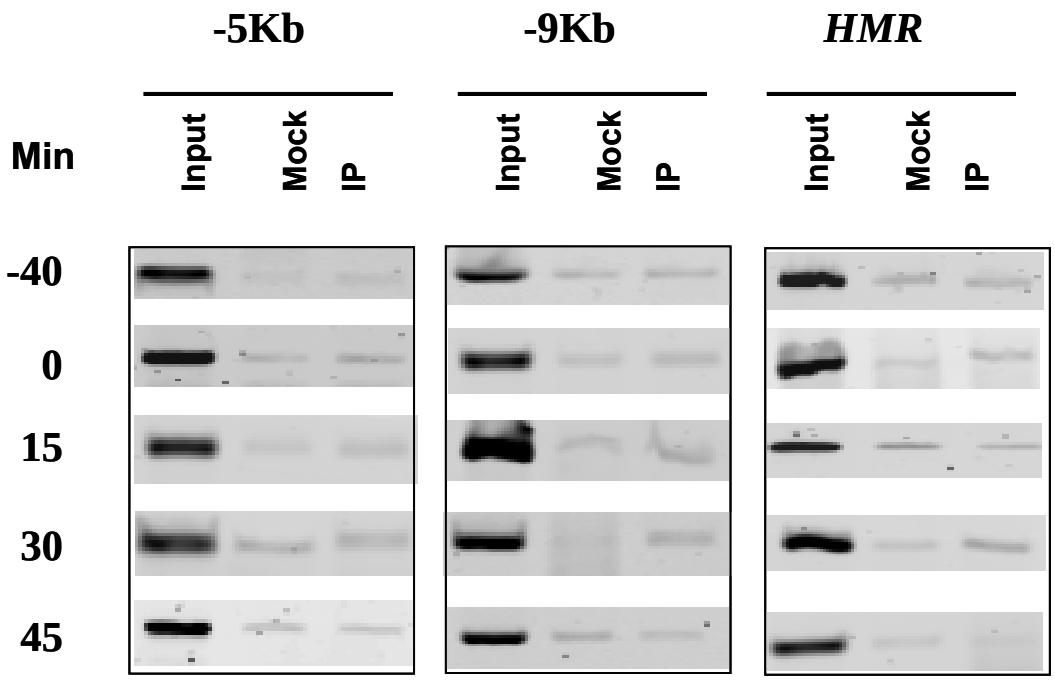
-5Kb
-9Kb
HMR
Input
Mock
IP
Input
Mock
IP
Input
Mock
IP
Min
-40
0
15
30
45

CHAPTER IV PARTNERS OF YKU80 IN MATING TYPE SWITCHING

Abstract:

The recombination enhancer (RE) plays a very important role in yeast mating type switching by ensuring the cell to choose the correct donor. Our previous experiments showed the DNA repair protein yKu80p is an essential regulator for RE function as well as its local chromatin structure. To further understand the molecular mechanism of this protein in switching, we exploited the tandem affinity purification (TAP) approached coupled with multi-dimensional protein identification technique (Mud-PIT) to identify proteins that associate with yKu80p during the course of switching. By comparing the mass-spec results of the switching and non-switching samples, we found that Rvb1p and Rvb2p bind to the yKu80p at early stage of DNA repairing. *In vitro* calmodulin pull down assay confirmed this strong but seemingly transient interaction. Moreover, as indicated in ChIP assay, Rvb1p exhibit a similar dynamic interaction pattern with the left arm of Chromosome III during switching like that of the yKu80p.

We also noticed the recruitment of γ-H2A, supposedly a landmark of double strand break, to the RE region in the very beginning of the switching process. Interestingly, the association of γ-H2A to the RE requires wild type yKu80p.

All the above results support the model proposing that the RE may serve as an entry point for the DSB for homolog searching.

4.1 Introduction

4.1.1 Yeast mating type switching and the function of the RE in donor preference

The haploid yeast cells exist in either of the two mating types: **a** or α which is determined by about 700bp DNA segment in the *MAT* locus on Chromosome III. Besides *MAT*, two other loci also contained the mating type information but they are both transcriptionally silenced. These two loci are called *HML* and *HMR*, located on either the left or the right arm of the same chromosome, respectively.

Yeast mating type conversion displays certain specificity. Switching only occurs in haploid cells during the late G_1 phase of the cell cycle. In addition, only the mother cell which has undergone cell division can switch its mating type (Haber, 1998). Switching begins with an *HO* endonuclease cut near the *MAT* locus. The generated double strand break (DSB) can then be repaired through homologous recombination using either *HML* or *HMR* as templates so that the silent mating type information stored there can be relocated to the active *MAT* region (Haber, 1998).

Mating switching generally follows the rule of "donor preference": **a** cells always choose *HML*α as a template to repair the DNA damage in *MAT* while α cells prefer to recombine with *HMR***a** 90% of the time**.** Previous reports indicated that the **a** and α cells employ different mechanisms to achieve the directionality of recombination (Wu and Haber, 1995; Wu and Haber, 1996). In α cells, the whole left arm of Chromosome III seems to be "cold" for all kinds of recombination. Consequently the *HML* is prevented from being used as a donor and the cell chooses *HMR* by default. On the other hand, in **a** cells, a 40kb large region of the left arm of Chromosome III, including the *HML*, is

activated so as to "out compete" *HMR* which leads it to be selected as the template (Wu and Haber, 1996; Wu et al., 1996).

A DNA element called the recombination enhancer (RE) is found to be vital in donor preference, especially in the **a** cells (Wu and Haber, 1996). This *cis*-acting segment is about 730bp long and located on the left arm of Chromosome III, 17kb from *HML* (Wu and Haber, 1996). The chromatin structure of the RE, is different in **a** and α cells (Weiss and Simpson, 1997). It has been shown that a MNase hypersensitive region flanked by two footprints is a characteristic feature of the RE structure in **a** cells, where RE actively promotes many recombination events on the left arm of Chromosome III. It is believed that this unique "open status" of chromatin may provide an interface for binding of protein required for activation. On the contrary, in α cells where the RE is repressed and the left arm of Chromosome III is inaccessible for recombination, RE is covered with arrays of tightly organized nucleosomes. This structure possibly shields it from interactions with *trans*-acting factors and cause it to be inactive (Weiss and Simpson, 1997) .

By comparing the RE sequence from *Saccharomyces cerevisiae* with its counterparts in *Saccharomyces carsbergensis* and *Saccharomyces bayanus*, Haber's group identified five conserved subdomains: A, B, C, D and E (Sun et al., 2002). Among them the C and D regions are shown to be indispensable for mating switching (Wu et al., 1998). The C region contains a Mcm1p/α2p binding site, while the D and E regions both include tandem repeats of TTT(G/A). Some of these TTT(G/A) stretches are thought to provide the binding site for the transcriptional activator Fkh1p which is essential for the RE function (Sun et al., 2002). A recent study showed that a mere two base pair mutation in

Mcm1p binding site caused drastic changes in the RE chromatin structure and defects in donor preference (Wu et al., 1998). However, when this binding site is substituted with a copper inducible promoter, the RE function is partially recovered when copper is provided in the media (Ercan and Simpson, unpublished). Collectively, it has been proposed that the function of the C region is to open up the chromatin structure in the RE. Binding of Mcm1p may assist such process and allows other trans-acting regulators to access to the region.

There are a few proteins that are known to bind to the RE. Mcm1p, not surprisingly, is crucial for maintaining the RE chromatin structure and its proper function (Wu et al., 1998). In a *mcm1* mutant strain, the characteristic footprints of the **a**-cell RE is lost and the hypersensitive sites becomes less distinguishable (Wu et al., 1998). Another transcriptional activator Fhk1p is also shown to interact with the RE and required for activation of RE in donor preference (Sun et al., 2002). On the other hand, Tup1p, a global organizer of the chromatin structure is also believed to function in establishing a repressive chromatin structure around the RE in α cells. Deletion of *TUP1* results in the loss of positioned nucleosomes around the RE and makes cells lose the ability to select the correct donor *HMR*. In this scenario, *HMR* and *HML* loci are chosen equally (Weiss and Simpson, 1997; Weiss and Simpson, 1998). In Chapter II, we demonstrate that yeast yKu80p, a homolog of human DNA repair protein Ku, is a novel regulator of the RE. The yeast yKu80p binds to the RE both *in vitro* and *in vivo* (Fig. 3.2 and 3.2). Deletion of yKu80p affects the local chromatin structure (Fig. 3.3). More importantly, RE's activity decreases by 40% in *yku80Δ* strain (Fig 3.4 and 3.5).

4.1.2 The repair of DSB

DNA damage caused by *HO* cleavage, ionizing radiation, UV radiation and DNA damaging chemicals can significantly affect the integrity of the genome (Bartek et al., 2004). Cells must use a sophisticated mechanism to sense such damages and repair them before they become deleterious to the cell. There are three major types of DNA damage: a base pair mismatch, thymidine dimer formation and double stranded break (DSB) (Bartek et al., 2004; Bartek and Lukas, 2003). Recent studies suggest that many DNA repair pathways interact with histones or chromatin associated factors and utilize chromatin structure to their advantage (Wuebbles and Jones, 2004). Several lines of evidence from yeast study suggest that acetylation of histone H3 and H4 are involved in DSB repair (Megee et al., 1995; Wuebbles and Jones, 2004). Rapid phosphorylation of a histone H2A species (H2A in yeast; H2AX in higher eukaroyes) coincides with most DSB and is very important step in response to DNA damage (Rogakou et al., 1999). In yeast cell, this event is mediated primarily by protein kinase Mec1p. It occurs very early during DSB repair and spans to a large segment of chromatin (up to 100kb) on both side of the DSB (Downs et al., 2000). Phosphorylated H2A (γ-H2A) may provide an interface for recruiting other protein factors that are involved in DNA repair (Lowndes and Toh, 2005).

There are two distinct but interconnected pathways that cells employ to repair DSB: non-homologous end joining (NHEJ) and homologous recombination (HR) (Collis et al., 2005). In the NHEJ pathway, immediately after DSB formation, a cluster of proteins including yKu80p/yku70p, Mre11p/Rad50p/Xrs2p (the MRX complex) bind to DSB for

protection and further recruit other factors (Aylon and Kupiec, 2004). After end processing, the Lif1p/Dnl4p DNA ligase complex is recruited to the DSB, resulting in ligation of the broken ends (Haber, 1999; Walker et al., 2001). Recently, several groups reported that chromatin modification complexes play essential roles in the early state of this process (Cairns, 2004). They found that phosphorylated H2A at the DSB initiates the recruitment of the INO80 complex, which in turn assists the repair process (Morrison et al., 2004; van Attikum et al., 2004). The cell can also use homologous recombination mechanism to repair the DSB (Haber, 2000). A classic example of this pathway is the repair process during yeast mating type switching, In this progress, several DSB factors such as Rad51p (a ss-DNA binding protein) and Rad52p (5′ to 3′ exonuclease) are necessary for protecting the protruding 3' DNA overhang produced by single-stranded degradation (Miyazaki et al., 2004). Subsequently the ss-DNA can invade the donor sequence and serve as a primer for DNA polymerization. After going through branch migration, reannealing and ligation, the DSB is eventually repaired by using either *HMR* or *HML* as a template. This process leads to the relocation of the donor loci to the *MAT* locus (Haber, 2000).

4.1.3 TAP and Mud-PIT

4.1.3.1 TAP purification

Tandem Affinity Purification (TAP) is a two step purification based on the affinity interaction between protein A and IgG as well as calmodulin and calmodulin binding protein (CBP) (Puig et al., 2001). In this method, the genomic copy of a specific gene is epitope-tagged with the TAP tag containing both protein A and CBP modules separated by a TEV protease cleavage site. The fusion protein along with its binding partners is first

bound to IgG agarose beads though its interaction the protein A module. The complex is then released by TEV protease cleavage. The eluate is then incubated with calmodulin resin in the presence of calcium. The complex is retained on the column through CBP module of tagged protein and is finally eluted with buffer containing EGTA and low salt concentration. This method allows us to rapidly purify high quality complexes from differently cultured yeast cells.

4.1.3.2 Mud-PIT mass spectrometry

Multi-dimensional Protein Identification Technology (Mud-PIT) mass spectrometry revolutionized the protein identification by providing a tool to rapidly identify proteins in a relative complex mixture (Washburn et al., 2001). This technique couples biochemical separation with mass spectrometry. Rather than use traditional 1-D or 2-D gel electrophoresis, MudPIT separates digested peptides using tandem liquid chromatography which are directly interfaced with the ion source of a mass spectrometer. This is especially advantageous in characterizing a protein complex because it eliminated the subjective sample handling and can forgo the elution step from polyacrylamide gel which unavoidably causes the partial loss of the samples.

In this study, we sought to search for the proteins which are dynamically interact with yKu80p during switching, then follow the functional links thereafter to understand the molecular mechanism of yKu80p in this process. By comparing proteins that co-purified with yKu80p under switching and non-switching conditions, we found that Rvb1p and Rvb2p, two essential subunits of Ino80.com, bind to the yKu80p at the early stage of DSB repair. This interaction was confirmed by calmodulin pull down assay. Furthermore, using ChIP analysis, we demonstrated that Rvb1p binds to the active RE in a yKu80p

dependent manner. In addition, it exhibits a directional movement from the RE to *HML* during switching, similar to yKu80p. We also discovered that γH2A, the landmark of the DSB is transiently enriched at RE at the beginning of switching and that yKu80p is required in this process.

Several pieces of evidence in this study implied INO80's involvement in mating type switching. Indeed, besides Rvb1p and Rvb2p, another key component of this complex, Arp5p, affects donor preference. However, it is not required for the enrichment of γH2A at RE. This leads us to speculate that instead of acting at the beginning of switching, INO80, with its nucleosome mobilization activity, may function in later homolog searching process.

4.2 Materials and methods

4.2.1 Yeast strains and media

The yeast strains used in this study are isogenic (except the *MAT* locus). **CWWT** *(ho HMLα MATa hmrΔ::HMRα-B ade1-100 ura3-53 leu2-3,112*) (S. Ercan, unpublished); **YCR701**(*ho HMLα MATa hmrΔ::HMRα-B ade1-100 ura3-53 leu2-3,112 YKU80*-TAP *KANMX6*); **YCR601***(MATa ade 2-101, ura3-52, his3-200, leu2-1, trp1-63, lys2-1 YKU80:: KANMX6)*; **YCR702** (*ho HMLα MATa hmrΔ::HMRα-B ade1-100 ura3-53 leu2-3,112 RVB1-myc KANMX6*); **YCR703** (*ho HMLα MATα hmrΔ::HMRα-B ade1-100 ura3-53 leu2-3,112 YKU80 URA3, RVB1-myc KANMX6*); **YCR704** (*ho HMLα MATα hmrΔ::HMRα-B ade1-100 ura3-53 leu2-3,112 YKU8::URA3, RVB1-myc KANMX6*); **YCR705** (*ho HMLα MATa hmrΔ::HMRα-B ade1-100 ura3-53 leu2-3,112 RVB13*-TAP *KANMX6*); **YCR706** (*ho HMLα MATα hmrΔ::HMRα-B ade1-100 ura3-53 leu2-3,112, RVB1-myc KANMX6*); **YCR707***(ho HMLα MATa hmrΔ::HMRα-B ade1-100 ura3-53 leu2-3,112 arp5::KANMX6*); **YCR603** *(ho HMLα MATa hmrΔ::HMRα-B ade1 112 lys5 leu2-3 ura3-52 trp1::hisG ade3::GAL HO YKU80::KANMX6 FKH1::URA3-1)***; YCR708** *(ho HMLα MATa hmrΔ::HMRα-B ade1 112 lys5 leu2-3 ura3-52 trp1::hisG ade3::GAL HO YKU80::KANMX6 YKU70::URA3-1)*. Strains used for the mating type switching assay are derived from DBY745 (Wu and Haber, 1995). Synthetic medium containing the appropriate supplements was used to select the deletion or epitope tagged proteins. The deletion and epitope tagged strains were generated by the standard one-step PCR method (Longtine et al., 1998).

4.2.2 Switching assay

Cells were grown to OD600 of 0.8 in 3% lactic acid media. *HO* expression was induced by adding 2% galactose to the media for 40 minutes. Cells were then changed to 2% dextrose media to stop *HO* cutting and start switching. The efficiency of switching was analyzed by DNA extracted from cells collected 2 hours after the start of switching, cut with *BamHI* and *HindIII* and then analyzed by Southern blots.

4.2.3 TAP purification of yKu80p and mass spectrometry

The TAP purification of yKu80p was carried out mainly as previously described (Puig et al., 2001) with minor modifications. Cells were collected 15 minutes after transferred to the dextrose media and lysed mechanically with glass beads in extraction buffer (40mM HEPES pH7.5, 350mM NaCl, 10% Glycerol, 0.1% Tween20). Soluable proteins were cleared by centrifugation at 12,000 rpm for 30 minutes followed by ultracentrifugation at 40,000 rpm for 90 minutes. The supernatant was then incubated with IgG sepharose beads at 4°C for 2 hours. The proteins bound to beads were washed with 30 ml IPP150 (10mM Tris-HCl pH 8.0, 150mM NaCl, 0.1% NP40) and 10mM TEV buffer (10mM Tris-HCl pH 8.0, 150mM NaCl, 0.1% NP40, 0.5mM EDTA, 1mM DTT). Proteins bound to IgG beads were eluted by incubating the beads with 100U TEV at 16°C for 3 hours. The eluate was then mixed with calmodulin beads in calmodulin binding buffer (CBB: 10mM Tris-HCl pH 8.0, 150mM NaCl, 0.1% NP40, 10mM β-Me, 1mM MgAc, 1mM imidazole, 2mM CaCl2) at 4°C for 2 hours. The beads were washed with 30ml of CBB and eluted with 5 times 200μl of calmodulin elution buffer (CEB: 10mM Tris-HCl pH 8.0, 150mM NaCl, 0.1% NP40, 10mM β-Me, 1mM MgAc, 1mM imidazole, 2mM EGTA). Proteins from TAP eluate were resolved using 10% SDS-PAGE and silver

stained. The factions of the purified complex were TCA precipitated and subject to Mud-PIT analysis by the Mass-Spectrometry facility at the Stowers Institute for Medical research.

4.2.4 Calmodulin pull-down and western blotting

Cells were collected at OD of 0.8 and resuspended in WCE buffer (50mM Tris pH8, 5mM EDTA, 0.8M NaCl, 15% glycerol, 0.01% NP40, 10mM DTT, 1mM PMSF, 1mM benzamidine-HCl, 10μg leupeptin, 10μg aprotinin, 1μg pepstatin). Subsequently, cells were mechanically lysed by vortexing with glass beads 6 times for 30 seconds with 1 minute intervals. Soluble proteins were separated by centrifugation at 14,000 rpm for 10 minutes at 4°C. Whole cell extracts were then incubated with calmodulin beads in the presence of calcium for 2 hours at 4°C. After washing with calmodulin binding buffer, proteins were eluted by SDS loading buffer. Purified proteins were separated on a 11% SDS-PAGE protein gel and transferred to nitrocellulose membrane and blotted with HRP conjugated anti-*myc* antibody. The result was visualized using the ECL detection kit (Amersham Biosciences).

4.2.5 Chromatin Immunoprecipitation (ChIP)

At different time points during the switching, cells were collected by centrifugation and cross-linked with 3% formaldehyde for 15 minutes at room temperature. Crude chromatin was extracted by disrupting the cells with glass beads which was then sheered by sonication to yield ~500bp fragments. The sonication was done using Branson Sonifier 450 at setting of 40% output, 90% duty cycle and with 15 times 12 second cycles. After reverse cross-link, all input DNA was checked on 2% agarose gel. The

antibodies used in the immunoprecipitation are: polyclonal antibody against γ-H2A (Upstate) and monoclonal anti-*myc* antibody mouse 9E10 (Upstate).

4.2.6 Quantitative PCR

The length of the primers were designed to be 21-23-mers, with average Tm of 58°C. Primer sequences are available upon request. The quantitative PCR was carried out as previously described (Li and Reese, 2001) with minor modification. The PCR cycles were as below: after incubating at 94°C for 5 minutes for denaturing, DNA was amplified for 25 cycles at 94°C for 30 seconds, 55°C for 30 second and 72°C for 45 seconds, followed by an extra 5 minutes extension at 72°C. The input DNA used in this reaction was diluted to 1/200, while dilution of the immunoprecipitated DNA is 1/40. The PCR products were then loaded to a 2% agarose gel containing ethidium bromide and detected by Typhoon (Amersham). All the quantification was done with Image Quant v5.0 software (Molecular Dynamics).

4.3 Results

4.3.1 Identification of proteins that dynamically associate with yKu80p upon *HO* cleavage

To better understand the role of yKu80p in donor preference, we began by looking for the proteins which are only associated with yKu80p during mating switching process. Our hope was that these factors may act in concert with yKu80p to regulate the RE function.

The TAP method was chosen because of its versatility and high quality. We tagged the yKu80p with a *C*-terminal TAP epitope in a strain which contains an *HO* gene under the control of the *GAL10* promoter. This strain enables us to artificially trigger the mating type switching. yKu80p and its associated factors are then isolated at a certain time point during the course of switching. We are especially interested in those proteins that associate with yKu80p at the beginning of switching. These proteins presumably should be involved in the initiation of HR repair.

Yeast cells were grown to early log phase in lactic acid media. The expression of *HO* was induced by adding 2% galactose to the culture for 40 minutes. During this period, a DSB was generated within the *MAT* locus. Cells were then changed into 2% glucose media to shut down the expression of *HO* and begin the DSB repair and recombination. 15 minutes after the start of switching, cells were harvested and subjected to TAP purification. The same strain grown under the uninduced condition also underwent the same purification process to serve as a negative control.

Proteins purified from both induced and uninduced situations were separated by SDS-PAGE electrophoresis and visualized by silver staining. As shown in Fig. 4.1, only two major bands with the size corresponding to that of yKu80p-CBP and yKu70p were detected in the non-switching cells. In contrast, multiple bands were observed in the switching sample, indicating that there are some proteins which dynamically bind to YKu80p/Yku70p during DSB repair. Both samples were then precipitated with TCA and subjected to Mud-PIT mass spectrometry analysis.

As shown in Table 4-1, we were able to detect multiple peptide hits of yKu80p and yKu70p from both samples, which is a good indication since we know that yKu80p/yKu70p forms an stable and static heterodimer. This also validates our experimental scheme and methodology. Using the software "CONTRAST", we compared the two Mud-PIT data sets. There are 35 proteins that are only present in the switching sample but not in the non-switching one. Four proteins previously reported to bind to yKu80p and involve in DSB repair are identified in this study (Table 4-1, colored in purple): Sir4p has been shown to relocate from telomere to DSB immediately after the *HO* cleavage along with yKu80p (Martin et al., 1999); Lif1-Dnl4, a DNA ligase complex involved in DSB repair, works in concert with yKu80p and yKu70p to promote the end joining process (Herrmann et al., 1998); In addition, the replication origin binding protein Rap1p is also known to associate with yKu80p and regulate DNA replication (Cosgrove et al., 2002). This indicates that the proteins we found in the Mud-PIT analysis are indeed the *bona fide* partners of yKu80p during switching.

Interestingly, two proteins, Rvb1p and Rvb2p, appear to be specifically present in the induced sample. They are the yeast homologs of bacterial RuVB proteins that is involved

in recombination and resolving Holliday Structure (Yamada et al., 2002; Yamada and Morikawa, 2002). Rvb1p, an ATP dependent 3'-5' helicase, is known to be present in two chromatin remodeling complexes, the INO80 complex and the SWR1 complex (Mizuguchi et al., 2004; Shen et al., 2000). INO80 possesses an ATP dependent nucleosome mobilizaton activity (Shen et al., 2003b) and has been shown to be recruited to the DSB after *HO* cutting (Morrison et al., 2004; van Attikum et al., 2004). Rvb1p and Rvb2p can also form a small complex containing only themselves and Yhr034c (Jonsson et al., 2004). However, we did not identify any other subunits from either the SWR1 complex or the small complex (Yhr034c) to be associated with yKu80p. Instead, we detected Arp5p and Arp8p (Table 4-1, colored in blue), which are presumably INO80 specific subunits. Despite missing the catalytic subunits, we did find multiple subunits from one particular complex. The functional involvement of INO80 in DSB repair leads us to speculate that the INO80 complex might dynamically interact with yKu80p and influence donor preference.

The other identified proteins included many enzymes contributing to carbohydrate metabolism (Table 4-1, colored in yellow). At this point, we did not consider these proteins relevant to mating type switching. We attribute their detection to the significant alteration of carbohydrate metabolism caused by carbon source changes during switching induction (from lactic acid to galactose then to glucose).

4.3.2 Rvb1p transiently interact with yKu80p at the beginning of the switching

To confirm this dynamic interaction between yKu80p and Rvb1p, we decided to exploit calmodulin pulldown technique to monitor the association of yKu80p and Rvb1p during the course of switching. A strain carrying both *myc-RVB1* and *TAP-YKU80* was

generated in the background of the *HO* gene under the control of the *GAL10* promoter. Cells were grown to an OD of 0.8 in lactic acid media. 2% galactose was then added to start the *HO* expression. After 40 minutes, cells were spun down and resuspended in YPD (2% dextrose) media to stop *HO* cutting and allow the DSB to be repaired. At different time points (-40, 0, 15, 30, 45 and 60 minutes) from the start of switching, cells were collected and whole cell extracts were made using the glass-beads disruption method. The extracts were then directly incubated with calmodulin beads in the presence of calcium for 2 hours at 4°C. After extensive washing, proteins were eluted with SDS-PAGE loading buffer and subjected to western blotting using anti-*myc* antibody and Peroxidase anti Peroxidase (PAP). As shown in Fig. 4.2 A, the steady level of yKu80p throughout the course of experiment indicates that our pull-down procedure is quantitative. No Rvb1p was detected with yKu80p before the *HO* cleavage. However, after the galactose induction, we began to see a robust signal, indicating a strong binding of the Rvb1p and yKu80p at this point. Their association remains till 15 minutes after the beginning of DNA repair and drops to background level after 30 minutes. This suggests that the Rvb1p transiently interact with yKu80p at the beginning of switching.

4.3.3 yKu80p is required for the binding of the Rvb1p to RE

The next question is whether the yKu80p-bound Rvb1p can also be recruited to the RE. A yeast strain containing genomic tagged *myc-RVB1* was cross-linked with formaldehyde and subjected to chromatin immunoprecipitation (ChIP) assay using an anti-*myc* antibody. Precipitated DNA was amplified by quantitative PCR using primer set covering the RE region (Fig. 3.2 A). As shown in Fig. 4.3, Rvb1p can only be cross-linked to the RE region in **a** cells (middle panel) but not α cells. To demonstrate the

stringency of our ChIP, we included two negative controls in this experiment. As expected, we did not detect any significant cross linking signal of Rvb1p with either the region 5 kb from the RE or the telomere. The similar occupancy between yKu80p and Rvb1p at the RE make us wonder if there is any interdependency of those two factors. This is indeed the case as we showed that the binding of the Rvb1p to the RE is completely abolished in a *yku80* deletion strain (Fig. 4.3 middle panel), indicating that the presence of Rvb1p at the RE is dependent upon yKu80p. The dependency is either through direct interaction or the binding of yKu80 making the RE accessible to Rvb1p.

The rationale we used to focus on the involvement of the INO80 complex at the RE is based on the assumption that Rvb proteins only exist in two known complexes Ino80.com and Swr1 complex (Korber and Horz, 2004; Shen et al., 2000). Although we ruled out the likelihood of the SWR1 complexes playing a role in switching, it is still possible that another Rvb1p containing complex, instead of the Ino80 complex, may participate in the switching process. To identify all the proteins associated with Rvb1p in **a** cells, we decided to purify Rvb1p containing complexes using a strain bearing a *C*-terminal TAP tagged Rvb1p. The resulting protein complexes were separated by 11% SDS-PAGE and visualized by silver staining. In Fig. 4.4, it shows that this mixture contains two major bands corresponding to Rvb1p and Rvb2p. Further Mud-PIT analysis revealed a comprehensive list of proteins which associate with Rvb1p (Table 4-2). Besides known subunits of the INO80 and SWR1, we also detected a novel protein Yhr034c which can also form a complex with Rvb1p. While this study was carried out, another independent report also reached the same conclusion (Jonsson et al., 2004). Intriguingly, under switching condition, neither Yhr034c nor any unique components of SWR1 complex

were detected to interact with yKu80p, indicating that they may not be involved in homologous recombination. Moreover, in this experiment, we did not identify yKu80p to be associated with Rvb1p. Given the fact that we also failed to detect any association between Rvb1p and yKu80-TAP under non-switching condition in our previous mass spectrometry analysis, we believe that this interaction must be conditionally and happens only upon the induction of switching.

4.3.4 Dynamic interaction of Rvb1p and the left arm of Chromosome III during switching

One of the prevailing hypotheses of donor preference proposed that the RE plays an important role in DSB homolog searching (Haber, 1998). It suggested that the RE may serve as an entry point for the DSB to the left arm of Chromosome III and assist it in finding the correct donor *HML*. The model is supported by our previous finding that the yKu80p, bound to both the RE and DSB, appeared to migrate from the RE towards *HML* along the left arm of the Chromosome III during switching. This movement is directional as it only goes towards the *HML* but not *HMR*.

Rvb1p was shown to interact strongly with yKu80p in the beginning of the switching process (Fig. 4.2). Considering the chromatin remodeling activity of INO80, it is reasonable to hypothesize that it might facilitate DSB migration during switching (Cairns, 2004). Therefore, we wonder if Rvb1p displays a similar movement pattern as that of the yKu80p. To this end, *myc*-epitope tagged Rvb1p was introduced into **a** cells with *HO* under the control of a *GAL10* promoter. Switching was induced as described above. At different time points (10, 25, 40, 60 and 90 minutes) after the beginning of switching, we collected cells. They were then cross-linked with formaldehyde and subjected to ChIP

assay. Primer sets were designed to specifically amplify the RE sequence and regions 2kb *HMR* proximal, 5kb and 11kb *HML* proximal and *HML* locus . Beginning as early as 10 minutes after the start of switching, as shown in Fig. 4.5A, we started to detect the cross-link signal of the Rvb1p at RE. This signal intensifies at the 25 minutes time point then fades away after 40 minutes. Rvb1p's interaction with the region 5kb proximal to *HML* peaks also about 25 minutes after the beginning of DNA repair whereas its association with the region11kb *HML* proximal does not reach its summit until 40 minutes. The cross-link signal of Rvb1p and the *HML* becomes strongest 60 minutes after the start of switching and the signal decreased to a great extent at the 90 minutes time point when the process of recombination is almost completed. These results suggest that, like yKu80p, Rvb1p directionally moved from the RE to the *HML*. Furthermore, no noticeable signals were produced on the locations above 2 kb *HMR* proximal from the RE region. This is consistent with the fact that the RE only assists the donor preference in **a** cells where the *HML* is the destined donor.

In conclusion, the dynamic interaction pattern of Rvb1p and the left arm of Chromosome III strikingly resembled that of the yKu80p. In addition, yKu80p is essential for recruiting Rvb1p to the RE. These results indicate that they might work together in homologous recombination.

4.3.5 γH2A is recruited to the RE in a yKu80p dependent manner

Based on the entry point model, we predicted that DSB should be recruited to the RE upon *HO* cleavage to start the homolog searching. If this scenario is true, we would expect that some DSB landmarks would be cross-linked to the RE during switching.

Both yKu80p and Rvb1p have been shown to be associated with the DSB and play important roles in mending the broken ends of DNA (Martin et al., 1999; Morrison et al., 2004). More importantly, consistent with the entry point hypothesis, we showed that both of the proteins also bind to the RE. One of the most significant features of broken DNA end is the enrichment of phosphorylated H2A (γ-H2A) (Lowndes and Toh, 2005). In an attempt to test the entry point hypothesis, we decided to exploit the ChIP technique to monitor the behavior of γ-H2A, as a DSB marker at the beginning of switching.

In this experiment, we used the artificial switching system with a *GAL10* controlled *HO* gene. Switching was induced as previously described. Before induction and at different time points (0, 15, 30, 45 and 60 minutes) into the switching, cells were collected and fixed with formaldehyde. Extracts were subjected to immunoprecipitation using polyclonal anti-γH2A antibody. Primers amplifying both the *MAT* and RE loci were designed to detect γH2A bound DNA. As expected, there is no phosphorylated H2A signal in either RE or *MAT* before *HO* expression (Fig. 4.6A and 4.6B). Immediately after the generating of DSB, signal was detected at the DSB locus indicating the enrichment of γH2A which is consistent with previous reports (Morrison et al., 2004). At this time, however, we did not detect any γH2A in the vicinity of the RE (Fig. 4.6B). The interaction of the γH2A and the DSB intensified until it reached its peaks 15 to 30 minutes after the beginning of switching (Fig. 4.6A). During this period of time, a strong cross-linking signal also emerged in the RE region. In contrast to the gradual decrease of the interactions between the DSB and γH2A, its contact with the RE seems to be very transient. Since yKu80p is an important protein regulator for the RE, we speculated that yKu80p may also play a role in the recruitment for the DSB to RE. To test this

hypothesis, we measured the enrichment of γH2A at DSB and the RE in the absence of the yKu80p.

Strains bearing *HO* under the control of *GAL10* promoter were deleted of either*YKU80* or *YKU80/YKU70*. They were grown to early log phase and their mating type was switched as previous described. 15 minutes into the beginning of switching, cells were collected and cross-linked for ChIP assay using polyclonal anti-γH2A antibody. As shown in Fig. 4.7A, left panel, deletion of yKu80p or yKu70p/80p does not appear to affect the enrichment of γH2A at DSB. In contrast, the interaction of γH2A and the RE is completely abolished in *yku80* and *yku80/70* strains (Fig. 4.7A, right panel). This data strongly suggests that yKu80p is the determinant in bringing the γH2A to the RE region.

In conclusion, our result provides another piece of evidence to support the hypothesis that the RE acts as an entry point for DSB and yKu80p plays an important role in this process.

4.3.6 Involvement of INO80 in mating type switching

Physical interaction between multiple subunits of INO80 (Arp5p, Arp8p, Rvb1p and Rvb2p) and yKu80p upon *HO* cleavage makes us suspect that INO80 might be involved in mating type switching. To test this idea, we chose to examine switching without a functional INO80 complex. To this end, a strain deleted of Arp5p is used. Arp5p is essential for the function of INO80 in both DNA repair and nucleosome remodeling since it is required for the binding of INO80 to nucleosome (Shen et al., 2003a).

In this study, yeast strain carrying the artificial switching system with a background of *ARP5* deletion (YCR707) was grown to OD of 0.6 before switching was induced.

Genomic DNA was then extracted and subjected to donor preference analysis. As expected, the deletion of Arp5p causes a significant defect in donor preference: the usage of *HML* dropped from 90% in wild type cells to 40% in *arp5* strain (Fig. 4.8). This data suggested that a functional INO80 is essential for correct mating type switching. However, Arp5p does not seem to be required for the enrichment of γH2A at RE. As shown in Fig. 4.7A, a strong cross-linking signal of γH2A was detected in the RE region in the absence of Arp5p. Considering the nucleosome mobilization activity of INO80, it is likely that, instead of participating in the recruitment of the DSB to the RE, the complex may be involved in later steps of switching like the homolog searching. In conclusion, INO80 complex may play an important role in regulating mating type switching. However, it might not be required in the early stage of the event.

4.4 Discussion

RE plays a very important role in determining which donor (*HML* or *HMR*) is used during yeast mating type switching (Wu et al., 1998). One of the proteins that regulate its function is yKu80p. In an effort to understand the molecular mechanism of yKu80p, we used a TAP approach together with Mud-PIT technique to identify novel proteins that interact with yKu80p during switching. Besides known yKu80p binding factors, Rvb1p, Rvb2p have been revealed to associate with yKu80p upon *HO* cleavage. Rvb1p, a homolog of bacterial RuvB helicase, is component of at least two nucleosome remodeling complexes: INO80 and SWR1 (Korber and Horz, 2004; Shen et al., 2000). The INO80 complex has been shown to bind to the DSB and involved in the non-homologous DNA damage repair (Morillon et al., 2003; van Attikum et al., 2004). In addition, it has been found to regulate the homologous recombination in *Arabidopsis* (Fritsch et al., 2004). The SWR1 complex, on the other hand, is involved in the deposition of histone variant Htz1p and the establishment of heterochromatin (Korber and Horz, 2004). Recently, a novel "light" Rvb1p containing complex has been found to contain only Rvb1p, Rvb2p and YHR034cp (Jonsson et al., 2004). Both Arp5p and Arp8p, which exist exclusively in the INO80 complex, were detected to associate with yKu80p by our Mud-PIT analysis. In contrast, none of the specific components of the other two complexes was identified. More importantly, we demonstrated that active INO80 is required for proper donor selection. This implies that like its plant counterpart, the yeast INO80 complex may play a role in homologous recombination and switching in conjunction with yKu80p.

Nevertheless, at this point, we can not rule out the possibility that other Rvb1p containing complexes might also be involved.

In addition, we showed that a functional INO80 is not required for introducing the γ-H2A to the RE (Fig. 4.7A), suggesting that INO80 regulates donor preference at a post-entry point step. Since INO80 does possess nucleosome mobility activity, we speculate that it may promote DSB migration and the homolog searching process.

Our experiments showed that Rvb1p interacted with yKu80p at the beginning of the switching and is subsequently recruited to the RE. Moreover, it also displays similar directional movement pattern like that of the yKu80p, indicating that they might work together in facilitate the homologous searching of the DSB. However, in spite of migrating together, the interaction between yKu80p and Rvb1p seemed to be transient and restricted in the beginning of the switching. Since the "recombisome" associated with the DSB is a massive complex, we speculate that in the course of switching, there might be some conformational change and yKu80p may not be tightly associated with Rvb1p in the later stage of the recombination.

The recruitment of γ-H2A to the vicinity of the RE at the beginning of switching is a very intriguing result. Because if indeed, γ-H2A can be used as a marker for DSB, it would greatly support the hypothesis that the RE served as an entry point and facilitated the homolog searching process. We showed that the phosphorylation of H2A at RE occurs in the early stage of switching. However, no cross-link signals of either yKu80p or Rvb1p was detected at this point, although both of them have been shown to bind to the RE before the start of switching. We believe that this may due to the masking of the *myc* epitope by other proteins. Because as indicated by the γ-H2A ChIP data, the DSB with all

the proteins associated with it might invade the RE region at this moment. Another interpretation of the enrichment of γ-H2A at the RE is that H2A is locally phosphorylated by Mec1p or Tel1p, possibly mediated by yKu80p. It has been shown that the human homolog of yKu80p, the Ku complex, contains a DNA-dependent protein kinase (DNA-PK) subunit. However, until present, no such DNA-PK has been found in yeast (Collis et al., 2005).

Figure 4.1 TAP purification of yKu80p during switching and non-switching situations.

Yeast strains containing TAP tagged yKu80p (YCR701) were grown to OD of 0.8 then induced to switching as described previously. Cells were collected 15 minutes after the start of switching and subjected to TAP purification. The same culture that did not undergo induction was used as a control. Two elution conditions with different concentration (150mM and 500mM) of NaCl were used in the purification, as indicated on top of each gel. 10% of the purified yKu80 complex was separated with 11% SDS-PAGE and visualized by silver staining. The arrows show the two protein bands whose sized corresponding to that of the TAP-yKu80p and yKu70p.

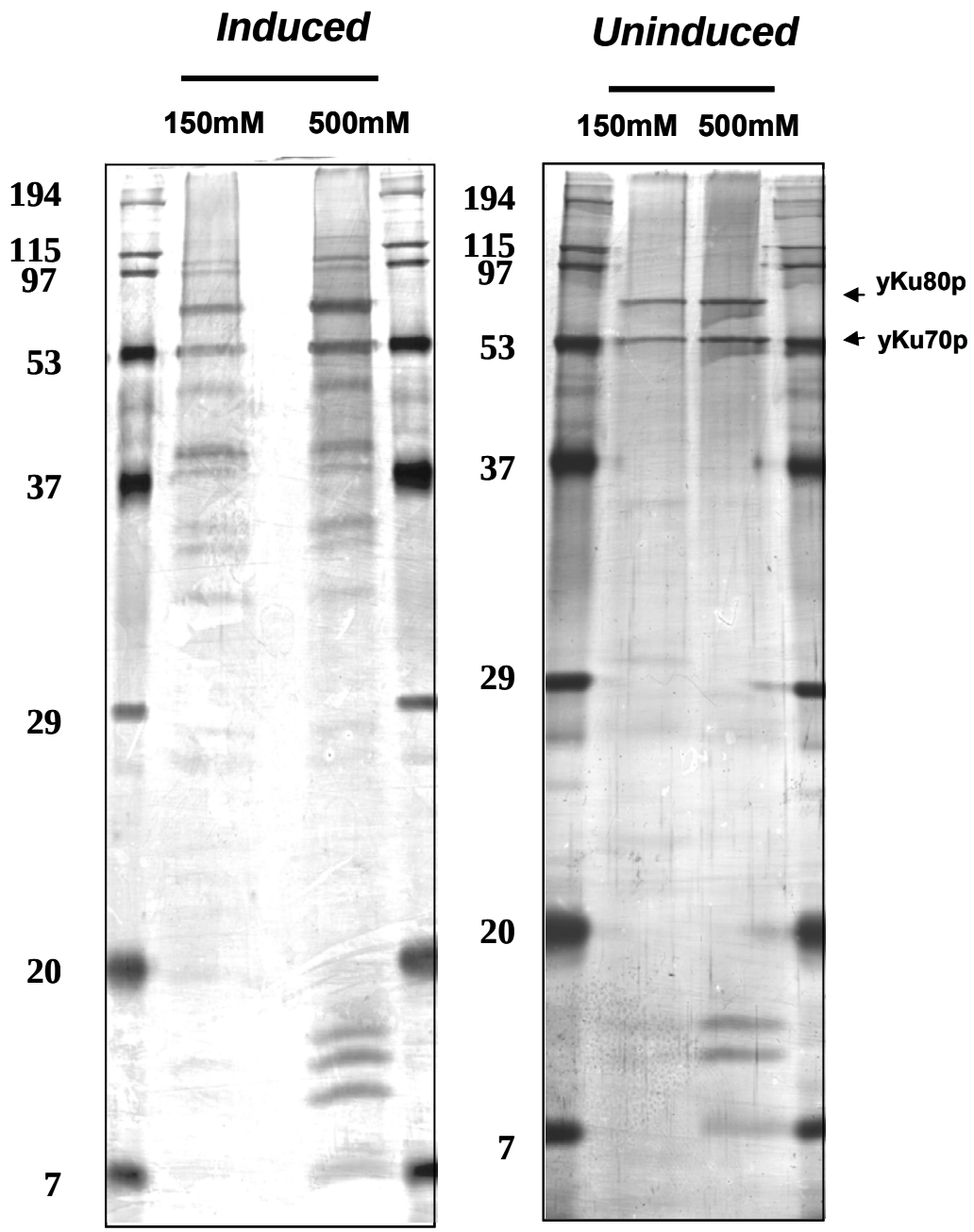
Induced
Uninduced
150mM
500mM
150mM
500mM
194
115
97
53
37
29
20
7
194
115
97
53
37
29
20
7
yKu80p
yKu70p

Figure 4.2: Transient interaction between Rvb1p and yKu80p strongly at the beginning of switching.

(A) Yeast strain containing TAP-tagged yKu80p and *myc*-tagged Rvb1p (YCR703) were grown to OD of 0.8 before it was induced for mating type switching. At different time points during this process (-40, 0, 15, 30, 45 and 60 minutes), cells were collected and subjected to protein extraction. TAP-yKu80 was affinity purified using calmodulin beads. Proteins eluted from the calmodulin column were separated on 11% SDS-PAGE gel, subsequently transfer to nitrocellulose membrane and subjected to western blotting using anti *myc* antibody. (B) The signal of the interaction between yKu80p and Rvb1p was quantified using ImageQuant. Error bars indicate three independent experiments.

A.

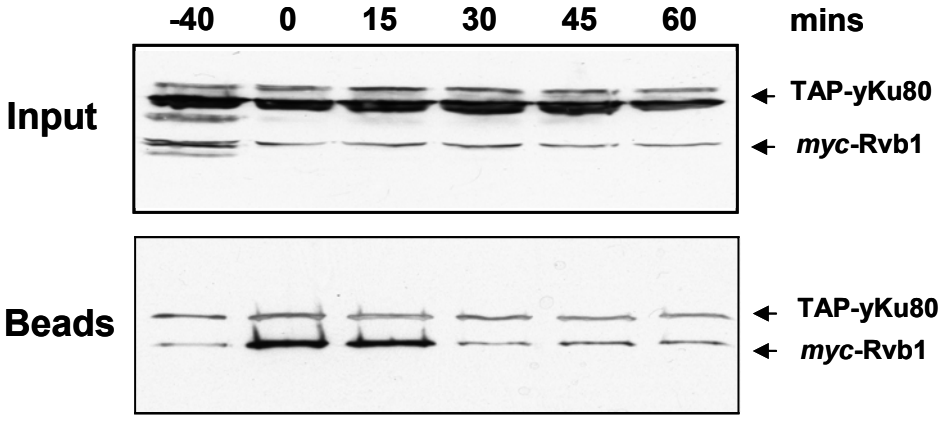
-40
0
15
30
45
60
mins
Input
TAP-yKu80
myc-Rvb1
Beads
TAP-yKu80
myc-Rvb1

B.

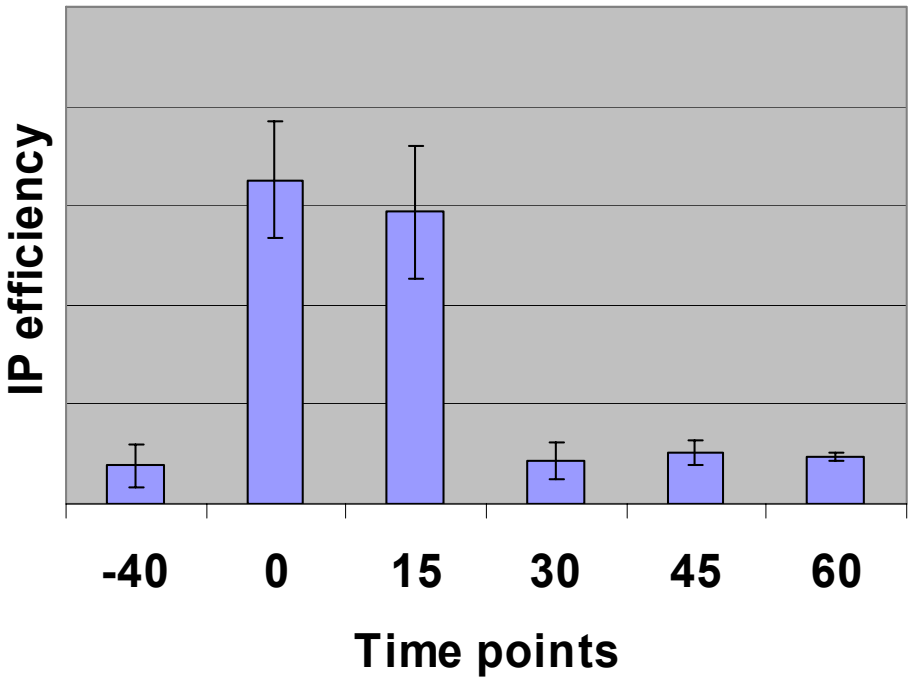
IP efficiency
-40
0
15
30
45
60
Time points

Figure 4.3: yKu80p is required for the binding of the Rvb1p to the RE.

ChIP assay was performed on strains containing *myc*-epitope tagged Rvb1p in **a** cells (YCR702), α cells (YCR703) and the *yku80* deleted **a** cells (YCR704). Cells were grown to OD of 1 before formaldehyde fixation and sonication. The chromatin fragments were then immunoprecipitated by anti-*myc* antibody. Quantitative PCR was carried out using primers that amplify the RE region.

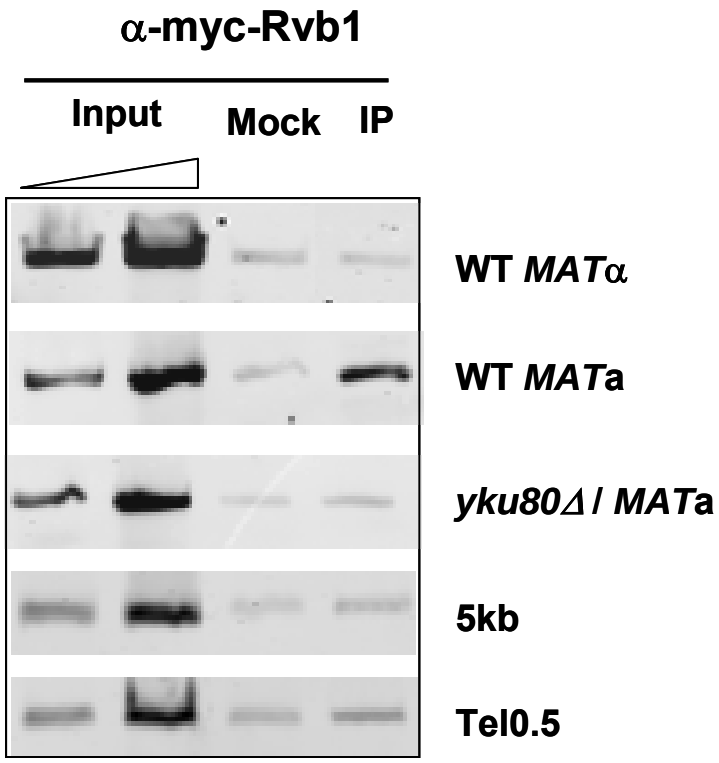

Figure 4.4: TAP purification of Rvb1p.

Yeast strain carrying *N*-terminal TAP tagged Rvb1p (YCR705) was grown to OD of 1.0. Cells were collected and subjected to TAP approach as described previously. The purified complex was separated by 11% SDS-PAGE and visualized by silver staining. The arrow indicates the protein band corresponding to the size of Rvb1p.

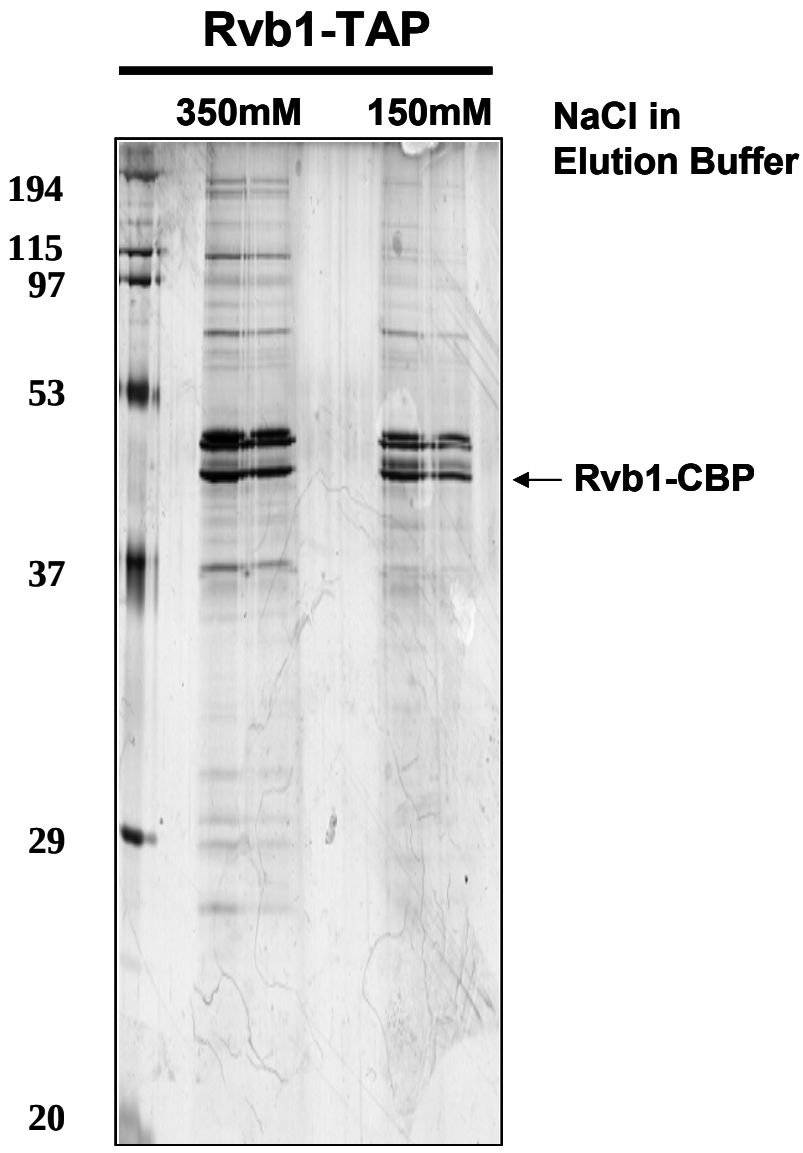

Figure 4.5: Dynamic interaction of Rvb1p and the left arm of Chromosome III during switching.

(A) A yeast strain containing a *myc*-tagged Rvb1p (YCR706) was induced for mating-type switching as described before. Cells were collected at 10, 25, 40, 60 and 90 minutes after the start of switching. DNA was extracted and subjected to ChIP analysis using primers designed to amplify regions of the RE, *HML*, 5kb and 11kb away from RE the *HML* proximal and 2Kb from the RE *HMR* proximal (see Fig.3.7 B) (B) DNA input of the above experiments. This experiment was repeated once with similar results.

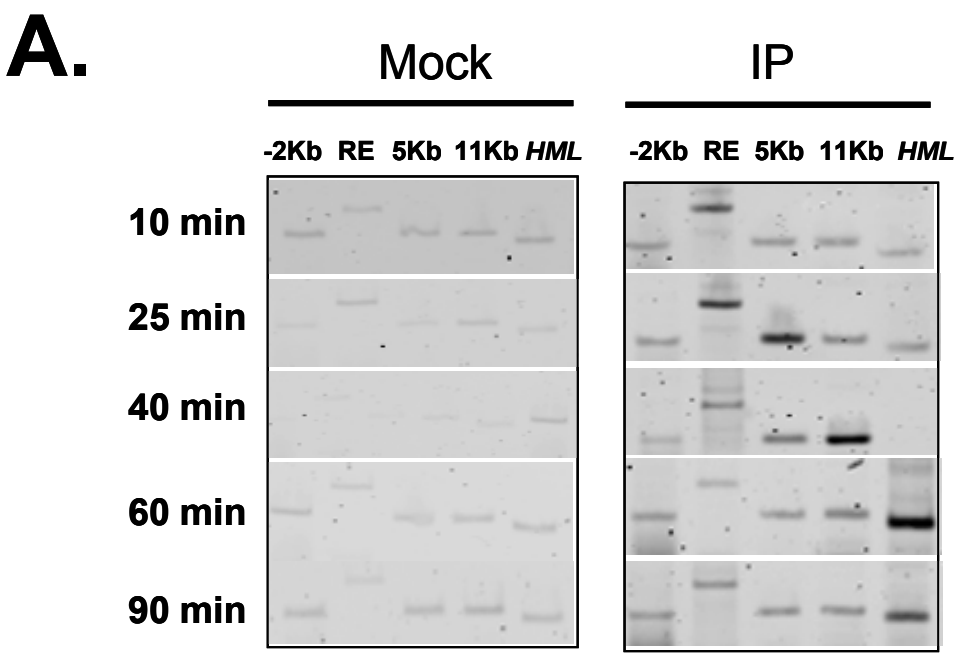
A.
Mock
IP
-2Kb RE 5Kb 11Kb HML
-2Kb RE 5Kb 11Kb HML
10 min
25 min
40 min
60 min
90 min

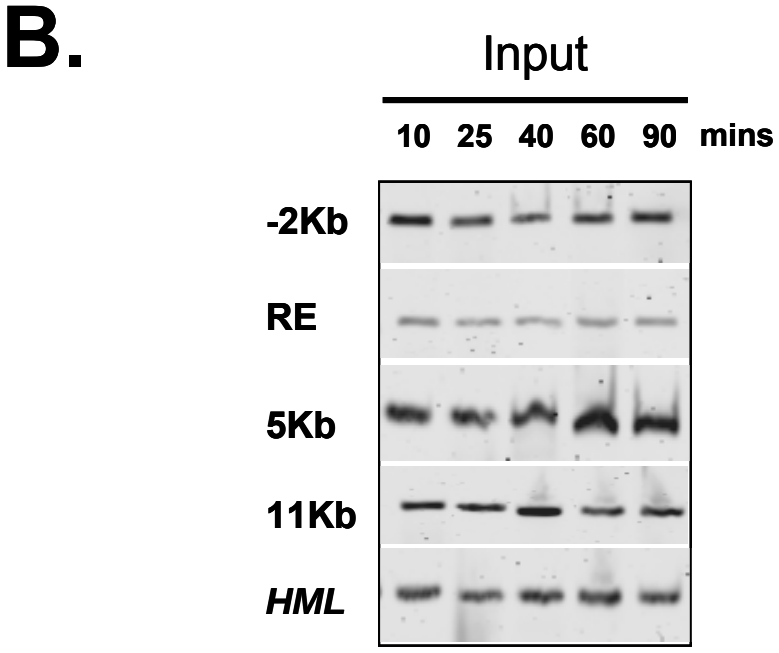
B.
Input
10 25 40 60 90 mins
-2Kb
RE
5Kb
11Kb
HML

Figure 4.6 γ-H2A is recruited to the RE region during the beginning of switching.

(A) The dynamic recruitment of γ-H2A to the DSB. Yeast cell carrying the artificial switching system (CWWT) was grown to OD of 0.8 and mating type switching was induced as described. At different time points of this process (-40, 0, 15, 30 and 45 minutes after switching), cells were collected and subjected to formaldehyde fixation and ChIP assay. Immunoprecipitation was performed using polyclonal anti γ-H2A antibody. PCR primers were designed to amplify the region adjacent to the *HO* cutting. Error bars represent three independent experiments. (B) γ-H2A is recruited to the RE during switching. ChIP assay was executed as described above and quantitative PCR was performed using primers covering the RE region.

A.

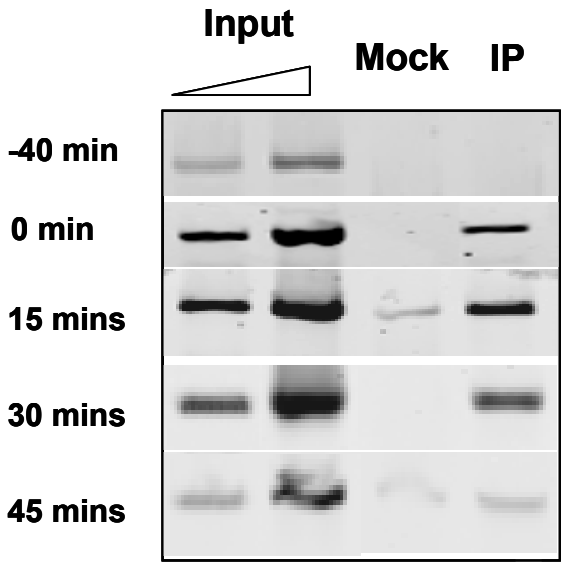
DSB locus
Input
Mock
IP
-40 min
0 min
15 mins
30 mins
45 mins

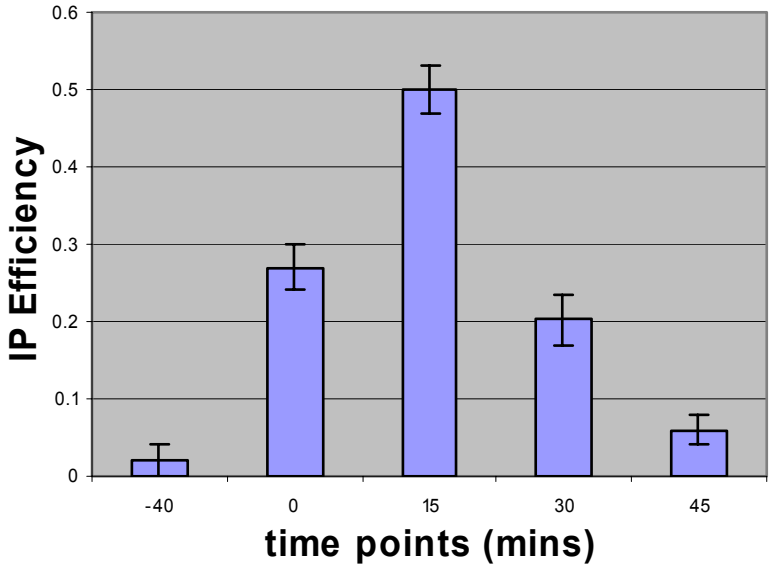
IP Efficiency
0.6
0.5
0.4
0.3
0.2
0.1
0
-40
0
15
30
45
time points (mins)

B.

RE locus

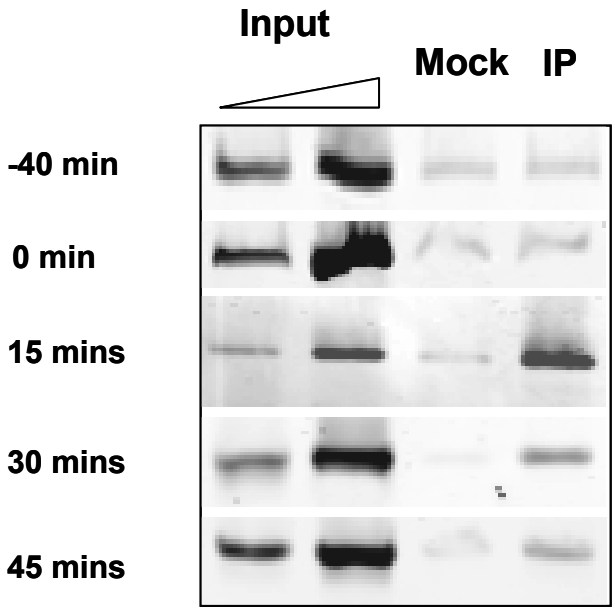
Input
Mock
IP
-40 min
0 min
15 mins
30 mins
45 mins

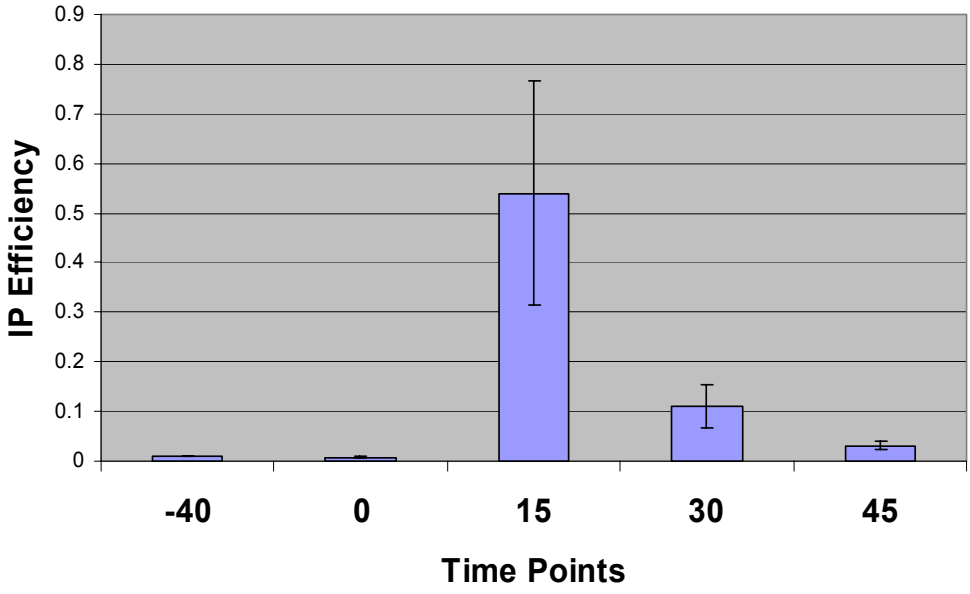
IP Efficiency
0.9
0.8
0.7
0.6
0.5
0.4
0.3
0.2
0.1
0
-40
0
15
30
45
Time Points

Figure 4.7 The recruitment of γ-H2A to the RE require yKu80p.

(A) Yeast strains carrying *HO* under the control of *GAL10* promoter with the background of *arp5Δ*, *yku80Δ*, *yku80Δ/yku70* and *yku80Δ/fkh1* (YCR707, YCR601, YCR708 and YCR603) were used in this experiment. Mating type switching was induced as described previously. Cells were collected 15 minutes after the beginning of DNA repair and fixed by formaldehyde. ChIP assays were performed as described above using primers amplifying both the DSB and the RE regions. (B) Graph shows the quantified IP data using ImageQuant. Error bars represent results from three independent experiments.

A.

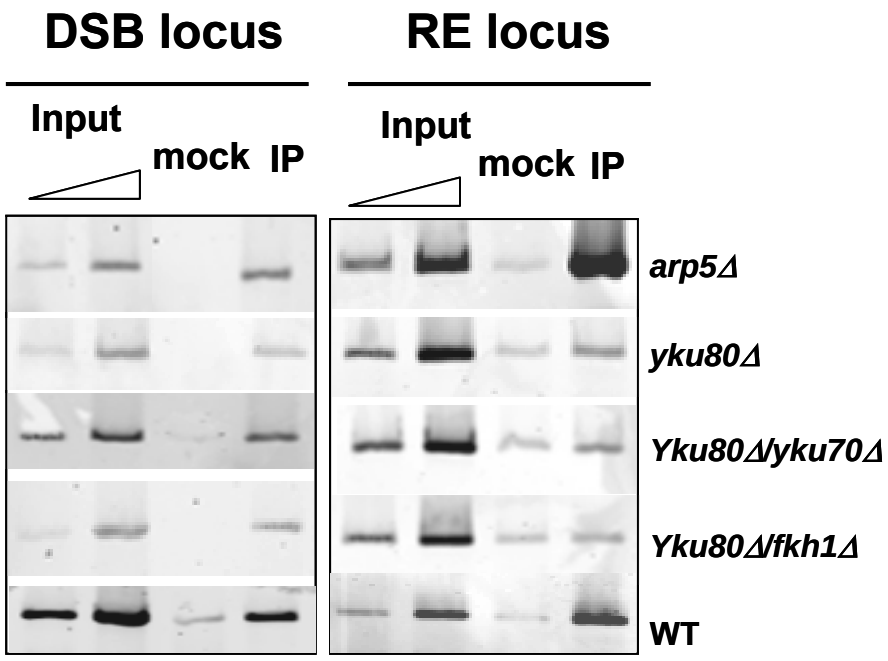
DSB locus
RE locus
Input
mock
IP
Input
mock
IP
arp5Δ
yku80Δ
Yku80Δ/yku70Δ
Yku80Δ/fkh1Δ
WT

B.

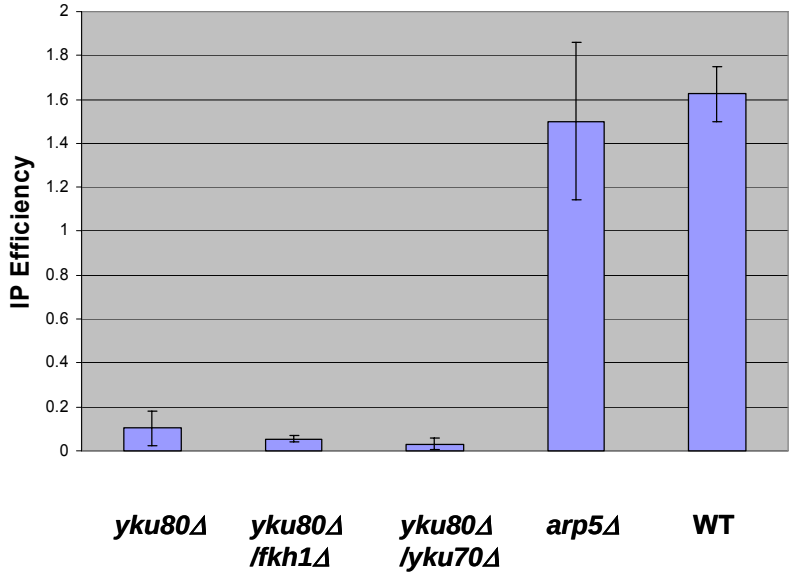
IP Efficiency
2
1.8
1.6
1.4
1.2
1
0.8
0.6
0.4
0.2
0
yku80Δ
yku80Δ /fkh1Δ
yku80Δ /yku70Δ
arp5Δ
WT

Figure 4.8: INO80 regualtes donor preference.

(A) Yeast strain carrying *HO* under *GAL10* control with *ARP5* deletion (YCR707) was used in this assay. Cells were grown to OD of 0.6 and switching was induced as described above. Three hours after switching, cells were collected and subjected to DNA purification and BamHI/HindIII double digestion. The digested genomic DNA were blotted with the Y_{α} probe which can detect four specific bands labeled above. Completion of switching generates *MAT*α band when cell chooses *HML* or *MAT*α-B band when *HMR* is used as the donor. (B) Chart illustrates the result of above experiments. Error bars indicate three independent switching assays.

A.

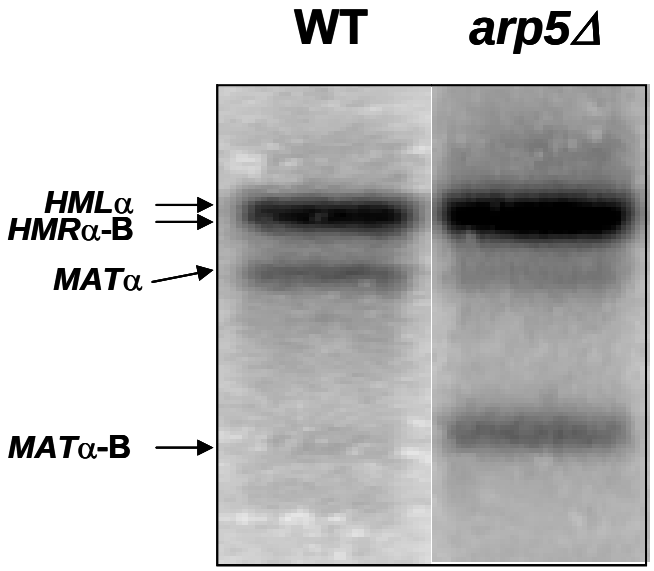
WT
arp5Δ
HMLα
HMRα-B
MATα
MATα-B

B.

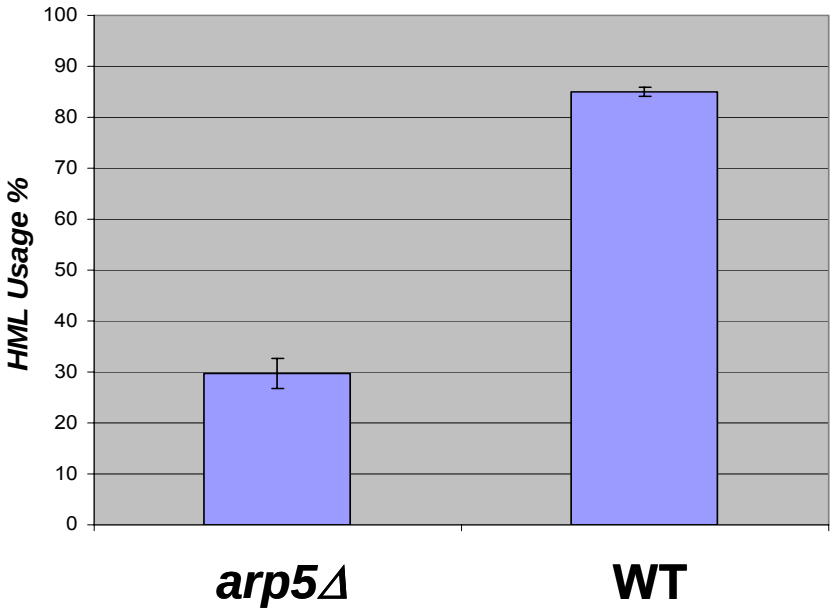
100
90
80
70
60
50
40
30
20
10
0
HML Usage %
arp5Δ
WT

Table 4-1 Mud-PIT result of purified TAP-yKu80p

Protein	Peptide hits Hits	Spec-Count	Seqence Coverage (I/U)	Peptide Sequence
yKu80p	31	210	41.5/15.7	K.SMAYLEYTLLNK.S
				F.QIQSFLAPVTTTATIGFIK.R
				F.LAPVTTTATIGFIK.R
				R.IILIDCGK.D
				R.IILIDCGKDTQEER.K
				I.LIDCGKDTQEER.K
				R.IYNMNELLVEITSPATSVVK.P
				R.IYNMNELLVEITSPATSVVK.P
				K.VEAFPATK.A
				K.SIIEYEIHNEGNK.K
				K.SIIEYEIHNEGNK.K
				K.SIIEYEIHNEGNKK.N
				K.NVSEDDQSGSSYIPVTISKDSVTK.A
				R.YGADYVVLPSVLVDQTVYESFPGLDLR.G
				L.VDQTVYESFPGLDLR.G
				R.YFLTSESSFITADTR.L
				K.DSEVNMCALCPVLIEHSNINSEK.K
				C.ALCPVLIEHSNINSEK.K
				K.SLTLCRLPFAEDER.V
				R.LPFAEDER.V
				R.LPFAEDER.V
				R.LPFAEDERVTDFPK.L
				N.YYQPIGEVTTDTTLPLPSLNK.D
				R.QQQVLLEWIHQL.M
				I.PELPDSLK.N
				K.LVEVLGIK.K
				K.LVEVLGIK.K
				K.IPDLETLLK.R
				I.PDLETLLK.R
				I.PDLETLLK.R
				K.RGEQHSR.G
yKu70	47	153	42.2/13.8	K.EGIYELFPLR.D
				K.EGIYELFPLR.D
				R.DINATFMK.K
				K.KLNDLLEDLSSGR.I
				K.LNDLLEDLSSGR.I
				K.LNDLLEDLSSGR.I
				R.ISLYDYFMFQQTGSEK.Q
				F.MLDTFLEEIPGQK.Q
				R.VFLFTDIDKPQEA.Q
				R.VFLFTDIDKPQEAQDIDER.A
				R.VFLFTDIDKPQEAQDIDER.A
				F.LFTDIDKPQEAQDIDER.A
				R.RLTIDLFDNK.V
				R.LTIDLFDNK.V

Table 4-1, continue

Protein	Peptide hits Hits	Spec-Count	Seqence Coverage (I/U)	Peptide Sequence
				R.LTIDLFDNK.V
				R.IMFQCPLILDEK.T
				R.IMFQCPLILDEK.T
				K.TNFIVGVK.G
				K.TNFIVGVK.G
				K.GYTMYTHEK.A
				K.GYTMYTHEK.A
				K.LVYEHEDIR.Q
				K.LVYEHEDIR.Q
				K.LVYEHEDIRQEAYSK.R
				R.KFLNPITGEDVTGK.T
				K.FLNPITGEDVTGK.T
				K.FLNPITGEDVTGK.T
				N.PITGEDVTGK.T
				K.SIHYFNNIDK.S
				K.SSFIVPDEAK.Y
				K.SSFIVPDEAK.Y
				K.SSFIVPDEAKYEGSIR.T
Sir4	2	3	2.6/0	
Lif1	11	21	25.9/0	
Dnl4	8	14	12.3/0	
Rap1	1	1	1.5/1.7	
Rvb1	4	7	15.8/0	K.TALALAISQELGPK.V
				K.VPFCPLVGSELYSVEVK.K
				K.EVYEGEVTELTPEDAENPLGGYGK.T
				R.GTEDVISPHGVPPDLIDR.L
Rvb2	4	7	13.2/0	K.TTDMETIYELGNK.M
				R.TQGFLALFTGDTGEIR.S
				R.AQEEEVELSSDALDLLTK.T
				R.YSSNLISVAQQIAMK.R
Arp5	1	1	4.4/0	R.TVAGFSNVELPQCIIPSSYIK.R
Arp8	1	1	2.2/0	R.DLFTNELNDWNSLSQFESK.E
Sir2	1	1	3.4/0	
Htb1/2	5	25	19.1/7.6	
Hhf1/2	6	20	39.8/18.4	
Hta1/2	2	2	12.1/0	
Hht1/2	2	5	14.7/0	
Hta3	2	3	15.7/0	
Rim1	1	3	10.2/0	
Bmh2	2	3	15/0	
Bmh1	2	3	14.7/0	
Sum1	7	8	10.4/0	
Isw1	4	7	3.8/0.6	
Tra1	1	2	0.2/0.2	
Htl1	2	3	33.3/0	
Rsc8	1	1	1.3/0	
Itc1	1	1	1.5/0	

Table 4-1, continue

Protein	Peptide hits Hits	Spec-Count	Seqence Coverage (I/U)	Peptide Sequence
Cdc19	18	30	38.6/0	
Ipp1	2	4	8.7/0	
Pgi1	2	3	5.2/0	
Ape3	1	1	2.0/0	
Pgk1	19	38	44.2/0	
Psa1	1	1	5.3/0	
Sam2	1	1	3.9/0	
Eno1	13	33	20.8/0	
Ahp1	1	2	11.4/0	
Rhr2	2	5	10.0/0	
Tdh1	7	23	22.0/0	
Pdc1	16	38	36.6/0	
Hxk1	1	2	3.7/0	
Hxk2	2	2	7.8/0	

Table 4-2 Mud-PIT result of purified TAP-Rvb1p

Complex	Protein	Pepetide hits	Spectrum count	Coverage %
Rvb	Rvb1	54	225	69.8
	Rvb2	56	293	78.3
Ino80.com	Act1	13	35	38.9
	Arp4	18	42	35.2
	Arp5	11	24	19.1
	Arp8	35	75	47.2
	Ino80	47	103	31
	Nhp10	6	10	31
	Ies1	14	29	29.9
	Ies3	10	23	52.4
	Rvb1	54	225	69.8
	Rvb2	56	293	78.3
SWR-C	Swr1	34	66	23.5
	Act1	13	35	38.9
	Arp4	18	42	35.2
	Arp6	2	3	6.2
	Yaf9	3	4	10.6
	Vps72	10	16	17.8
	Vps71	2	4	3.6
	Aor1	5	7	20.8
	Swc7	4	5	28
	Swc4	5	8	16.4
	Swc1	8	11	11
	Rvb1	54	225	69.8
	Rvb2	56	293	78.3
Small Complex	Rvb1	54	225	69.8
	Rvb2	56	293	78.3
	Yhr034c	7	13	30.5

CHAPTER V FUTURE STUDIES

5.1 Further optimizing the MAP method

The minichromosome affinity purification method has been proved to be a very useful tool to explore *in vivo* chromatin structure under its different functional state. However, it still has some technical drawbacks that need further optimization.

The current approach relies on the interaction between the *lac* operator and its repressor to achieve affinity purification. Theoretically, we would be able to retrieve the minichromosome bound to the *lac*I/Z beads by simply adding IPTG to compete off the binding of the *lac* operator to the *lac* repressor. However, in our hand, IPTG alone can not efficiently elute minichromosome from the affinity column and we were forced to increase the NaCl concentration in the elution buffer to produce efficient yields. The raise of ionic strength is potentially problematic since it may interfere the binding of some protein factors. To circumvent this problem, we sought to replace the *lac* operator in the minichromosome backbone with a calmodulin binding domain (CBD). In this case, the minichromosome will be isolated by the interaction of CBD and the calmodulin beads in the presence of calcium. It will subsequently be eluted with EGTA in a low NaCl buffer. Preliminary cloning experiments are in progress in our lab (Wang and Chakraborty, unpublished).

Two-step affinity purification of the minichromosome is also a feasible way to improve the quality if the there is information available of its associating factors. Since we identified yKu80p to be a minichromosome binding protein, I tried to exploit another affinity purification step after MAP. To this end, I first attempted to isolate the RE minichromosome in TAP tagged *YKU80* strain. The minichromosome elute from the *lac* repressor column was subjected to small scale IgG/calmodulin column affinity

purification. However, like the result of the sucrose gradient, the protein yield from this 3-step affinity approach was very low. 20% of the total protein obtain from 2 liters of cell was barely detectable by silver staining. Therefore, for this method, a larger amount of starting material may be needed.

5.2 Detailed mechanism of yKu80p in donor preference

Our study of yKu80p provides a lot of insights into how the activity of the RE is regulated during switching. However, the detailed mechanism of the directionality of donor preference is still elusive.

Haber's lab used the LacI-*lac*O system described previously to visualize the mobility of *HML*, *HMR* and *MAT* loci in living cells. They found that neither *HML* or *HMR* is paired with *MAT* prior to the start of switching (Bressan et al., 2004). However, the *MAT* and the correct donor do align to each other after the DSB is generated (Simon et al., 2002). These results bring an interesting question: how is the DSB at the *MAT* brought together with the accurate donor?

The yKu80p dependent enrichment of γH2A in RE at the beginning of switching is a very intriguing observation. Since the phosphorylated H2A was proved to be associated with the DSB, this result indicated the directional recruitment of the DSB to the left arm of Chromosome III by RE and its associated proteins. In mammalian cells, yKu80p has been shown to be able to bring the broken DNA end to its binding site (Walker et al., 2001). Therefore, it is reasonable to speculate that its yeast counterpart functions similarly.

In attempt to directly address this question, we sought to investigate the direct interaction between the DSB and the RE. Dekker et al described a straightforward

approach to detect the protein mediated long range interaction of different regions of chromosome (Dekker, 2003). The "chromosome conformation capture" (3C) method uses formaldehyde to cross-link two associated DNA fragments and the proteins that assist their interaction. The DNA-Proteins complex was then diluted and digested with site specific endonuclease. In the ligation step afterward, the two interacting DNA fragments will be preferably ligated since both of then are bound to the same protein complex and are closer to each other than the free fragments. The ligated DNA which represents the interaction between chromatin segments can then be detected by PCR. This technique has been used to detect the long range interaction of enhancer and promoter upon the activation of the β-globulin locus (Tolhuis et al., 2002). In our case, this method could be applied to detect the association of DSB and the RE and test if yKu80p are directly involved in this process. However, there were some technical details that need to be worked out. Switching is a very quick process. As shown in the ChIP assay (Fig. 4.6), γH2A started to appear in the RE 15 minutes after the start of DNA repair and left there after 30 minutes. However, the original 3C method applies formaldehyde cross-linking after the isolation of nuclei which takes hours to complete. Therefore, the transient interaction between different chromosomal regions during switching could be difficult to be captured.

An alternative approach to address the local phosphorylation in the RE is by monitoring its movement during switching. If the γH2A enrichment were proven to be restrained to the RE, the local phosphorylation model would be favored. Otherwise, if γH2A went through similar directional movement along the left arm of Chromosome III like that of the yKu80p and Rvb1p, it would support the idea that the enrichment of γH2A

at RE is indeed resulted from the DSB entering the RE. Our preliminary ChIP result showed that γH2A is not confined to the RE during switching. Instead, it moves along the left arm of Chromosome III toward *HML*.

Another interpretation of the enrichment of phosphorylated H2A at RE upon *HO* induction is that RE-bound yKu80p may directly recruit Mec1p or Tel1p to locally phosphorylate histone H2A. We designed one experiment trying to address this possibility. Many chemicals, such as camptothecin, can induce random double stranded break in yeast cells, which in turn gives rise to γH2A (Redon et al., 2003). This reagent provides a mean for us to monitor the enrichment of γH2A at RE under non-switching condition. If, indeed, the γH2A at RE is a result from yKu80p mediated local phosphorylation upon DNA damage, we would expect to see the γH2A cross-linking signal at RE when camptothecin is applied at a appropriate concentration so that robust level of total γH2A can be detected. In contrast, if we can not detect any enrichment of γH2A at RE under such condition, it would argue that random DSB could not cause the RE chromatin to be phosphorylated. Therefore it would be logical to conclude that the γH2A enrichment at RE during switching is indeed caused by looping the DSB to the RE region because, first, *HO* cleavage only generates a single γH2A bound DSB and second, this enrichment of γH2A have also been shown to exist at a DNA segment that does not have any broken ends.

REFERENCES

Aalfs, J. D., and Kingston, R. E. (2000). What does 'chromatin remodeling' mean? Trends Biochem Sci *25*, 548-555.

Angus-Hill, M. L., Schlichter, A., Roberts, D., Erdjument-Bromage, H., Tempst, P., and Cairns, B. R. (2001). A Rsc3/Rsc30 zinc cluster dimer reveals novel roles for the chromatin remodeler RSC in gene expression and cell cycle control. Mol Cell *7*, 741-751.

Aylon, Y., and Kupiec, M. (2004). DSB repair: the yeast paradigm. DNA Repair (Amst) *3*, 797-815.

Bannister, A. J., Schneider, R., and Kouzarides, T. (2002). Histone methylation: dynamic or static? Cell *109*, 801-806.

Bartek, J., Lukas, C., and Lukas, J. (2004). Checking on DNA damage in S phase. Nat Rev Mol Cell Biol *5*, 792-804.

Bartek, J., and Lukas, J. (2003). DNA repair: Damage alert. Nature *421*, 486-488.

Becker, P. B., and Horz, W. (2002). ATP-dependent nucleosome remodeling. Annu Rev Biochem *71*, 247-273.

Belmont, A. S. (2001). Visualizing chromosome dynamics with GFP. Trends Cell Biol *11*, 250-257.

Bennett, P. M. (2004). Genome plasticity: insertion sequence elements, transposons and integrons, and DNA rearrangement. Methods Mol Biol *266*, 71-113.

Bird, A. P., and Wolffe, A. P. (1999). Methylation-induced repression--belts, braces, and chromatin. Cell *99*, 451-454.

Boulton, S. J., and Jackson, S. P. (1996). Saccharomyces cerevisiae Ku70 potentiates illegitimate DNA double-strand break repair and serves as a barrier to error-prone DNA repair pathways. Embo J *15*, 5093-5103.

Brachmann, R. K., Yu, K., Eby, Y., Pavletich, N. P., and Boeke, J. D. (1998). Genetic selection of intragenic suppressor mutations that reverse the effect of common p53 cancer mutations. Embo J *17*, 1847-1859.

Brandt, V. L., and Roth, D. B. (2004). V(D)J recombination: how to tame a transposase. Immunol Rev *200*, 249-260.

Bressan, D. A., Vazquez, J., and Haber, J. E. (2004). Mating type-dependent constraints on the mobility of the left arm of yeast chromosome III. J Cell Biol *164*, 361-371.

Cairns, B. R. (2004). Around the world of DNA damage INO80 days. Cell *119*, 733-735.

Cairns, B. R., Schlichter, A., Erdjument-Bromage, H., Tempst, P., Kornberg, R. D., and Winston, F. (1999). Two functionally distinct forms of the RSC nucleosome-remodeling complex, containing essential AT hook, BAH, and bromodomains. Mol Cell *4*, 715-723.

Cary, R. B., Peterson, S. R., Wang, J., Bear, D. G., Bradbury, E. M., and Chen, D. J. (1997). DNA looping by Ku and the DNA-dependent protein kinase. Proc Natl Acad Sci U S A *94*, 4267-4272.

Casellas, R., Nussenzweig, A., Wuerffel, R., Pelanda, R., Reichlin, A., Suh, H., Qin, X. F., Besmer, E., Kenter, A., Rajewsky, K., and Nussenzweig, M. C. (1998). Ku80 is required for immunoglobulin isotype switching. Embo J *17*, 2404-2411.

Cervelli, T., and Galli, A. (2000). Effects of HDF1 (Ku70) and HDF2 (Ku80) on spontaneous and DNA damage-induced intrachromosomal recombination in Saccharomyces cerevisiae. Mol Gen Genet *264*, 56-63.

Chantalat, L., Nicholson, J. M., Lambert, S. J., Reid, A. J., Donovan, M. J., Reynolds, C. D., Wood, C. M., and Baldwin, J. P. (2003). Structure of the histone-core octamer in KCl/phosphate crystals at 2.15 A resolution. Acta Crystallogr D Biol Crystallogr *59*, 1395-1407.

Clikeman, J. A., Khalsa, G. J., Barton, S. L., and Nickoloff, J. A. (2001). Homologous recombinational repair of double-strand breaks in yeast is enhanced by MAT heterozygosity through yKU-dependent and -independent mechanisms. Genetics *157*, 579-589.

Collis, S. J., Deweese, T. L., Jeggo, P. A., and Parker, A. R. (2005). The life and death of DNA-PK. Oncogene *24*, 949-961.

Cooper, J. P., Roth, S. Y., and Simpson, R. T. (1994). The global transcriptional regulators, SSN6 and TUP1, play distinct roles in the establishment of a repressive chromatin structure. Genes Dev *8*, 1400-1410.

Corona, G., and Toffoli, G. (2004). High throughput screening of genetic polymorphisms by matrix-assisted laser desorption ionization time-of-flight mass spectrometry. Comb Chem High Throughput Screen *7*, 707-725.

Cosgrove, A. J., Nieduszynski, C. A., and Donaldson, A. D. (2002). Ku complex controls the replication time of DNA in telomere regions. Genes Dev *16*, 2485-2490.

Cuthbert, G. L., Daujat, S., Snowden, A. W., Erdjument-Bromage, H., Hagiwara, T., Yamada, M., Schneider, R., Gregory, P. D., Tempst, P., Bannister, A. J., and Kouzarides, T. (2004). Histone deimination antagonizes arginine methylation. Cell *118*, 545-553.

Davie, J. R., and Moniwa, M. (2000). Control of chromatin remodeling. Crit Rev Eukaryot Gene Expr *10*, 303-325.

de Bruin, D., Zaman, Z., Liberatore, R. A., and Ptashne, M. (2001). Telomere looping permits gene activation by a downstream UAS in yeast. Nature *409*, 109-113.

Dean, A., Pederson, D. S., and Simpson, R. T. (1989). Isolation of yeast plasmid chromatin. Methods Enzymol *170*, 26-41.

Dekker, J. (2003). A closer look at long-range chromosomal interactions. Trends Biochem Sci *28*, 277-280.

Doherty, A. J., and Jackson, S. P. (2001). DNA repair: how Ku makes ends meet. Curr Biol *11*, R920-924.

Doherty, A. J., Jackson, S. P., and Weller, G. R. (2001). Identification of bacterial homologues of the Ku DNA repair proteins. FEBS Lett *500*, 186-188.

Donze, D., Adams, C. R., Rine, J., and Kamakaka, R. T. (1999). The boundaries of the silenced HMR domain in Saccharomyces cerevisiae. Genes Dev *13*, 698-708.

Donze, D., and Kamakaka, R. T. (2001). RNA polymerase III and RNA polymerase II promoter complexes are heterochromatin barriers in Saccharomyces cerevisiae. Embo J *20*, 520-531.

Dorigo, B., Schalch, T., Kulangara, A., Duda, S., Schroeder, R. R., and Richmond, T. J. (2004). Nucleosome arrays reveal the two-start organization of the chromatin fiber. Science *306*, 1571-1573.

Downs, J. A., Kosmidou, E., Morgan, A., and Jackson, S. P. (2003). Suppression of homologous recombination by the Saccharomyces cerevisiae linker histone. Mol Cell *11*, 1685-1692.

Downs, J. A., Lowndes, N. F., and Jackson, S. P. (2000). A role for Saccharomyces cerevisiae histone H2A in DNA repair. Nature *408*, 1001-1004.

Dror, V., and Winston, F. (2004). The Swi/Snf chromatin remodeling complex is required for ribosomal DNA and telomeric silencing in Saccharomyces cerevisiae. Mol Cell Biol *24*, 8227-8235.

Ducker, C. E., and Simpson, R. T. (2000). The organized chromatin domain of the repressed yeast a cell-specific gene STE6 contains two molecules of the corepressor Tup1p per nucleosome. Embo J *19*, 400-409.

Edmondson, D. G., Smith, M. M., and Roth, S. Y. (1996). Repression domain of the yeast global repressor Tup1 interacts directly with histones H3 and H4. Genes Dev *10*, 1247-1259.

Ercan, S., Carrozza, M. J., and Workman, J. L. (2004). Global nucleosome distribution and the regulation of transcription in yeast. Genome Biol *5*, 243.

Ercan, S., and Simpson, R. T. (2004). Global chromatin structure of 45,000 base pairs of chromosome III in a- and alpha-cell yeast and during mating-type switching. Mol Cell Biol *24*, 10026-10035.

Feldmann, H., Driller, L., Meier, B., Mages, G., Kellermann, J., and Winnacker, E. L. (1996). HDF2, the second subunit of the Ku homologue from Saccharomyces cerevisiae. J Biol Chem *271*, 27765-27769.

Feldmann, H., and Winnacker, E. L. (1993). A putative homologue of the human autoantigen Ku from Saccharomyces cerevisiae. J Biol Chem *268*, 12895-12900.

Ferguson, P. L., and Smith, R. D. (2003). Proteome analysis by mass spectrometry. Annu Rev Biophys Biomol Struct *32*, 399-424.

Flaus, A., and Owen-Hughes, T. (2001). Mechanisms for ATP-dependent chromatin remodelling. Curr Opin Genet Dev *11*, 148-154.

Fritsch, O., Benvenuto, G., Bowler, C., Molinier, J., and Hohn, B. (2004). The INO80 protein controls homologous recombination in Arabidopsis thaliana. Mol Cell *16*, 479-485.

Fry, C. J., and Peterson, C. L. (2001). Chromatin remodeling enzymes: who's on first? Curr Biol *11*, R185-197.

Gavin, I. M., and Simpson, R. T. (1997). Interplay of yeast global transcriptional regulators Ssn6p-Tup1p and Swi-Snf and their effect on chromatin structure. Embo J *16*, 6263-6271.

Goldmark, J. P., Fazzio, T. G., Estep, P. W., Church, G. M., and Tsukiyama, T. (2000). The Isw2 chromatin remodeling complex represses early meiotic genes upon recruitment by Ume6p. Cell *103*, 423-433.

Gonzalez, I., Buonomo, S. B., Nasmyth, K., and von Ahsen, U. (1999). ASH1 mRNA localization in yeast involves multiple secondary structural elements and Ash1 protein translation. Curr Biol *9*, 337-340.

Gotta, M., and Gasser, S. M. (1996). Nuclear organization and transcriptional silencing in yeast. Experientia *52*, 1136-1147.

Grant, P. A. (2001). A tale of histone modifications. Genome Biol *2*, REVIEWS0003.

Gravel, S., Larrivee, M., Labrecque, P., and Wellinger, R. J. (1998). Yeast Ku as a regulator of chromosomal DNA end structure. Science *280*, 741-744.

Haber, J. E. (1998). Mating-type gene switching in Saccharomyces cerevisiae. Annu Rev Genet *32*, 561-599.

Haber, J. E. (1999). Sir-Ku-itous routes to make ends meet. Cell *97*, 829-832.

Haber, J. E. (2000). Lucky breaks: analysis of recombination in Saccharomyces. Mutat Res *451*, 53-69.

Haber, J. E. (2002). Uses and abuses of HO endonuclease. Methods Enzymol *350*, 141-164.

Haber, J. E., Ira, G., Malkova, A., and Sugawara, N. (2004). Repairing a double-strand chromosome break by homologous recombination: revisiting Robin Holliday's model. Philos Trans R Soc Lond B Biol Sci *359*, 79-86.

Havas, K., Whitehouse, I., and Owen-Hughes, T. (2001). ATP-dependent chromatin remodeling activities. Cell Mol Life Sci *58*, 673-682.

Hawthorne, D. C. (1963). A Deletion in Yeast and Its Bearing on the Structure of the Mating Type Locus. Genetics *48*, 1727-1729.

Hecht, A., Strahl-Bolsinger, S., and Grunstein, M. (1999). Mapping DNA interaction sites of chromosomal proteins. Crosslinking studies in yeast. Methods Mol Biol *119*, 469-479.

Herrmann, G., Lindahl, T., and Schar, P. (1998). Saccharomyces cerevisiae LIF1: a function involved in DNA double-strand break repair related to mammalian XRCC4. Embo J *17*, 4188-4198.

Huang, J., Hsu, J. M., and Laurent, B. C. (2004). The RSC nucleosome-remodeling complex is required for Cohesin's association with chromosome arms. Mol Cell *13*, 739-750.

Huang, J., and Laurent, B. C. (2004). A Role for the RSC chromatin remodeler in regulating cohesion of sister chromatid arms. Cell Cycle *3*, 973-975.

Hughes, T. R., Marton, M. J., Jones, A. R., Roberts, C. J., Stoughton, R., Armour, C. D., Bennett, H. A., Coffey, E., Dai, H., He, Y. D., Kidd, M. J., King, A. M., Meyer, M. R., Slade, D., Lum, P. Y., Stepaniants, S. B., Shoemaker, D. D., Gachotte, D., Chakraburtty, K., Simon, J., Bard, M., and Friend, S. H. (2000). Functional discovery via a compendium of expression profiles. Cell *102*, 109-126.

Iyer, V., and Struhl, K. (1995). Poly(dA:dT), a ubiquitous promoter element that stimulates transcription via its intrinsic DNA structure. Embo J *14*, 2570-2579.

Jenuwein, T., and Allis, C. D. (2001). Translating the histone code. Science *293*, 1074-1080.

Jones, J. M., and Gellert, M. (2004). The taming of a transposon: V(D)J recombination and the immune system. Immunol Rev *200*, 233-248.

Jonsson, Z. O., Jha, S., Wohlschlegel, J. A., and Dutta, A. (2004). Rvb1p/Rvb2p recruit Arp5p and assemble a functional Ino80 chromatin remodeling complex. Mol Cell *16*, 465-477.

Kay, G. F. (1998). Xist and X chromosome inactivation. Mol Cell Endocrinol *140*, 71-76.

Kay, G. F., Penny, G. D., Patel, D., Ashworth, A., Brockdorff, N., and Rastan, S. (1993). Expression of Xist during mouse development suggests a role in the initiation of X chromosome inactivation. Cell *72*, 171-182.

Kladde, M. P., Xu, M., and Simpson, R. T. (1999a). DNA methyltransferases as probes for chromatin structure in yeast. Methods Mol Biol *119*, 395-416.

Kladde, M. P., Xu, M., and Simpson, R. T. (1999b). DNA methyltransferases as probes of chromatin structure in vivo. Methods Enzymol *304*, 431-447.

Korber, P., and Horz, W. (2004). SWRred not shaken; mixing the histones. Cell *117*, 5-7.

Kostriken, R., and Wedeen, C. J. (2001). Engineered interphase chromosome loops guide intrachromosomal recombination. Embo J *20*, 2907-2913.

Kurokawa, Y., Kanemaki, M., Makino, Y., and Tamura, T. A. (1999). A notable example of an evolutionary conserved gene: studies on a putative DNA helicase TIP49. DNA Seq *10*, 37-42.

Laroche, T., Martin, S. G., Gotta, M., Gorham, H. C., Pryde, F. E., Louis, E. J., and Gasser, S. M. (1998). Mutation of yeast Ku genes disrupts the subnuclear organization of telomeres. Curr Biol *8*, 653-656.

Lee, C. K., Shibata, Y., Rao, B., Strahl, B. D., and Lieb, J. D. (2004). Evidence for nucleosome depletion at active regulatory regions genome-wide. Nat Genet *36*, 900-905.

Li, B., and Reese, J. C. (2001). Ssn6-Tup1 regulates RNR3 by positioning nucleosomes and affecting the chromatin structure at the upstream repression sequence. J Biol Chem *276*, 33788-33797.

Li, Q., Peterson, K. R., Fang, X., and Stamatoyannopoulos, G. (2002). Locus control regions. Blood *100*, 3077-3086.

Liao, M., and Fang, F. (2000). [Yeast one-hybrid system--one effective method studying DNA-protein interaction]. Zhongguo Yi Xue Ke Xue Yuan Xue Bao *22*, 388-391.

Lieb, J. D. (2003). Genome-wide mapping of protein-DNA interactions by chromatin immunoprecipitation and DNA microarray hybridization. Methods Mol Biol *224*, 99-109.

Liebler, D. C. (2002). Proteomic approaches to characterize protein modifications: new tools to study the effects of environmental exposures. Environ Health Perspect *110 Suppl 1*, 3-9.

Link, A. J., Eng, J., Schieltz, D. M., Carmack, E., Mize, G. J., Morris, D. R., Garvik, B. M., and Yates, J. R., 3rd (1999). Direct analysis of protein complexes using mass spectrometry. Nat Biotechnol *17*, 676-682.

Lohr, D. (1997). Nucleosome transactions on the promoters of the yeast GAL and PHO genes. J Biol Chem *272*, 26795-26798.

Longtine, M. S., McKenzie, A., 3rd, Demarini, D. J., Shah, N. G., Wach, A., Brachat, A., Philippsen, P., and Pringle, J. R. (1998). Additional modules for versatile and economical PCR-based gene deletion and modification in Saccharomyces cerevisiae. Yeast *14*, 953-961.

Lowndes, N. F., and Toh, G. W. (2005). DNA Repair: The Importance of Phosphorylating Histone H2AX. Curr Biol *15*, R99-R102.

Luger, K., Mader, A. W., Richmond, R. K., Sargent, D. F., and Richmond, T. J. (1997). Crystal structure of the nucleosome core particle at 2.8 A resolution. Nature *389*, 251-260.

Luger, K., and Richmond, T. J. (1998a). DNA binding within the nucleosome core. Curr Opin Struct Biol *8*, 33-40.

Luger, K., and Richmond, T. J. (1998b). The histone tails of the nucleosome. Curr Opin Genet Dev *8*, 140-146.

Mages, G. J., Feldmann, H. M., and Winnacker, E. L. (1996). Involvement of the Saccharomyces cerevisiae HDF1 gene in DNA double-strand break repair and recombination. J Biol Chem *271*, 7910-7915.

Mai, X., Chou, S., and Struhl, K. (2000). Preferential accessibility of the yeast his3 promoter is determined by a general property of the DNA sequence, not by specific elements. Mol Cell Biol *20*, 6668-6676.

Manis, J. P., Gu, Y., Lansford, R., Sonoda, E., Ferrini, R., Davidson, L., Rajewsky, K., and Alt, F. W. (1998). Ku70 is required for late B cell development and immunoglobulin heavy chain class switching. J Exp Med *187*, 2081-2089.

Marahrens, Y., and Stillman, B. (1992). A yeast chromosomal origin of DNA replication defined by multiple functional elements. Science *255*, 817-823.

Martin, S. G., Laroche, T., Suka, N., Grunstein, M., and Gasser, S. M. (1999). Relocalization of telomeric Ku and SIR proteins in response to DNA strand breaks in yeast. Cell *97*, 621-633.

Masneuf, I., Hansen, J., Groth, C., Piskur, J., and Dubourdieu, D. (1998). New hybrids between Saccharomyces sensu stricto yeast species found among wine and cider production strains. Appl Environ Microbiol *64*, 3887-3892.

Megee, P. C., Morgan, B. A., and Smith, M. M. (1995). Histone H4 and the maintenance of genome integrity. Genes Dev *9*, 1716-1727.

Mills, K. D., Sinclair, D. A., and Guarente, L. (1999). MEC1-dependent redistribution of the Sir3 silencing protein from telomeres to DNA double-strand breaks. Cell *97*, 609-620.

Miyazaki, T., Bressan, D. A., Shinohara, M., Haber, J. E., and Shinohara, A. (2004). In vivo assembly and disassembly of Rad51 and Rad52 complexes during double-strand break repair. Embo J *23*, 939-949.

Mizuguchi, G., Shen, X., Landry, J., Wu, W. H., Sen, S., and Wu, C. (2004). ATP-driven exchange of histone H2AZ variant catalyzed by SWR1 chromatin remodeling complex. Science *303*, 343-348.

Morillon, A., Karabetsou, N., O'Sullivan, J., Kent, N., Proudfoot, N., and Mellor, J. (2003). Isw1 chromatin remodeling ATPase coordinates transcription elongation and termination by RNA polymerase II. Cell *115*, 425-435.

Morrison, A. J., Highland, J., Krogan, N. J., Arbel-Eden, A., Greenblatt, J. F., Haber, J. E., and Shen, X. (2004). INO80 and gamma-H2AX interaction links ATP-dependent chromatin remodeling to DNA damage repair. Cell *119*, 767-775.

Morse, R. H., Pederson, D. S., Dean, A., and Simpson, R. T. (1987). Yeast nucleosomes allow thermal untwisting of DNA. Nucleic Acids Res *15*, 10311-10330.

Nasmyth, K. (1983). Molecular analysis of a cell lineage. Nature *302*, 670-676.

Nasmyth, K., Stillman, D., and Kipling, D. (1987). Both positive and negative regulators of HO transcription are required for mother-cell-specific mating-type switching in yeast. Cell *48*, 579-587.

Neverova, I., and Van Eyk, J. E. (2005). Role of chromatographic techniques in proteomic analysis. J Chromatogr B Analyt Technol Biomed Life Sci *815*, 51-63.

Nugent, C. I., Bosco, G., Ross, L. O., Evans, S. K., Salinger, A. P., Moore, J. K., Haber, J. E., and Lundblad, V. (1998). Telomere maintenance is dependent on activities required for end repair of double-strand breaks. Curr Biol *8*, 657-660.

Nussenzweig, A., Chen, C., da Costa Soares, V., Sanchez, M., Sokol, K., Nussenzweig, M. C., and Li, G. C. (1996). Requirement for Ku80 in growth and immunoglobulin V(D)J recombination. Nature *382*, 551-555.

Olave, I. A., Reck-Peterson, S. L., and Crabtree, G. R. (2002). Nuclear actin and actin-related proteins in chromatin remodeling. Annu Rev Biochem *71*, 755-781.

Olins, A. L., and Olins, D. E. (1974). Spheroid chromatin units (v bodies). Science *183*, 330-332.

Olins, D. E., and Olins, A. L. (2003). Chromatin history: our view from the bridge. Nat Rev Mol Cell Biol *4*, 809-814.

Orlando, V. (2000). Mapping chromosomal proteins in vivo by formaldehyde-crosslinked-chromatin immunoprecipitation. Trends Biochem Sci *25*, 99-104.

Oshima, Y., and Takano, I. (1971). Mating types in Saccharomyces: their convertibility and homothallism. Genetics *67*, 327-335.

Patterton, H. G., and Simpson, R. T. (1994). Nucleosomal location of the STE6 TATA box and Mat alpha 2p-mediated repression. Mol Cell Biol *14*, 4002-4010.

Pazin, M. J., Hermann, J. W., and Kadonaga, J. T. (1998). Promoter structure and transcriptional activation with chromatin templates assembled in vitro. A single Gal4-VP16 dimer binds to chromatin or to DNA with comparable affinity. J Biol Chem *273*, 34653-34660.

Peterson, C. L. (1996). Multiple SWItches to turn on chromatin? Curr Opin Genet Dev *6*, 171-175.

Peterson, C. L., and Laniel, M. A. (2004). Histones and histone modifications. Curr Biol *14*, R546-551.

Puig, O., Caspary, F., Rigaut, G., Rutz, B., Bouveret, E., Bragado-Nilsson, E., Wilm, M., and Seraphin, B. (2001). The tandem affinity purification (TAP) method: a general procedure of protein complex purification. Methods *24*, 218-229.

Ravindra, A., Weiss, K., and Simpson, R. T. (1999). High-resolution structural analysis of chromatin at specific loci: Saccharomyces cerevisiae silent mating-type locus HMRa. Mol Cell Biol *19*, 7944-7950.

Rea, S., Eisenhaber, F., O'Carroll, D., Strahl, B. D., Sun, Z. W., Schmid, M., Opravil, S., Mechtler, K., Ponting, C. P., Allis, C. D., and Jenuwein, T. (2000). Regulation of chromatin structure by site-specific histone H3 methyltransferases. Nature *406*, 593-599.

Redon, C., Pilch, D. R., Rogakou, E. P., Orr, A. H., Lowndes, N. F., and Bonner, W. M. (2003). Yeast histone 2A serine 129 is essential for the efficient repair of checkpoint-blind DNA damage. EMBO Rep *4*, 678-684.

Roch, F. A., Hobi, R., Berchtold, M. W., and Kuenzle, C. C. (1997). V(D)J recombination frequency is affected by the sequence interposed between a pair of recombination signals: sequence comparison reveals a putative recombinational enhancer element. Nucleic Acids Res *25*, 2303-2310.

Rogakou, E. P., Boon, C., Redon, C., and Bonner, W. M. (1999). Megabase chromatin domains involved in DNA double-strand breaks in vivo. J Cell Biol *146*, 905-916.

Roth, S. Y., Shimizu, M., Johnson, L., Grunstein, M., and Simpson, R. T. (1992). Stable nucleosome positioning and complete repression by the yeast alpha 2 repressor are disrupted by amino-terminal mutations in histone H4. Genes Dev *6*, 411-425.

Sandor, Z., Calicchio, M. L., Sargent, R. G., Roth, D. B., and Wilson, J. H. (2004). Distinct requirements for Ku in N nucleotide addition at V(D)J- and non-V(D)J-generated double-strand breaks. Nucleic Acids Res *32*, 1866-1873.

Shakibai, N., Kumar, V., and Eisenberg, S. (1996). The Ku-like protein from Saccharomyces cerevisiae is required in vitro for the assembly of a stable multiprotein complex at a eukaryotic origin of replication. Proc Natl Acad Sci U S A *93*, 11569-11574.

Shen, X., Mizuguchi, G., Hamiche, A., and Wu, C. (2000). A chromatin remodelling complex involved in transcription and DNA processing. Nature *406*, 541-544.

Shen, X., Ranallo, R., Choi, E., and Wu, C. (2003a). Involvement of actin-related proteins in ATP-dependent chromatin remodeling. Mol Cell *12*, 147-155.

Shen, X., Xiao, H., Ranallo, R., Wu, W. H., and Wu, C. (2003b). Modulation of ATP-dependent chromatin-remodeling complexes by inositol polyphosphates. Science *299*, 112-114.

Shi, Y., Lan, F., Matson, C., Mulligan, P., Whetstine, J. R., Cole, P. A., and Casero, R. A. (2004). Histone demethylation mediated by the nuclear amine oxidase homolog LSD1. Cell *119*, 941-953.

Shimizu, M., Roth, S. Y., Szent-Gyorgyi, C., and Simpson, R. T. (1991). Nucleosomes are positioned with base pair precision adjacent to the alpha 2 operator in Saccharomyces cerevisiae. Embo J *10*, 3033-3041.

Sieweke, M. (2000). Detection of transcription factor partners with a yeast one hybrid screen. Methods Mol Biol *130*, 59-77.

Simon, P., Houston, P., and Broach, J. (2002). Directional bias during mating type switching in Saccharomyces is independent of chromosomal architecture. Embo J *21*, 2282-2291.

Simpson, R. T. (1990). Nucleosome positioning can affect the function of a cis-acting DNA element in vivo. Nature *343*, 387-389.

Simpson, R. T. (1999). In vivo methods to analyze chromatin structure. Curr Opin Genet Dev *9*, 225-229.

Simpson, R. T., Ducker, C. E., Diller, J. D., and Ruan, C. (2004). Purification of native, defined chromatin segments. Methods Enzymol *375*, 158-170.

Sivolob, A., and Prunell, A. (2004). Nucleosome conformational flexibility and implications for chromatin dynamics. Philos Transact A Math Phys Eng Sci *362*, 1519-1547.

Smith, D. L., and Johnson, A. D. (1994). Operator-constitutive mutations in a DNA sequence recognized by a yeast homeodomain. Embo J *13*, 2378-2387.

Smith, R. L., and Johnson, A. D. (2000). Turning genes off by Ssn6-Tup1: a conserved system of transcriptional repression in eukaryotes. Trends Biochem Sci *25*, 325-330.

Smith, R. L., Redd, M. J., and Johnson, A. D. (1995). The tetratricopeptide repeats of Ssn6 interact with the homeo domain of alpha 2. Genes Dev *9*, 2903-2910.

Sprague, G. F., Jr., Rine, J., and Herskowitz, I. (1981). Control of yeast cell type by the mating type locus. II. Genetic interactions between MAT alpha and unlinked alpha-specific STE genes. J Mol Biol *153*, 323-335.

Sugawara, N., Wang, X., and Haber, J. E. (2003). In vivo roles of Rad52, Rad54, and Rad55 proteins in Rad51-mediated recombination. Mol Cell *12*, 209-219.

Sun, K., Coic, E., Zhou, Z., Durrens, P., and Haber, J. E. (2002). Saccharomyces forkhead protein Fkh1 regulates donor preference during mating-type switching through the recombination enhancer. Genes Dev *16*, 2085-2096.

Svaren, J., and Horz, W. (1995). Interplay between nucleosomes and transcription factors at the yeast PHO5 promoter. Semin Cell Biol *6*, 177-183.

Szeto, L., and Broach, J. R. (1997). Role of alpha2 protein in donor locus selection during mating type interconversion. Mol Cell Biol *17*, 751-759.

Szeto, L., Fafalios, M. K., Zhong, H., Vershon, A. K., and Broach, J. R. (1997). Alpha2p controls donor preference during mating type interconversion in yeast by inactivating a recombinational enhancer of chromosome III. Genes Dev *11*, 1899-1911.

Taddei, A., and Gasser, S. M. (2004). Multiple pathways for telomere tethering: functional implications of subnuclear position for heterochromatin formation. Biochim Biophys Acta *1677*, 120-128.

Taddei, A., Hediger, F., Neumann, F. R., Bauer, C., and Gasser, S. M. (2004). Separation of silencing from perinuclear anchoring functions in yeast Ku80, Sir4 and Esc1 proteins. Embo J *23*, 1301-1312.

Takano, I., and Oshima, Y. (1970). Mutational nature of an allele-specific conversion of the mating type by the homothallic gene HO alpha in Saccharomyces. Genetics *65*, 421-427.

Tamura, K., Adachi, Y., Chiba, K., Oguchi, K., and Takahashi, H. (2002). Identification of Ku70 and Ku80 homologues in Arabidopsis thaliana: evidence for a role in the repair of DNA double-strand breaks. Plant J *29*, 771-781.

Tolhuis, B., Palstra, R. J., Splinter, E., Grosveld, F., and de Laat, W. (2002). Looping and interaction between hypersensitive sites in the active beta-globin locus. Mol Cell *10*, 1453-1465.

Tsukamoto, T., Hashiguchi, N., Janicki, S. M., Tumbar, T., Belmont, A. S., and Spector, D. L. (2000). Visualization of gene activity in living cells. Nat Cell Biol *2*, 871-878.

Tsukiyama, T. (2002). The in vivo functions of ATP-dependent chromatin-remodelling factors. Nat Rev Mol Cell Biol *3*, 422-429.

Tsukiyama, T., Palmer, J., Landel, C. C., Shiloach, J., and Wu, C. (1999). Characterization of the imitation switch subfamily of ATP-dependent chromatin-remodeling factors in Saccharomyces cerevisiae. Genes Dev *13*, 686-697.

Unal, E., Arbel-Eden, A., Sattler, U., Shroff, R., Lichten, M., Haber, J. E., and Koshland, D. (2004). DNA damage response pathway uses histone modification to assemble a double-strand break-specific cohesin domain. Mol Cell *16*, 991-1002.

Ushinsky, S. C., Bussey, H., Ahmed, A. A., Wang, Y., Friesen, J., Williams, B. A., and Storms, R. K. (1997). Histone H1 in Saccharomyces cerevisiae. Yeast *13*, 151-161.

van Attikum, H., Fritsch, O., Hohn, B., and Gasser, S. M. (2004). Recruitment of the INO80 complex by H2A phosphorylation links ATP-dependent chromatin remodeling with DNA double-strand break repair. Cell *119*, 777-788.

van der Woude, M. W., and Baumler, A. J. (2004). Phase and antigenic variation in bacteria. Clin Microbiol Rev *17*, 581-611, table of contents.

Vignali, M., and Workman, J. L. (1998). Location and function of linker histones. Nat Struct Biol *5*, 1025-1028.

Wai, L. K. (2004). Telomeres, telomerase, and tumorigenesis--a review. MedGenMed *6*, 19.

Walker, J. R., Corpina, R. A., and Goldberg, J. (2001). Structure of the Ku heterodimer bound to DNA and its implications for double-strand break repair. Nature *412*, 607-614.

Wang, X., and Simpson, R. T. (2001). Chromatin structure mapping in Saccharomyces cerevisiae in vivo with DNase I. Nucleic Acids Res *29*, 1943-1950.

Ward, I., and Chen, J. (2004). Early events in the DNA damage response. Curr Top Dev Biol *63*, 1-35.

Washburn, M. P., Wolters, D., and Yates, J. R., 3rd (2001). Large-scale analysis of the yeast proteome by multidimensional protein identification technology. Nat Biotechnol *19*, 242-247.

Watson, A. D., Edmondson, D. G., Bone, J. R., Mukai, Y., Yu, Y., Du, W., Stillman, D. J., and Roth, S. Y. (2000). Ssn6-Tup1 interacts with class I histone deacetylases required for repression. Genes Dev *14*, 2737-2744.

Weiler, K. S., Szeto, L., and Broach, J. R. (1995). Mutations affecting donor preference during mating type interconversion in Saccharomyces cerevisiae. Genetics *139*, 1495-1510.

Weiss, K., and Simpson, R. T. (1997). Cell type-specific chromatin organization of the region that governs directionality of yeast mating type switching. Embo J *16*, 4352-4360.

Weiss, K., and Simpson, R. T. (1998). High-resolution structural analysis of chromatin at specific loci: Saccharomyces cerevisiae silent mating type locus HMLalpha. Mol Cell Biol *18*, 5392-5403.

Widom, J. (1998a). Chromatin structure: linking structure to function with histone H1. Curr Biol *8*, R788-791.

Widom, J. (1998b). Structure, dynamics, and function of chromatin in vitro. Annu Rev Biophys Biomol Struct *27*, 285-327.

Woodcock, C. L., and Horowitz, R. A. (1997). Electron microscopy of chromatin. Methods *12*, 84-95.

Woodcock, C. L., and Horowitz, R. A. (1998). Electron microscopic imaging of chromatin with nucleosome resolution. Methods Cell Biol *53*, 167-186.

Wu, C., Weiss, K., Yang, C., Harris, M. A., Tye, B. K., Newlon, C. S., Simpson, R. T., and Haber, J. E. (1998). Mcm1 regulates donor preference controlled by the recombination enhancer in Saccharomyces mating-type switching. Genes Dev *12*, 1726-1737.

Wu, X., and Haber, J. E. (1995). MATa donor preference in yeast mating-type switching: activation of a large chromosomal region for recombination. Genes Dev *9*, 1922-1932.

Wu, X., and Haber, J. E. (1996). A 700 bp cis-acting region controls mating-type dependent recombination along the entire left arm of yeast chromosome III. Cell *87*, 277-285.

Wu, X., Moore, J. K., and Haber, J. E. (1996). Mechanism of MAT alpha donor preference during mating-type switching of Saccharomyces cerevisiae. Mol Cell Biol *16*, 657-668.

Wuebbles, R. D., and Jones, P. L. (2004). DNA repair in a chromatin environment. Cell Mol Life Sci *61*, 2148-2153.

Xu, M., Kladde, M. P., Van Etten, J. L., and Simpson, R. T. (1998). Cloning, characterization and expression of the gene coding for a cytosine-5-DNA methyltransferase recognizing GpC. Nucleic Acids Res *26*, 3961-3966.

Yamada, K., Miyata, T., Tsuchiya, D., Oyama, T., Fujiwara, Y., Ohnishi, T., Iwasaki, H., Shinagawa, H., Ariyoshi, M., Mayanagi, K., and Morikawa, K. (2002). Crystal structure of the RuvA-RuvB complex: a structural basis for the Holliday junction migrating motor machinery. Mol Cell *10*, 671-681.

Yamada, K., and Morikawa, K. (2002). [Three-dimensional structural view of the mechanism of Holliday junction migration]. Seikagaku *74*, 1251-1259.

Yates, J. R., 3rd, Eng, J. K., McCormack, A. L., and Schieltz, D. (1995). Method to correlate tandem mass spectra of modified peptides to amino acid sequences in the protein database. Anal Chem *67*, 1426-1436.

Zhou, Z., Sun, K., Lipstein, E. A., and Haber, J. E. (2001). A Saccharomyces servazzii clone homologous to Saccharomyces cerevisiae chromosome III spanning KAR4, ARS 304 and SPB1 lacks the recombination enhancer but contains an unknown ORF. Yeast *18*, 789-795.

CURRICULUM VITAE

Name: Chun Ruan

Education and Professional Experience:

1998-2005	Ph.D in Cell and Developmental Biology, Huck Institutes of Life Sciences, Pennsylvania State University
1995-1998	M.S. in Molecular Biology, College of Life Science, Peking University, Beijing, China
1994-1995	Research assistant of National Lab of Plant Molecular Biology, Peking University, Beijing, China
1990-1994	B.S. in Microbiology, Dept. of Microbiology, Beijing Agricultural University, Beijing, China

Academic Honors and Awards:

1998	Fellowship of Life Science Consortium, Penn State University
1995	Weiming Fellowship, Peking University
1993	Guo Zhaoming Fellowship, Beijing Agricultural University
1990-1994	People fellowship, Beijing Agricultural University